Dielectric Relaxation Behavior of Poly(3-hydroxybutyrate)

by
Taigyoo Park

Dissertation submitted to the Faculty of the
Virginia Polytechnic Institute and State University
in partial fulfillment of the requirements for the degree of

DOCTOR OF PHILOSOPHY

in

Chemistry

APPROVED:

T.C. Ward, Chairman

H.W. Gibson

H. Marand

M.R. Anderson

J.S. Riffle

April, 1994

Blacksburg, Virginia

Dielectric Relaxation Behavior of Poly(3-hydroxybutyrate)

by
Taigyoo Park

Committee Chairman: Thomas C. Ward
Chemistry

(Abstract)

The importance of Poly(3-hydroxybutyrate) (PHB) as a biodegradable material is well known. Due to ever increasing environmental awareness, significant efforts have been made to utilize PHB or its derivatives in producing disposable products. However, brittle mechanical properties of PHB hinder the direct application of this material in useful commodity items. In order to achieve toughened PHB, blending with other polymers which possess high relaxation behavior at room temperature seems attractive. Prior to such development, the fundamental characterization of the relaxation behavior of PHB itself is extremely important in order to assess the effect of any attempt to improve the situation in a quantitative manner.

Dielectric thermal analysis was used in the study of the relaxation behavior of melt processed PHB. The approach was largely phenomenological, that was, based on the macroscopic theory of dielectric relaxation. The mean relaxation time of melt processed PHB was evaluated while PHB was undergoing crystallization at room temperature. The experimental conditions were kept as close as possible to actual shelf-

life conditions. Dynamic temperature sweep experiments revealed multiple relaxation peaks at the glass transition region. Temperature plane curve resolution revealed, in the early stage of crystallization, two dynamically changing peaks whose behaviors, as the extent of crystallization progressed, were quite opposite in terms of the magnitude of the loss property. By analyzing the temperature dependence of loss property and mean relaxation time, it was concluded that the peak located at the lower temperature is related to pure amorphous chain movement, and the peak located at the higher temperature is related to the movement of amorphous chains which are confined in-between crystalline phases, such as lamellae and spherulites. For the evaluation of the mean relaxation time of binary blends or multiple relaxations arising from homopolymers and copolymers, an empirical model has been developed which is grounded in the theory of linear viscoelasticity with the aim of quantitatively assessing the effect of attempts to improve the toughness of PHB. In the course of data reduction and model development, the majority of empirical dielectric relaxation functions has been reviewed including the Havriliak-Negami model and the Kohlrausch-Williams-Watts stretched exponential function. It was found that the center of relaxation time in the Havriliak-Negami model was skewed toward short time scale of relaxation, while mean relaxation time reflected the relaxation behavior of PHB chains on average, including movement of chains which relax with difficulty as the extent of crystallization progresses.

ACKNOWLEDGEMENTS

First of all, I wish to express my deep gratitude to my advisor Professor Thomas Carl Ward. His teaching was always concise and to the point, leaving a lot for me to think about again and again. Nevertheless all his teaching materials were always delivered in an unbelievably exciting manner. Although I grew up in a country where the teaching of Confucius prevails, I have never seen a teacher who is closer to Confucius than my advisor in terms of balanced teaching and personality. I just feel sorry about the unfortunate destiny of my son since, he would never find, and never have an opportunity to learn from a teacher like Professor Ward.

I would like to thank Professor Gibson for his teaching organic polymer chemistry as well as sacrificing his invaluable time in serving on my committee. I would like to thank Professor Marand first, for his teaching of physical chemistry, second, for his guidance through the PHB project, and third, for sacrificing his invaluable time in serving on my committee. I would like to thank Professor Anderson, from whom I learned electrochemistry, for serving on my committee. Also I would like to thank Professor Riffle for her teaching on many occasions here at Tech as well as serving on my committee. I would like to thank Professor Allan Shultz, who let me have a practical learning opportunity from one of the finest minds of all American intellectuals for academic advice given on numerous occasions during lab life. I would like to thank Dr. C. Frederick Battrell, for he showed me the quality of mind which I have always envied but never attained in my life. I would like to thank Chad Snyder, who worked with me through the PHB project, for his work on the crystallization study which he kindly rendered to me to include in part in this dissertation and for his always bright personality and attitude.

I am indebted to all my colleagues in my lab. In order not to forget their names together with all the happiness and misunderstandings caused by my ignorance of American culture, which I always enjoyed, I record their names here. Celene, John Hellgeth, Paul Vail, Janis Cartwright, Dan Hahn, Yan Yang, David Porter, Tony Williams, Mark Vrana, Mark Muggli, Jesse, and Kermit Kwan. I especially thank Steven Wilkinson, for he encouraged me a lot through the cumulative exams and then the thermal degradation experiment. I thank Mike Zumbrum for his contributions to the lab by which we all benefited tremendously. I thank George Dallas for his teaching during the Torlon project as well as the great hospitality he showed. I thank Joyce Kaltenecker, together with Pascal, for a lot of help during my exams and advice on the experiments. Nobody influenced me as much as Saikat Joardar did in my lab life. With his amazing scientific prowess, he taught me many details about dielectric experiment and all the other aspects of physical sciences without which I could not have survived up to this moment. All my lab members helped me learn many things, from computers to American English, beers to whiskies, and OOzos. I would like to thank the Korean students who taught, encouraged, and helped me whenever I had a troubled mind; Sanghun Lee, Sang Pak, Ojin Kwon, and Yongjoon Lee. I would like to especially thank Taeho Yoon and Guangjin Choi, who helped me during the first month of my family's American life, for their continual advice on life, as well as academic problems. I would like to thank Donggeon Kim for his teaching about the constrained parameter method with his SAS program even during his busy schedule. I would like to thank Youngjun Kim, Myungho Pyo, and Kyungil Kim, for they taught me chemistry and helped me pass the GRE exam with a top grade so that I could come to this country for advanced study. They also gave me tremendous advice, and encouragement in life. I would like to thank Professor Changkyun Choi of Seoul National University from whom I learned transport phenomena and thermodynamics, for he first guided me into the polymer industry and

later wrote a recommendation letter to Virginia Tech. Before I came to the States, many people helped me to prepare both in basic skills and mental maturity and I would like to thank them here. I especially thank my high school English teacher, Youngbok Jeong, and my mathematics teacher, Jooan Ok. I would like to thank violinist, Hwanam Park, for teaching me violin as well as many disciplines of life for five years. I would like to thank musician and audiovisual specialist Gaegeun Song for his teaching about music theory, audio, and showing me a role model of professionalism. I particularly thank Gaegeun Song and Geungi Park for their companionship to my father during my study here at Tech. I would like to thank my uncles-in-law Saewon Kim, M.D. who unfortunately passed away during my stay here, and Bonghoon Lee for they taught me many disciplines of life in ways no other people except for my parents could do more intimately. I also would like to thank Sookhee Hong, M.D. who delivered me into this world and showed me a spiritually positive way of life.

I also thank myself, that I was able to resist so many temptations in this country; jazz piano, radios, wines and whiskies. I would like to thank my brother Taicheol and sister Jinsook for their filial duties to my parents, for I know that should have been my duty. I am feeling really sorry for the life that my wife spent with me just in the hope of a better family life. I will repay her for all her patience and encouragement as time permits from now on. Also, I would like to thank my son, Junhyung, and daughter, Karen, for they provided me endless agony and intermittent happiness so that I would not lose the feeling of life. When I think of my father and mother, sorrow touches my heart more than any other feeling. For my survival up to this moment, no other human can be credited more than my mother and father who sacrificed their whole life for me. From now on, it is my turn to sacrifice for whatever they need.

Finally, I thank Jesus Christ who showed me that no human can be unfortunate.

Dedication

to

my father, *Bongryeol Park*

and

my mother, *Seonhee Kim Park*

who lacked the opportunity for higher education, but sacrificed their lives for me
so that I could grow in place of them

and

my wife, *Giyoung Kim Park*

who began to sacrifice her life ever since we met

TABLE OF CONTENTS

LIST OF FIGURES

LIST OF TABLES

Chapter 1. Introduction and Research Objective

Poly(3-hydroxybutyrate) (PHB) is a biodegradable polymer which has significance for possible commercial application in the fields of medical, agricultural, and disposable products. However, there are three main hindrances to these industrially attractive materials, even in these days of the Green Peace movement. One is its brittle mechanical properties, which supposedly come from thermally induced strain during the crystallization process. The toughness of PHB itself is very far from what is required by the standards of many packaging industries. Second, melt processing of PHB in the manufacture of films and bottles requires extrusion and blow molding processes, which require appreciable melt strength. PHB has low melt strength and degrades thermally just above its melting temperature. This trait is another discouraging factor against the successful application of this material on an industrial scale. Third, the crystallization rate of this material is very slow in the short term scale, which is comparable to the injection molding cycle time of conventional commodity polymers, thus lowering its productivity. In the long term scale, which is related to the shelf-life of the material, its highly regular chemical structure renders great ultimate extent of crystallization with a slow crystallization rate, and therefore requires careful attention in the quality control of PHB during the storage period.

The solution of the problems mentioned above may take several different approaches, such as copolymerization and blending of PHB with other toughening material. However, the ultimate success might come from the balance of many scientific and engineering endeavors, such as understanding mechanical properties, enhancing its melt strength with a smaller tendency toward thermal degradation, developing engineering techniques which process PHB with less thermal degradation, controlling its

crystallization rate for the specific melt process or discovering a totally new process which requires small capital.

No matter what type of approach is taken, the characterization of how much improvement has occurred, and why a specific attempt was successful is a natural curiosity to engineers and scientists, as well as capital investors.

As such, this study is focused on the characterization of the crystallization process of PHB over relatively long time, meaning days, weeks and months in order to attempt to correlate any engineering work on PHB with the relaxation behavior of PHB molecules at the conditions under which most commercial products might be stored. It is to be noted in the beginning that since long term behavior of crystalline material is far from ideal behavior which is predicted by theory, the approach of this study is purely phenomenological. If the time scale of the experiment is long, the uncertainty and unexpected error caused by many variables, whose influences to the final outcome are very hard to understand and predict, increase over time. This might be one possible excuse for many researchers who use the phenomenological approach to the problem.

The characterization tool of this study is dielectric relaxation analysis, based on the macroscopic theory of dielectric relaxation, together with the empiricism of temperature plane curve resolution and mean relaxation time analysis. Also, in the hope of predicting the relaxation behavior of binary blends of PHB with toughening components in future applications, empirical modeling work which is rooted in linear viscoelasticity theory has been attempted. Several computer programs were written and tested from scratch, notably using the Levenberg-Marquardt algorithm with constrained parameters. Also many phenomenological relaxation models currently used by many researchers in this field have been reviewed in a coherent manner with unified units and notations for the down-to-earth understanding of advantages and disadvantages of utilizing a specific relaxation model.

Chapter 2. Macroscopic Theory of Dielectric Relaxation

2.1 Basics

The dielectric relaxation behavior of polymer has been the subject of many academic fields including physics[1], electrical engineering[2] and polymer physical chemistry.[3] As various academic fields have been using different notations and unit systems, it may be worthwhile to define all terms which will be used in this study from the simple parallel plate capacitor, and to derive important equations in a coherent manner.

2.1.1 Capacitor

A capacitor[4] is a device for storing electric charge and it consists of two conducting objects placed near one another. A typical capacitor consists of a pair of parallel plates of area A separated by a small distance d as shown in Figure 1. If a potential V is applied to a capacitor, then the capacitor is charged. It is found that the amount of charge acquired by each plate is proportional to the potential V.

$$Q = CV \qquad \text{Eq.(2.1.1-1)}$$

The constant of proportionality, C, is called the capacitance of the capacitor. The unit of capacitance is coulombs per volt and this unit is called a Farad. The relation between electric field $\tilde{E}$ and potential V is given by

$$V_{ba} = -\int_a^b \tilde{E} \cdot d\tilde{l} \qquad \text{Eq.(2.1.1-2)}$$

where $\tilde{l}$ denotes the distance vector whose direction is from a to b.

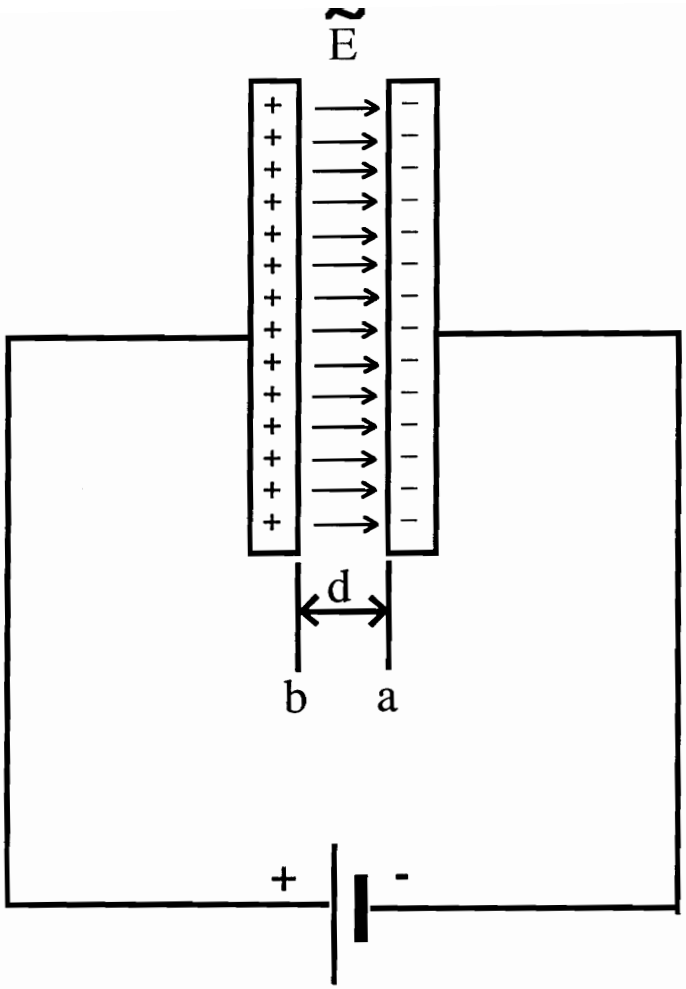

Figure 1. **Schematic: Parallel plate capacitor connected to a battery**

The electric field between two parallel plates is related to the surface charge density σ by Eq.(2.1.1-3).

$$E = \sigma / \varepsilon_0 \qquad \text{Eq.(2.1.1-3)}$$

Then Eq.(2.1.1-2) becomes

$$V = \int_a^b E\, dl = \frac{Q}{\varepsilon_0 A}\int_a^b dl = \frac{Qd}{\varepsilon_0 A} \qquad \text{Eq.(2.1.1-4)}$$

By comparison of Eq.(2.1.1-1) and Eq.(2.1.1-4), it follows

$$C_0 = \frac{Q}{V} = \varepsilon_0 \frac{A}{d} \qquad \text{Eq.(2.1.1-5)}$$

where the subscript zero denotes vacuum states and ε_0 is the permittivity of free space, ~8.85419×10^{-12} C^2/Nm^2. When dielectric material is inserted between the plates of the capacitor, the capacitance is increased by a factor ε, called the dielectric constant.

$$C = \varepsilon\varepsilon_0 \frac{A}{d} = \varepsilon_m \frac{A}{d} \qquad \text{Eq.(2.1.1-6)}$$

where ε_m is the permittivity of the dielectric and equals $\varepsilon\varepsilon_0$.

It is extremely important to pay attention to the fact that Eq.(2.1.1-1) holds whether or not potential is kept constant after dielectric material is placed in-between the capacitor. Suppose that a capacitor without dielectric material is charged with potential V_0 to accumulate charge Q_0. Then, before inserting the dielectric, the battery is disconnected. Now when the dielectric is inserted the charge Q_0 on each plate is unchanged. In this case, it is found that the potential decreases by a factor ε

$$V = \frac{V_0}{\varepsilon} \qquad \text{Eq.(2.1.1-7)}$$

Then, again the capacitance becomes

$$C = \frac{Q_0}{(V_0/\varepsilon)} = \varepsilon C_0$$

which is consistent with Eq.(2.1.1-1), Eq.(2.1.1-5) and Eq.(2.1.1-6).

The electric field within a parallel plate capacitor is altered due to the presence of dielectric. When no dielectric is present, the electric field between the plates of a parallel plate capacitor is given by

$$E_0 = \frac{V_0}{d} \qquad \text{Eq.(2.1.1-8)}$$

If the capacitor is isolated as before so that the charge remains fixed on the plates when a dielectric is inserted, the potential drops from V_0 to V_0/ε. Thus the electric field in the dielectric becomes

$$E = \frac{V_0}{\varepsilon d} \quad \text{or} \quad E = \frac{E_0}{\varepsilon} \qquad \text{Eq.(2.1.1-9)}$$

and the electric field within the dielectric is reduced by a factor equal to ε. This phenomenon may be explained in detail using the concept of "electric field lines" as follows.

Consider a capacitor whose plates are separated by an air gap as in Figure 2, (a). The capacitor is charged to have charge Q on both plates and then isolated. Now a dielectric is inserted between the plates as in Figure 2, (a). The dielectric material may be polar (with permanent dipole moment) or non polar (with an induced dipole moment). The electric field will exert a torque on the dipoles, tending to rotate them so they are parallel to the field. Thermal motion of the molecules will prevent perfect alignment of all dipoles but the greater the field, the better the alignment. The net effect is as if there were a net negative charge on the outer edge of the dielectric facing the positive plate, and a net positive charge on the opposite side as in Figure 2, (c). This is called induced charge. Because of this, some of the electric field lines do not pass through the dielectric

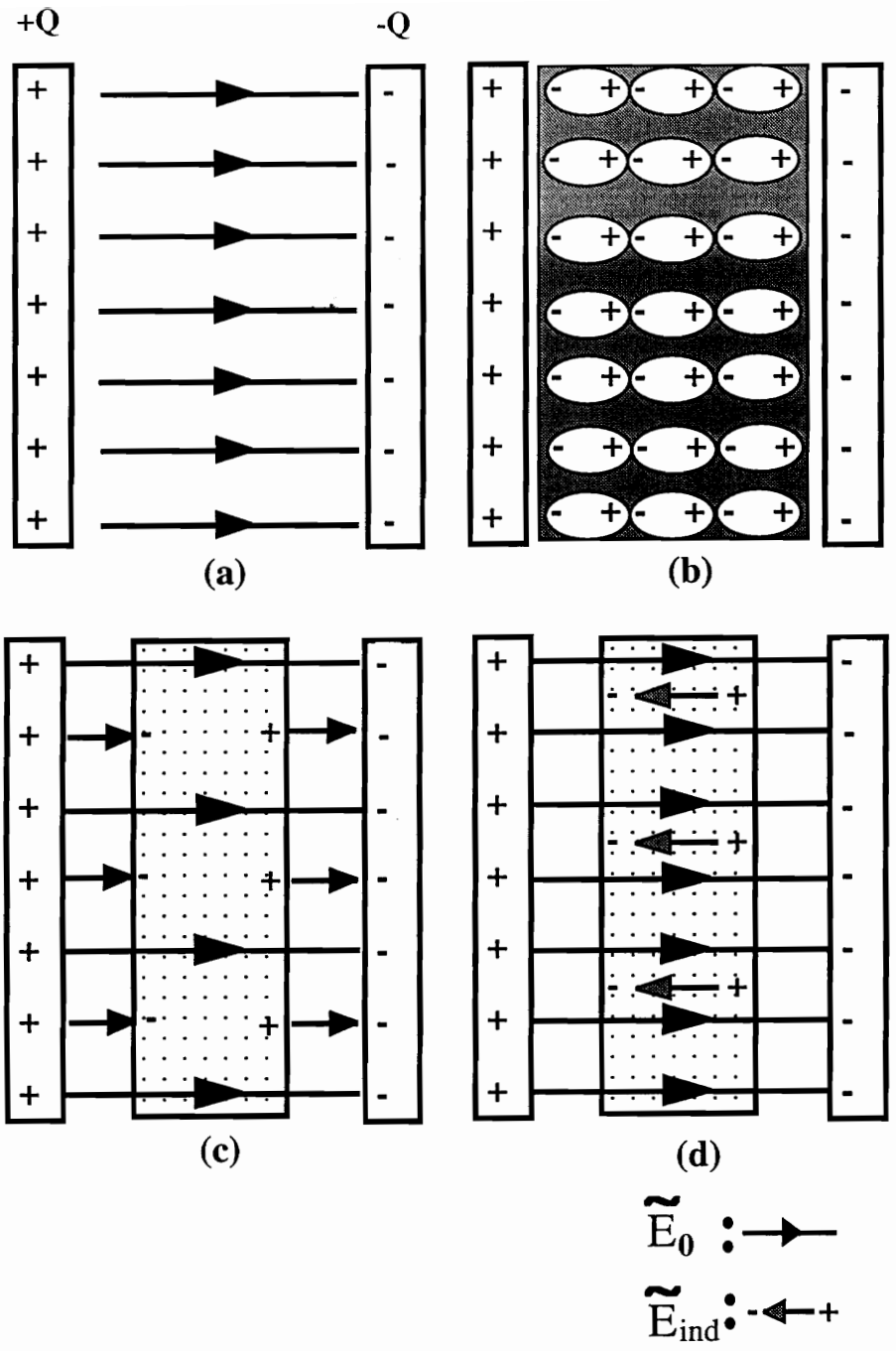

Figure 2. **Schematic: Molecular view of the effects of a dielectric on the electric field within a parallel plate capacitor**

hence the electric field within the dielectric is less than that in the air. The electric field within the dielectric can be considered as the vector sum of the electric field $\widetilde{E}_0$ due to the "free" charges, Q, on the conducting plates, and the field $\widetilde{E}_{ind}$ due to the "induced charge", Q_{ind}, on the dielectric. Since they are in opposite directions, the net field within the dielectric $\widetilde{E}_0 - \widetilde{E}_{ind}$ is less than $\widetilde{E}_0$ as shown in Figure 2, (d).

Using Eq.(2.1.1-9), the relationship between $\widetilde{E}_0$ and $\widetilde{E}_{ind}$ is obtained in terms of the dielectric constant ε.

$$\widetilde{E} = \widetilde{E}_0 - \widetilde{E}_{ind} = \frac{\widetilde{E}_0}{\varepsilon}$$

or

$$\widetilde{E}_{ind} = \widetilde{E}_0 \left(1 - \frac{1}{\varepsilon}\right) \qquad \text{Eq.(2.1.1-10)}$$

From the relationship of surface charge density and electric field as in Eq.(2.1.1-3), electric fields due to free and induced charge can be expressed in terms of respective charges.

$$E_0 = \frac{\sigma}{\varepsilon_0} = \frac{Q}{\varepsilon_0 A}$$

$$E_{ind} = \frac{\sigma_{ind}}{\varepsilon_0} = \frac{Q_{ind}}{\varepsilon_0 A} \qquad \text{Eq.(2.1.1-11)}$$

Induced charge is often called "bound charge" since it is on the surface of an insulator and it is not free to move as the electrons in a conductor are. From Eq.(2.1.1-10) and Eq.(2.1.1-11), the relationship between $\widetilde{E}_0$ and $\widetilde{E}_{ind}$ can be written in terms of the dielectric constant.

$$\frac{E_{ind}}{E_0} = \frac{\sigma_{ind}}{\sigma} = \frac{Q_{ind}}{Q} = 1 - \frac{1}{\varepsilon} \qquad \text{Eq.(2.1.1-12)}$$

The concept of induced charge as established so far is useful in defining electric displacement $\widetilde{D}$ from which a governing equation of linear dielectric relaxation is easily developed.

2.1.2 Polarization and Electric Displacement

Consider a parallel plate capacitor completely filled with a dielectric as shown in Figure 3 (a). It is assumed that the plates are large (of area A) compared to the separation d so that $\widetilde{E}$ is uniform and perpendicular to the plates. For a Gaussian surface, the long rectangular box indicated by the dashed lines, which just barely reaches into the dielectric is chosen. The surface encloses both the free charge Q on the conductor and the induced bound charge Q_{ind} on the dielectric.

Then Gauss' law may be written for this surface as

$$\int_s \widetilde{E} \cdot d\widetilde{A} = \frac{Q - Q_{ind}}{\varepsilon_0} \qquad \text{Eq.(2.1.2-1)}$$

With Eq.(2.1.1-10) and Eq.(2.1.1-12), this is further reduced to

$$\int_s \widetilde{E} \cdot d\widetilde{A} = \frac{Q}{\varepsilon\, \varepsilon_0} \qquad \text{Eq.(2.1.2-2)}$$

The left hand side of Eq.(2.1.2-2) can be decomposed into six terms arising from six Gaussian surfaces as in Figure 3, (b). The terms arising from the four surfaces which are parallel with the electric field becomes null because of the orthogonality of $d\widetilde{A}$ and $\widetilde{E}$. Also, in the conductor side surface, there exists no electric field (no electric field within the conductor). Only the surface which faces the dielectric has an electric field $\widetilde{E}$. Then Eq.(2.1.2-2) becomes

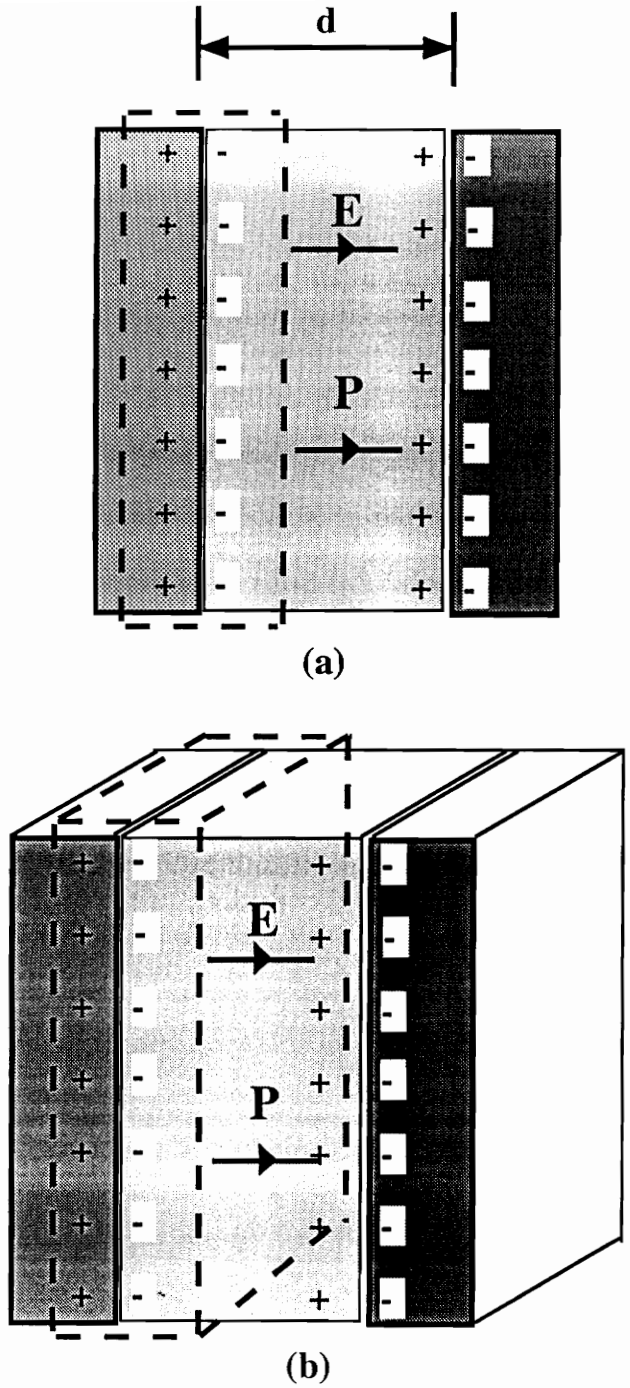

Figure 3. **Schematic: Gaussian surface for the parallel plate capacitor**

$$EA = \frac{Q}{\varepsilon \varepsilon_0} \qquad \text{Eq.(2.1.2-3)}$$

The dielectric between the plates in Figure 3, (a) has a dipole moment whose magnitude is $Q_{ind}d$. For this dielectric material, the polarization vector P is defined as the dipole moment per unit volume with scalar magnitude as

$$P = \frac{Q_{ind}d}{Ad} = \frac{Q_{ind}}{A} = \sigma_{ind} \qquad \text{Eq.(2.1.2-4)}$$

Thus polarization P represents the induced bound charge. The polarization vector P points from negative to positive induced charge (as usually defined in dipole moment). With the same argument used in the evaluation of the surface integral of Eq.(2.1.2-3), it follows

$$\int_s \tilde{P} \cdot d\tilde{A} = PA = Q_{ind} \qquad \text{Eq.(2.1.2-5)}$$

where the last part of Eq.(2.1.2-5) comes from Eq.(2.1.2-4).

Combining Eq.(2.1.2-5) and Eq.(2.1.2-1) gives

$$\int_s \tilde{E} \cdot d\tilde{A} = \frac{Q}{\varepsilon_0} - \frac{1}{\varepsilon_0}\int_s \tilde{P} \cdot d\tilde{A}$$

or

$$\int_s (\varepsilon_0 \tilde{E} + \tilde{P}) \cdot d\tilde{A} = Q \qquad \text{Eq.(2.1.2-6)}$$

Eq.(2.1.2-6) is a general expression of Gauss' law when a dielectric is present in-between the capacitor. Now if a new vector electric displacement $\tilde{D}$ is defined as

$$\tilde{D} = \varepsilon_0 \tilde{E} + \tilde{P} \qquad \text{Eq.(2.1.2-7)}$$

Then Gauss' law becomes

$$\int_S \tilde{D} \cdot d\tilde{A} = Q \qquad \text{Eq.(2.1.2-8)}$$

From Eq.(2.1.2-8), it is easily seen that $\tilde{D}$ is associated with free charge only whereas $\tilde{E}$ is associated with all charges as seen in Eq.(2.1.2-1) and $\tilde{P}$ is associated with bound charges as in Eq.(2.1.2-4). Eq.(2.1.2-7) signifies that the study of $\tilde{D}$ in relation with $\tilde{E}$ may yield the polarization behavior of dielectric material. In order to see this point more clearly, comparison of Eq.(2.1.2-2) and Eq.(2.1.2-8) gives

$$\tilde{D} = \varepsilon \varepsilon_0 \tilde{E} \qquad \text{Eq.(2.1.2-9)}$$

While Eq.(2.1.2-7) does not contain the dielectric constant ε, Eq.(2.1.2-9) explicitly does . Thus, it follows naturally that the dielectric constant ε encompasses polarization P.

It is worthwhile to note that Eq.(2.1.2-9) is derived under a static electric field without any system dynamics of dielectric material. However, if the dielectric is purely elastic in polarization, it is also valid for an oscillating field. When dielectric material possesses viscoelasticity and the electric field is oscillating sinusoidally as in Eq.(2.1.2-10), electric displacement would occur with a phase difference of a certain phase angle δ.

$$E = E_0 \cos \omega t \qquad \text{Eq.(2.1.2-10)}$$

$$D = D_0 \cos (\omega t - \delta)$$

$$= D_0 \cos \delta \cos \omega t + D_0 \sin \delta \sin \omega t \qquad \text{Eq.(2.1.2-11)}$$

In Eq.(2.1.2-11), electric displacement is composed of two terms, one which is in phase with the field and the other out of phase by π/2 radians. The ratio of the magnitude of D which is out of phase to that which is in phase is conveniently expressed using δ.

$$\frac{D_0 \sin \delta}{D_0 \cos \delta} = \tan \delta \qquad \text{Eq.(2.1.2-12)}$$

In order to relate δ to the dielectric constant ε and exploit the simple form of Eq.(2.1.2-9), the complex form of D, E, and ε namely D^*, E^*, and ε^* have been found useful as follows.

$$D^* = \varepsilon^* \varepsilon_0 E^*$$

$$\varepsilon^* = \frac{D^*}{\varepsilon_0 E^*} = \frac{D_0 e^{i(\omega t - \delta)}}{\varepsilon_0 E_0 e^{i\omega t}} = \varepsilon' - i\varepsilon''$$

where

$$\varepsilon' = \frac{D_0 \cos \delta}{\varepsilon_0 E_0} \quad , \quad \varepsilon'' = \frac{D_0 \sin \delta}{\varepsilon_0 E_0} \qquad \text{Eq.(2.1.2-13)}$$

Eq.(2.1.2-13) is correct with respect to units, and moreover, the ratio $\varepsilon''/\varepsilon'$ gives phase difference information δ as

$$\frac{\varepsilon''}{\varepsilon'} = \tan \delta \qquad \text{Eq.(2.1.2-14)}$$

This outcome justifies the direct use of complex forms in the equations developed so far. The reason why complex forms are utilized in the study of dielectric relaxation or generally in linear viscoelastic theory is the same as in the case of solving ordinary linear differential equations using complex variables. This convenient formalism is valid only when the system to be solved is linear.

2.1.3 Boltzmann's Superposition Principle

In order to formulate dielectric relaxation behavior phenomenologically, Boltzmann's superposition principle is necessary. It states that the viscoelastic property at any time t is a linear superposition of past perturbations. There certainly exists a limit in

the magnitude of perturbation for this to be true and the following discussion is made within this limit. The concept of a normalized time decaying function $\Phi(t)$ plays a key role in developing general linear viscoelastic theory in which dielectric relaxation study occupies a small niche. Also, it is possible to define a normalized function $\Psi(t)$ which increases over time in such a manner that the sum of $\Phi(t)$ and $\Psi(t)$ at any time t always equals one as shown in Figure 4.

$$\Phi(t) + \Psi(t) = 1$$
$$\Phi(t) = 1\,, \quad \Psi(t) = 0 \quad \text{for} \quad t = 0 \qquad \text{Eq.(2.1.3-1)}$$
$$\Phi(t) = 0\,, \quad \Psi(t) = 1 \quad \text{for} \quad t = \infty$$

When a static electric field E_0 is applied to a dielectric, electric displacement D(t) at any time t may be expressed in terms of $\Psi(t)$ as follows.

$$D(t) = \varepsilon_0 [\varepsilon_\infty + (\varepsilon_s - \varepsilon_\infty) \Psi(t)] E_0 \qquad \text{Eq.(2.1.3-2)}$$

where ε_∞ is the unrelaxed (high frequency) dielectric constant and ε_s is the relaxed (low frequency) dielectric constant. According to Boltzmann's superposition principle , if extra field is added at time $t = t_1$, the total electric displacement at times $t > t_1$ would be

$$D(t) = \varepsilon_0 [\varepsilon_\infty + (\varepsilon_s - \varepsilon_\infty) \Psi(t)] E_0 + \varepsilon_0 [\varepsilon_\infty + (\varepsilon_s - \varepsilon_\infty) \Psi(t - t_1)] E(t_1)$$

where E_0 may be interpreted as E(0).

In general, for a series of field increments, electric displacement becomes

$$D(t) = \sum_{t_i = -\infty}^{t_i = t} \varepsilon_0 [\varepsilon_\infty + (\varepsilon_s - \varepsilon_\infty) \Psi(t - t_i)] E(t_i) \qquad \text{Eq.(2.1.3-3)}$$

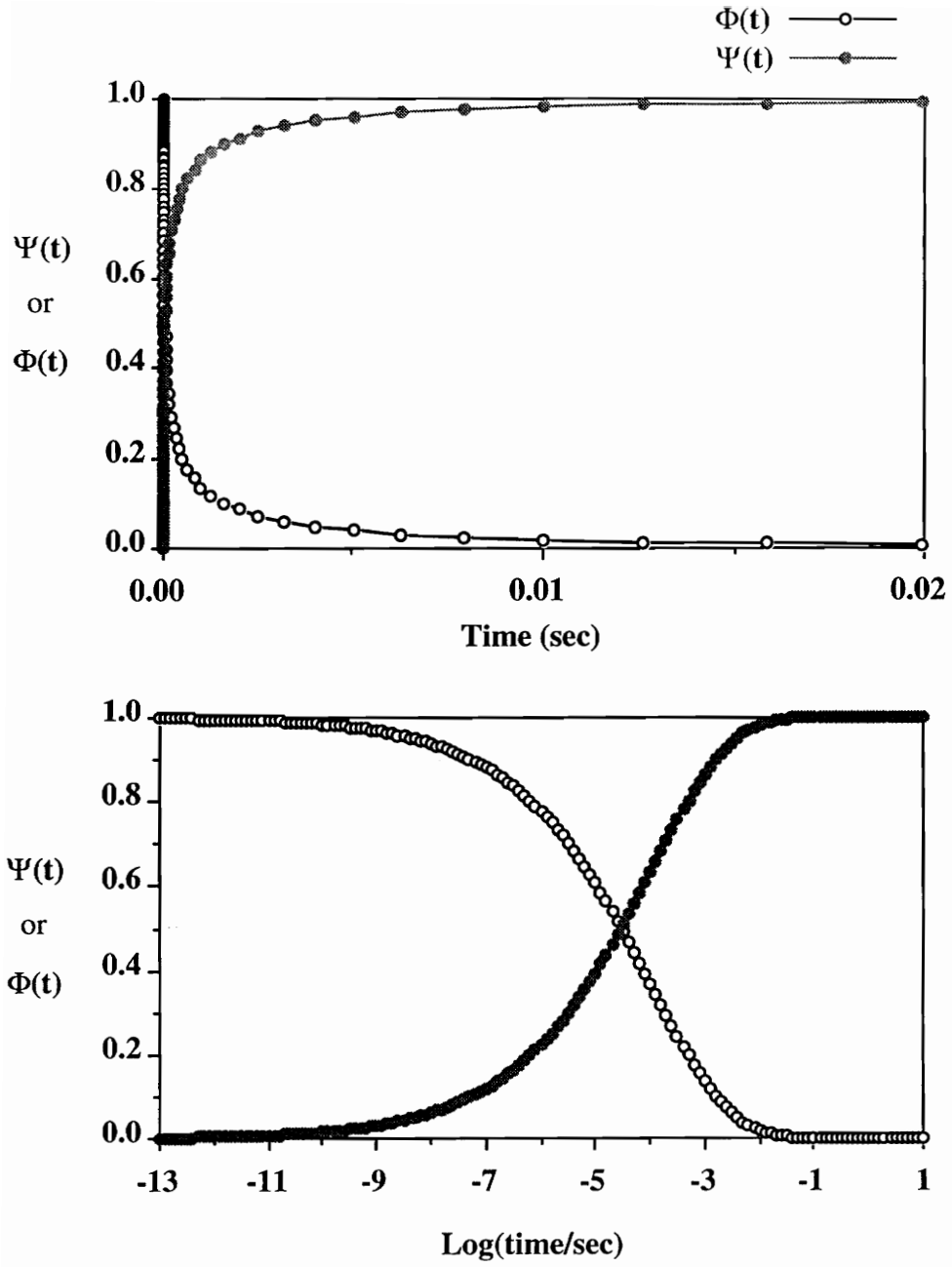

Figure 4. **Normalized relaxation function $\Psi(t)$ and time decaying function $\Phi(t)$, example when $\tau = 10^{-4}$**

For a continuously varying field, Eq.(2.1.3-3) may be integrated over t_i with the condition $E(-\infty) = 0$.

$$D(t) = \varepsilon_0 \varepsilon_\infty E(t) + \varepsilon_0 (\varepsilon_s - \varepsilon_\infty) \int_{-\infty}^{t} \Psi(t - s) \frac{\partial E(s)}{\partial s} ds \qquad \text{Eq.(2.1.3-4)}$$

The second term on the right hand side of Eq.(2.1.3-4) can be further integrated by parts.

$$\int_{-\infty}^{t} \Psi(t - s) \frac{\partial E(s)}{\partial s} ds = [\Psi(t - s)E(s)]_{-\infty}^{t} - \int_{-\infty}^{t} \frac{\partial \Psi(t - s)}{\partial s} E(s)\, ds$$

$$= + \int_{-\infty}^{t} \frac{\partial \Psi(t - s)}{\partial (t - s)} E(s)\, ds \qquad = \int_{-\infty}^{t} \alpha(t-s)\, E(s)\, ds$$

where $\alpha(k)$ is defined as

$$\alpha(k) = \frac{d\Psi(k)}{dk}$$

Then Eq.(2.1.3-4) becomes

$$D(t) = \varepsilon_0 \varepsilon_\infty E(t) + \varepsilon_0 (\varepsilon_s - \varepsilon_\infty) \int_{-\infty}^{t} \alpha(t - s)\ E(s)\, ds \qquad \text{Eq.(2.1.3-5)}$$

By making the substitution $t - s = x$ with proper limits, D(t) may be rewritten once more

$$D(t) = \varepsilon_0 \varepsilon_\infty E(t) + \varepsilon_0 (\varepsilon_s - \varepsilon_\infty) \int_{0}^{\infty} \alpha(x)\ E(t-x)\, dx \qquad \text{Eq.(2.1.3-6)}$$

Eq.(2.1.3-6) is the master equation from which single relaxation, and multiple relaxation by the linear superposition of single relaxation under static and dynamic electric fields can be modeled. When the electric field is oscillating, Eq.(2.1.3-6) together with $E^*(t) = E_0 e^{-i\omega t}$ becomes

$$D^*(t) = \varepsilon_0 \varepsilon_\infty E^*(t) + \varepsilon_0 (\varepsilon_s - \varepsilon_\infty) E^*(t) \int_0^\infty e^{-i\omega x} \alpha(x)\, dx \qquad \text{Eq.(2.1.3-7)}$$

Dividing Eq.(2.1.3-7) by $\varepsilon_0 E^*(t)$ yields

$$\varepsilon^*(t) = \frac{D^*(t)}{\varepsilon_0 E^*(t)} = \varepsilon_\infty + (\varepsilon_s - \varepsilon_\infty) \int_0^\infty e^{-i\omega x} \alpha(x)\, dx \qquad \text{Eq.(2.1.3-8)}$$

Rearranging and exchanging the dummy variable x with t, Eq.(2.1.3-8) becomes

$$\frac{\varepsilon^* - \varepsilon_\infty}{\varepsilon_s - \varepsilon_\infty} = \int_0^\infty e^{-i\omega t} \left[- \frac{d\Phi(t)}{dt} \right] dt \qquad \text{Eq.(2.1.3-9)}$$

since

$$\alpha(t) = \frac{d\Psi(t)}{dt} = - \frac{d\Phi(t)}{dt}$$

This equation may be called the master equation for the dynamic dielectric experiment. There are several different forms of Eq.(2.1.3-9). For example, integrating the right hand side of Eq.(2.1.3-9) by parts yields

$$\frac{\varepsilon^* - \varepsilon_\infty}{\varepsilon_s - \varepsilon_\infty} = 1 - (i\omega) \int_0^\infty e^{-i\omega t} \Phi(t)\, dt \qquad \text{Eq.(2.1.3-10)}$$

Also, Eq.(2.1.3-9) can be expanded to give the real and imaginary parts specifically as below

$$\frac{\varepsilon'(\omega) - \varepsilon_\infty}{\varepsilon_s - \varepsilon_\infty} = \int_0^\infty \cos \omega t \left[- \frac{d\Phi(t)}{dt} \right] dt \qquad \text{Eq.(2.1.3-11)}$$

$$\frac{\varepsilon''(\omega)}{\varepsilon_s - \varepsilon_\infty} = \int_0^\infty \sin \omega t \left[- \frac{d\Phi(t)}{dt} \right] dt \qquad \text{Eq.(2.1.3-12)}$$

These last two equations show the very important fact that $\varepsilon'(\omega)$ is the even function of ω and $\varepsilon''(\omega)$ is the odd function of ω. This becomes the basis for deriving the Fourier transform pairs involving $\varepsilon'(\omega)$ and $\varepsilon''(\omega)$

2.1.4 Fourier Transform

The experimental study of dielectric relaxation often starts either with the collection of $\varepsilon'(\omega)$ and $\varepsilon''(\omega)$ or $\Phi(t)$ data. If one starts from the time decaying function, $\Phi(t)$, the derivative of it together with Eq.(2.1.3-11) and Eq.(2.1.3-12) will yield the information about normalized dielectric constants. On the other hand, if one starts from collecting $\varepsilon'(\omega)$ and $\varepsilon''(\omega)$, the Fourier transforms of Eq.(2.1.3-11) and Eq.(2.1.3-12) are required in order to get the time decaying function $\Phi(t)$.

Fourier transform pairs[5] may be written as

$$f(t) = \int_{-\infty}^{\infty} g(\omega) e^{i\omega t} d\omega \qquad \text{Eq.(2.1.4-1)}$$

$$g(\omega) = \frac{1}{2\pi} \int_{-\infty}^{\infty} f(t) e^{-i\omega t} dt. \qquad \text{Eq.(2.1.4-2)}$$

Sometimes it is found that the conversion factor $1/2\pi$ is distributed symmetrically between the transform and the inversion. It does not matter as long as the product of the conversion factors of the transform and inversion equals $1/2\pi$. In order to exploit the even or odd character of functions to be Fourier transformed, the above pair of equations needs some manipulation. Changing the dummy variable ω in Eq.(2.1.4-1) to τ and substituting it into Eq.(2.1.4-2) gives

$$g(\omega) = \frac{1}{2\pi}\int_{-\infty}^{\infty}\int_{-\infty}^{\infty} g(\tau)e^{it(\tau-\omega)}dt$$

$$= \frac{1}{2\pi}\int_{-\infty}^{\infty}\int_{-\infty}^{\infty} g(\tau)\cos t(\tau-\omega)d\tau dt + \frac{i}{2\pi}\int_{-\infty}^{\infty}\int_{-\infty}^{\infty} g(\tau)\sin t(\tau-\omega)d\tau dt \qquad \text{Eq.(2.1.4-3)}$$

The fact that sin $t(\tau-\omega)$ is an odd function of t makes the second integral always zero and indeed this must be the case since $g(\omega)$ is purely real. Then

$$g(\omega) = \frac{1}{2\pi}\int_{-\infty}^{\infty}\int_{-\infty}^{\infty} g(\tau)\cos t(\tau-\omega)d\tau dt \qquad \text{Eq.(2.1.4-4)}$$

Since the integrand of Eq.(2.1.4-4) is an even function of t, the integration limit of t may be changed.

$$g(\omega) = \frac{1}{\pi}\int_{0}^{\infty}\int_{-\infty}^{\infty} g(\tau)\cos t(\tau-\omega)d\tau dt \qquad \text{Eq.(2.1.4-5)}$$

Depending on whether $g(\omega)$ is an odd or even function, further simplifications are possible. In order to see this more clearly, first expand the cosine term in the integrand of Eq.(2.1.4-5), and then rewrite the integration limit of τ.

$$g(\omega) = \frac{1}{\pi}\int_{0}^{\infty}\left[\int_{-\infty}^{0} g(\tau)\cos t\tau\cos t\omega d\tau + \int_{0}^{\infty} g(\tau)\cos t\tau\cos t\omega d\tau\right]dt$$

$$+ \frac{1}{\pi}\int_{0}^{\infty}\left[\int_{-\infty}^{0} g(\tau)\sin t\tau\sin t\omega d\tau + \int_{0}^{\infty} g(\tau)\sin t\tau\sin t\omega d\tau\right]dt$$

Next, the partial substitution $t = -z$ with the proper limit gives

$$g(\omega) = \frac{1}{\pi}\int_0^{\infty} [\int_{-\infty}^{0} g(-z)\cos(-tz)\cos t\omega\,(-dz) + \int_0^{\infty} g(\tau)\cos t\tau \cos t\omega d\tau]dt \qquad \text{Eq.(2.1.4-6)}$$

$$+\frac{1}{\pi}\int_0^{\infty} [\int_{-\infty}^{0} g(-z)\sin(-tz)\sin t\omega(-dz) + \int_0^{\infty} g(\tau)\sin t\tau \sin t\omega d\tau]dt$$

If $g(\tau)$ is an even function, the two inner integrals in the first term in Eq.(2.1.4-6) become identical. Similarly, the two inner integrals in the second term turn out to be negatives of each other. Hence

$$g(\omega) = \frac{2}{\pi}\int_0^{\infty}\int_0^{\infty} g(\tau)\cos(t\tau)\cos(t\omega)\,d\tau dt \qquad ; g(\omega) \text{ even} \qquad \text{Eq.(2.1.4-7)}$$

If $g(\omega)$ is an odd function, then the two inner integrals in the first term in Eq.(2.1.4-6) are negatives of each other and the inner integrals in the second term are equal. Hence

$$g(\omega) = \frac{2}{\pi}\int_0^{\infty}\int_0^{\infty} g(\tau)\sin(t\tau)\sin(t\omega)\,d\tau dt \qquad ; g(\omega) \text{ odd} \qquad \text{Eq.(2.1.4-8)}$$

Eq.(2.1.4-7) and Eq.(2.1.4-8) can be viewed in terms of transform pairs defined as follows.

When $g(\omega)$ is even:

$$g(\omega) = \int_0^{\infty} f(t)\cos\omega t\,dt$$

$$f(t) = \frac{2}{\pi}\int_0^{\infty} g(\tau)\cos(t\tau)\,d\tau = \frac{2}{\pi}\int_0^{\infty} g(\omega)\cos(\omega t)\,d\omega \qquad \text{Eq.(2.1.4-9)}$$

When $g(\omega)$ is odd:

$$g(\omega) = \int_0^{\infty} f(t)\sin\omega t\,dt$$

$$f(t) = \frac{2}{\pi}\int_0^{\infty} g(\tau)\sin(t\tau)\,d\tau = \frac{2}{\pi}\int_0^{\infty} g(\omega)\sin(\omega t)\,d\omega \qquad \text{Eq.(2.1.4-10)}$$

The final results of the previous sections, Eq.(2.1.3-11) and Eq.(2.1.3-12), show that $\varepsilon'(\omega)$ is an even function of ω and $\varepsilon''(\omega)$ is an odd function of ω. By identifying $g(\omega)$ as

$$\frac{\varepsilon'(\omega)-\varepsilon_\infty}{\varepsilon_s-\varepsilon_\infty}$$

and $f(t)$ as

$$-\frac{d\Phi(t)}{dt}$$

and utilizing Eq.(2.1.4-9), since $\varepsilon'(\omega)$, and consequently $g(\omega)$, is an even function, it follows that

$$-\frac{d\Phi(t)}{dt} = \frac{2}{\pi}\int_0^{\infty} \left(\frac{\varepsilon'(\omega)-\varepsilon_\infty}{\varepsilon_s-\varepsilon_\infty}\right)\cos\omega t\,d\omega \qquad \text{Eq.(2.1.4-11)}$$

In the same manner for $\varepsilon''(\omega)$, it is deduced that

$$-\frac{d\Phi(t)}{dt} = \frac{2}{\pi}\int_0^{\infty} \left(\frac{\varepsilon''(\omega)}{\varepsilon_s-\varepsilon_\infty}\right)\sin\omega t\,d\omega \qquad \text{Eq.(2.1.4-12)}$$

For expressions explicitly in terms of $\Phi(t)$, integration of Eq.(2.1.4-11) and Eq.(2.1.4-12) yields Eq.(2.1.4-13) and Eq.(2.1.4-14) respectively.

$$\Phi(t) = \frac{2}{\pi}\int_0^{\infty} \left(\frac{\varepsilon_\infty-\varepsilon'(\omega)}{\varepsilon_s-\varepsilon_\infty}\right)\frac{\sin\omega t}{\omega}\,d\omega \qquad \text{Eq.(2.1.4-13)}$$

$$\Phi(t) = \frac{2}{\pi}\int_0^{\infty} \left(\frac{\varepsilon''(\omega)}{\varepsilon_s-\varepsilon_\infty}\right)\frac{\cos\omega t}{\omega}\,d\omega \qquad \text{Eq.(2.1.4-14)}$$

It is to be noted that Eq.(2.1.4-13) fails when t equals zero. Thus, it is easy to see that the condition of the above transform is that t be positive. Using Eq.(2.1.4-14), the time decaying function $\Phi(t)$ can be obtained from a half sided, or one sided, cosine transform of normalized dielectric loss data. Of course, Eq.(2.1.4-13) may be used for this purpose. However, in this case, there is one more parameter ε_∞ which must be known explicitly from experiment. Thus Eq.(2.1.4-14) is preferred for practical purpose.

2.1.5 Kramers-Kronig Relation

Any physical property X which satisfies the relation

$$X(i\omega) = \int_0^\infty e^{-i\omega t} Y(t)\, dt \qquad \text{Eq.(2.1.5-1)}$$

where Y(t) is a response function in the time domain having the properties

i) $Y(t) = 0 \quad \text{for} \quad t < 0$

ii) $\lim_{t \to \infty} Y(t) = 0$

iii) $\int_0^\infty Y(t)\, dt$ is finite

obeys Kramers-Kronig relation.[6] This relation states that the knowledge of one part (real or imaginary) of a complex property X permits the knowledge of the other. From Eq.(2.1.3-9), it is readily seen that the normalized complex dielectric constant obeys the Kramers-Kronig relation. Rigorous proof of the Kramers-Kronig relation which utilizes contour integration in the complex plane of frequency can be found readily.[7, 8] Rather simple proof may be borrowed to illustrate this relation as follows.[9]

Substitution of Eq.(2.1.4-12) into Eq.(2.1.3-11) gives

$$\frac{\varepsilon'(\omega)-\varepsilon_\infty}{\varepsilon_S-\varepsilon_\infty} = \int_0^\infty \cos\omega t \left[\frac{2}{\pi} \int_0^\infty \left(\frac{\varepsilon''(\nu)}{\varepsilon_S-\varepsilon_\infty}\right) \sin\nu t \, d\nu \right] dt \qquad \text{Eq.(2.1.5-2)}$$

$$= \frac{2}{\pi} \int_0^\infty \frac{\varepsilon''(\nu)}{\varepsilon_S-\varepsilon_\infty} \, d\nu \int_0^\infty \cos\omega t \sin\nu t \, dt$$

The integrals containing the product of cosine and sine term may be expanded into the sum of two sine terms and then integrated with respect to t as

$$= \frac{2}{\pi} \int_0^\infty \frac{\varepsilon''(\nu)}{\varepsilon_S-\varepsilon_\infty} \, d\nu \, \frac{1}{2}\left[\frac{-\cos(\omega+\nu)t}{\omega+\nu} + \frac{\cos(\omega-\nu)t}{\omega-\nu}\right]_0^\infty$$

$$= \frac{2}{\pi} \lim_{R\to\infty} \int_0^\infty \frac{\varepsilon''(\nu)}{\varepsilon_S-\varepsilon_\infty} \, d\nu \, \frac{1}{2}\left[\frac{-\cos(\omega+\nu)t}{\omega+\nu} + \frac{\cos(\omega-\nu)t}{\omega-\nu}\right]_0^R$$

$$= \frac{2}{\pi} \lim_{R\to\infty} \int_0^\infty \frac{\varepsilon''(\nu)}{\varepsilon_S-\varepsilon_\infty} \, \frac{1}{2}\left[\left(\frac{-\cos R(\omega+\nu)}{\omega+\nu} + \frac{\cos R(\omega-\nu)}{\omega-\nu}\right) - \left(\frac{-1}{\omega+\nu} + \frac{1}{\omega-\nu}\right)\right] d\nu$$

At this moment, it would be convenient to assess the effect of the following function on the final integration result.

$$\left(\frac{-\cos R(\omega+\nu)}{\omega+\nu} + \frac{\cos R(\omega-\nu)}{\omega-\nu}\right) \qquad \text{namely} \qquad -\left(\frac{\cos R(\nu+\omega)}{\nu+\omega} + \frac{\cos R(\nu-\omega)}{\nu-\omega}\right)$$

since cosine is an even function of ν.

This effect is easily illustrated with the function $f(\nu)$ defined as

$$f(\nu) = \frac{\cos R(\nu+c)}{\nu+c}$$

where c is a constant ω or $-\omega$ in the ν domain.

The function f(ν) multiplied by a continuous non-oscillating function of ν, namely $\varepsilon''(\nu)$, behaves in the ν domain schematically as shown in Figure 5. The property $\varepsilon''(0) = 0$ and the decreasing amplitude of f(ν) are the guide lines for the drawing. In Figure 5, it is easily seen that as R increases to infinity, the positive area rapidly cancels the negative area signifying that the contribution of cosine terms in the integration is null since R in f(ν) corresponds to angular frequency in the ν domain with period $T = 2\pi / R$.

As such, with

$$-\left(\frac{-1}{\omega + \nu} + \frac{1}{\omega - \nu}\right) = \frac{\nu}{\nu^2 - \omega^2}$$

Eq.(2.1.5-2) becomes

$$\frac{\varepsilon'(\omega)-\varepsilon_\infty}{\varepsilon_s-\varepsilon_\infty} = \frac{2}{\pi}\int_0^\infty \left(\frac{\varepsilon''(\nu)}{\varepsilon_s-\varepsilon_\infty}\right)\frac{\nu}{\nu^2 - \omega^2}d\nu \qquad \text{Eq.(2.1.5-3)}$$

From Eq.(2.1.5-3), it is obvious that the knowledge of $\varepsilon''(\omega)$ automatically determines that of $\varepsilon'(\omega)$, which is the Kramers-Kronig relation as stated in the beginning of this section.

2.1.6 Single and Multiple Relaxation Model

Based on the Boltzmann's superposition principle, two important models, single and multiple relaxation models can be formulated. The single relaxation model has special meaning in that Debye derived the same form from a molecular level model.[10] For polymeric systems, this model is hard to rationalize because of the broad relaxation range of polymers, which at the very least excludes the possibility of a single relaxation mechanism. As will be discussed in detail in subsequent chapters, there might be many causes for this behavior. Leaving alone the exact causes of broad relaxation, it is to be

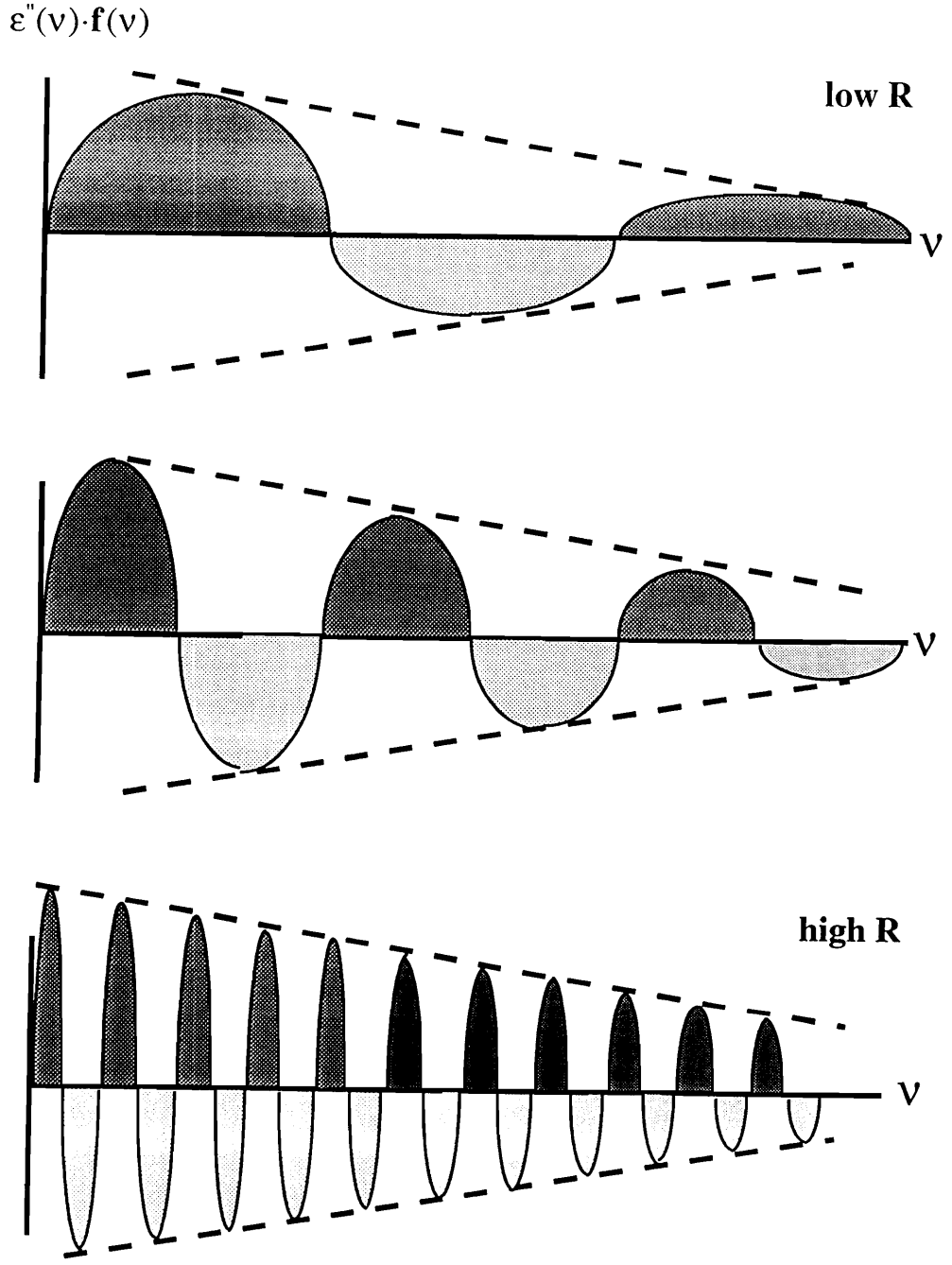

Figure 5. **Schematic: Behavior of $\varepsilon''(\nu)\cdot f(\nu)$ with increasing R**

noted that a multiple relaxation model can assimilate the broad relaxation behavior of polymeric systems quite successfully. The formalism of the multiple relaxation model is based on the linear combination of the single relaxation model.

For the single relaxation model, the time decaying function is

$$\Phi(t) = e^{-t/\tau} \qquad \text{Eq.(2.1.6-1)}$$

where τ is relaxation time.

Substitution of Eq.(2.1.6-1) into Eq.(2.1.3-9) followed by integration with respect to t gives

$$\frac{\varepsilon^* - \varepsilon_\infty}{\varepsilon_s - \varepsilon_\infty} = \frac{1}{1 + i\omega\tau} \qquad \text{Eq.(2.1.6-2)}$$

Separation of the real and imaginary parts of Eq.(2.1.6-2) results in the following equations which may be used in fitting experimental data to evaluate relaxation time.

$$\frac{\varepsilon'(\omega) - \varepsilon_\infty}{\varepsilon_s - \varepsilon_\infty} = \frac{1}{1 + \omega^2\tau^2} \quad , \quad \frac{\varepsilon''(\omega)}{\varepsilon_s - \varepsilon_\infty} = \frac{\omega\tau}{1 + \omega^2\tau^2} \quad , \quad \tan\delta = \frac{\varepsilon''}{\varepsilon'} = \frac{(\varepsilon_s - \varepsilon_\infty)\omega\tau}{\varepsilon_s + \varepsilon_\infty\omega^2\tau^2}$$

This result is identical to Debye equations in the form if τ is replaced with what Debye defined originally.

The time decaying function of the multiple relaxation model is the linear summation of the time decaying function of the single relaxation model. Then

$$\Phi(t) = \sum_i A(\tau_i) e^{-t/\tau_i} \qquad \text{Eq.(2.1.6-3)}$$

where $A(\tau_i)$ is the fraction of single relaxation mechanism with relaxation time τ_i.

In continuous form, Eq.(2.1.6-3) becomes

$$\Phi(t) = \int_0^\infty \rho(\tau) e^{-t/\tau}\, d\tau \qquad \text{Eq.(2.1.6-4)}$$

and the time derivative of it is

$$-\frac{d\Phi(t)}{dt} = \int_0^\infty \frac{\rho(\tau)}{\tau} e^{-t/\tau}\, d\tau \qquad \text{Eq.(2.1.6-5)}$$

where $\rho(\tau)$ is the distribution function of relaxation time which satisfies the normalization condition

$$\int_0^\infty \rho(\tau) d\tau = 1$$

Also by changing variables with $\chi = 1/\tau$, it is easily seen that Eq.(2.1.6-4) is the Laplace transform

$$\Phi(t) = \int_0^\infty \frac{\rho(1/\chi)}{\chi^2} e^{-t\chi}\, d\chi = \mathcal{L}\left(\frac{\rho(1/\chi)}{\chi^2}\right)$$

Substitution of Eq.(2.1.6-5) into Eq.(2.1.3-9) followed by integration with respect to t yields

$$\frac{\varepsilon^* - \varepsilon_\infty}{\varepsilon_s - \varepsilon_\infty} = \int_0^\infty \frac{\rho(\tau)}{1 + i\omega\tau}\, d\tau \qquad \text{Eq.(2.1.6-6)}$$

Separation of the real and imaginary parts of Eq.(2.1.6-6) gives

$$\frac{\varepsilon'(\omega) - \varepsilon_\infty}{\varepsilon_s - \varepsilon_\infty} = \int_0^\infty \frac{\rho(\tau)}{1 + \omega^2\tau^2}\, d\tau \qquad \text{Eq.(2.1.6-7)}$$

$$\frac{\varepsilon''(\omega)}{\varepsilon_s - \varepsilon_\infty} = \int_0^\infty \frac{\rho(\tau)\omega\tau}{1 + \omega^2\tau^2}\, d\tau \qquad \text{Eq.(2.1.6-8)}$$

These last two equations are the starting point for modeling complex dielectric relaxation which appears as a close association of many distinctively different types of relaxations as described in Chapter 5.

2.2 Empirical Dielectric Relaxation Functions.

2.2.1 Cole-Cole Model

When pairs of data $\varepsilon'(\omega)$ and $\varepsilon''(\omega)$ are plotted in a complex plane over a wide range of frequencies, an arc shape is generally obtained. For the single relaxation time model, a plot of $\varepsilon''(\omega)$ versus $\varepsilon'(\omega)$ gives a semi-circle represented by Eq.(2.2.1-1). Experimental results for many polar liquids give excellent agreement with the theoretical semi-circle curve predicted by Eq.(2.2.1-1), their relaxation time being on the order of 10^{-11} second.[11]

$$\left[\varepsilon' - \frac{(\varepsilon_s + \varepsilon_\infty)}{2}\right]^2 + [\varepsilon'']^2 = \left[\frac{(\varepsilon_s - \varepsilon_\infty)}{2}\right]^2 \qquad \text{Eq.(2.2.1-1)}$$

As stated in the previous section, for the dielectric relaxation of many polymeric systems, the single relaxation time model as represented by Eq.(2.1.6-2) is found to be unsatisfactory. Consequently, various empirical relations between loss and storage dielectric constants have been proposed. Probably the simplest known empirical equation is that of Cole and Cole.[12] From the plot of normalized loss dielectric constant versus $\log\omega\tau_0$, they found a considerably broader frequency range of dispersion together with a smaller maximum value of $\varepsilon''(\omega)$ than is predicted by the single relaxation time model. Such behavior is represented by a depressed semi-circle in an Argand diagram of $\varepsilon'(\omega)$ versus $\varepsilon''(\omega)$, which is also called a Cole-Cole diagram in memory of Cole and Cole who

initiated its wide use. Cole and Cole formulated Eq.(2.2.1-2) after working on the geometry of complex dielectric constants in an Argand diagram.

$$\frac{\varepsilon^{*}-\varepsilon_{\infty}}{\varepsilon_{s}-\varepsilon_{\infty}} = \frac{1}{1+(i\omega\tau_{0})^{1-\alpha}} \qquad \text{Eq.(2.2.1-2)}$$

where τ_0 is considered as the central relaxation time and α has limit of $0 \leq \alpha < 1$. This equation reduces to the Debye expression for $\alpha = 0$. As α approaches one, the dispersion region becomes broader and the maximum value of $\varepsilon''(\omega)$ for $\omega = 1 / \tau_0$ decreases in the frequency domain. In the Cole-Cole diagram, the Cole-Cole model represents a depressed semi-circle whose center is below the abscissa (Eq.(2.2.1-3)) as shown in Figure 6.

$$\left[\varepsilon' - \frac{(\varepsilon_s + \varepsilon_\infty)}{2}\right]^2 + \left[\varepsilon'' + \frac{(\varepsilon_s - \varepsilon_\infty)}{2}\cot\frac{(1-\alpha)\pi}{2}\right]^2 = \left[\frac{(\varepsilon_s - \varepsilon_\infty)}{2}\operatorname{cosec}\frac{(1-\alpha)\pi}{2}\right]^2 \qquad \text{Eq.(2.2.1-3)}$$

The phenomenological meaning of this model corresponds to a superposition of a group of single relaxation processes with a range of relaxation times that are symmetrically distributed about τ_0.

2.2.2 Davidson-Cole Model

Modification of the Cole-Cole Model was proposed by Davidson and Cole after they discovered an even broader range of dispersion especially at higher frequencies. This model has significance since " high frequency " means frequencies which approach optical frequencies and their model could encompass much of the difference between the dielectric constants of radio frequencies and optical frequencies.[13] Their concept is formulated in the following empirical equation.

$$\frac{\varepsilon^*-\varepsilon_\infty}{\varepsilon_s-\varepsilon_\infty} = \frac{1}{(1+i\omega\tau_0)^\gamma} \qquad \text{Eq.(2.2.2-1)}$$

where γ is a parameter with the constraint, $0 < \gamma \leq 1$

In the Cole-Cole diagram, Eq.(2.2.2-1) appears as a skewed distribution of relaxation times about τ_0 as shown in Figure 6. To be more precise, τ_0 is the upper bound of the distribution of relaxation times as will be discussed in the next section. The smaller the gamma, the more skewed the resulting semicircle becomes. There may be several reasons for the broadening of the loss curve at higher frequencies. In some cases, two or more discrete relaxations which overlap at a given temperature are assumed.[14] In other interpretations, intrinsically such behavior is presumed. For example, Glarum derived the Davidson-Cole model using a diffusion model.[15,16] However, it is enough at this moment that the Davidson-Cole model can be used as an empirical model which can handle skew-symmetric distribution of relaxation times.

2.2.3 Havriliak-Negami Model

Both Cole-Cole and Davidson-Cole equations may be viewed as one parameter models which intend to incorporate the symmetric and skew symmetric distribution of relaxation times respectively. For them, the majority of experimental objects were simple organic alcohols or low molecular weight glycols. Fuoss and Kirkwood, on the other hand, developed an empirical model for the loss dielectric constant which was applied to bulk polymers such as poly vinyl chloride-diphenyl systems.[17] Although this work was pioneering in the study of bulk polymers, their empirical formulation is not popular today since it is not based on a simple complex functional form which models the relation between loss and storage dielectric constant concisely. With their model, application of

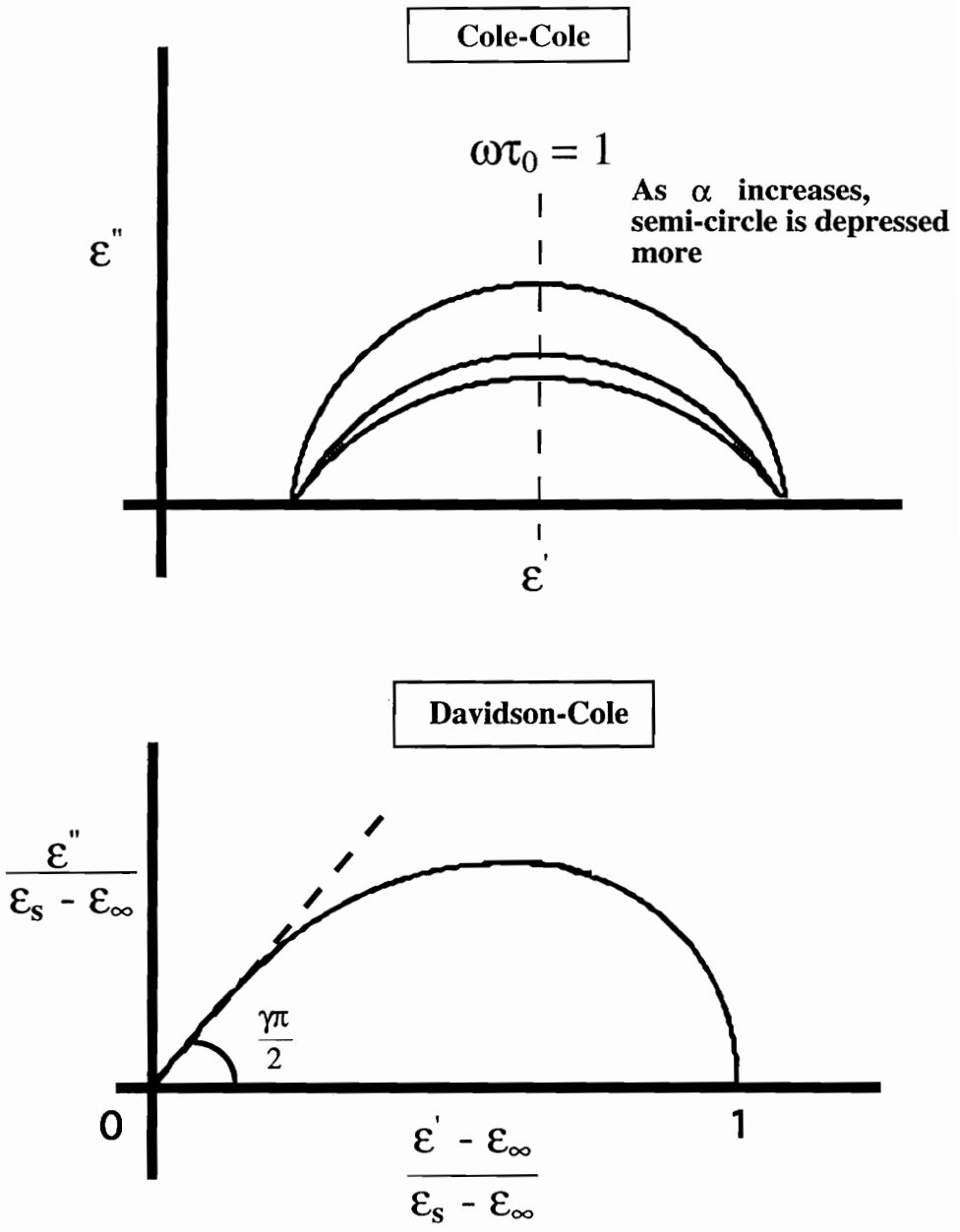

Figure 6. Schematic: Plot of Cole-Cole and Davidson-Cole model

various integral transforms which permit more complete knowledge of viscoelastic properties of solid polymers is not easy.

Havriliak-Negami fused together the concept of the Cole-Cole and the Davidson-Cole models as in Eq.(2.2.3-1).

$$\frac{\varepsilon^{*}-\varepsilon_{\infty}}{\varepsilon_{s}-\varepsilon_{\infty}} = \frac{1}{(1+(i\omega\tau_{0})^{1-\alpha})^{\gamma}} \qquad \text{Eq.(2.2.3-1)}$$

Although there existed efforts which yielded results close to Eq.(2.2.3-1) by other workers at about the same time[20], Havriliak and Negami were the first to actually test the model for various polymers in bulk form. Eq.(2.2.3-1) may be viewed as a two parameter model of α and γ which has one more degree of freedom than previous models in the data fitting of experimental results. Parameters α and γ in this model retain their original meanings and constraints as in the Cole-Cole and Davidson-Cole models. Once a complex form of an empirical equation is given, the corresponding $\varepsilon'(\omega)$ and $\varepsilon''(\omega)$ is readily derived using De Moivre's theorem. In the case of Havriliak-Negami equation, two successive applications of De Moivre's theorem, first with α, then with γ, with the pure imaginary number $i\omega\tau_0$ in the form of

$$i\omega\tau_0 = \omega\tau_0(\cos\frac{\pi}{2} + i\sin\frac{\pi}{2})$$

yields in a straightforward manner the following results.

$$\varepsilon'(\omega)-\varepsilon_{\infty} = r^{-\gamma/2}(\varepsilon_{s}-\varepsilon_{\infty})\cos(\theta\gamma)$$

$$\varepsilon''(\omega) = r^{-\gamma/2}(\varepsilon_{s}-\varepsilon_{\infty})\sin(\theta\gamma)$$

$$r = \left(1+(\omega\tau_0)^{1-\alpha}\sin(\alpha\pi/2)\right)^2 + \left((\omega\tau_0)^{1-\alpha}\cos(\alpha\pi/2)\right)^2$$

$$\theta = \arctan\left(\frac{(\omega\tau_0)^{1-\alpha}\cos(\alpha\pi/2)}{1+(\omega\tau_0)^{1-\alpha}\sin(\alpha\pi/2)}\right) \qquad \text{Eq.(2.2.3-2)}$$

Table 1 summarizes the original expressions of $\varepsilon'(\omega)$ and $\varepsilon''(\omega)$ for the Cole-Cole and the Davidson-Cole models which are derived in the same manner. Of course Eq.(2.2.3-2) reduces into the equations in Table 1 with proper values of α and γ.

2.3 Distribution of Relaxation Times

2.3.1 Introduction

The various empirical equations discussed in section 2.2. have been developed because the relaxation behavior in many dielectric systems is too complex to be described in terms of a single relaxation time model. This has been shown to be true in a wide variety of materials including organic liquids, solutions, polymers, and in particular many glass forming materials. It is true that rigorous theories have not yet been developed which fully describe non-exponential relaxation behavior.[21] Two main approaches to explain non-exponential relaxation behavior in dielectrics have been taken. One approach is from molecular level interpretation. The other is from macroscopic theory which interprets the non-exponential relaxation behavior of the materials in terms of a superposition of exponentially relaxing processes which leads to a distribution of relaxation times. So far it is not known which approach is more correct. If the macroscopic theory is taken, then the distribution of exponentially relaxing processes becomes important in order to understand the relaxation behavior of dielectrics. In macroscopic theory, three properties ε^*, $\Phi(t)$, and $\rho(\tau)$ are often employed, which are the complex dielectric constant, the time decaying function (TDF), and the distribution

Table 1.

Original form of $\varepsilon'(\omega)$ and $\varepsilon''(\omega)$ for Cole-Cole and Cole-Davidson

Model	Cole-Cole	Davidson-Cole
$\frac{\varepsilon'(\omega)-\varepsilon_\infty}{\varepsilon_s-\varepsilon_\infty}$	$\frac{1+(\omega\tau_0)^{1-\alpha}\sin(\alpha\pi/2)}{1+2(\omega\tau_0)^{1-\alpha}\sin(\alpha\pi/2)+(\omega\tau_0)^{2(1-\alpha)}}$ or $\frac{1}{2}\left(1-\frac{\sinh[(1-\alpha)\ln(\omega\tau_0)]}{\cosh[(1-\alpha)\ln(\omega\tau_0)]+\cos(\alpha\pi/2)}\right)$	$(\cos\phi)^\gamma\cos(\phi\gamma)$ $\phi=\arctan(\omega\tau_0)$
$\frac{\varepsilon''(\omega)}{\varepsilon_s-\varepsilon_\infty}$	$\frac{(\omega\tau_0)^{1-\alpha}\cos(\alpha\pi/2)}{1+2(\omega\tau_0)^{1-\alpha}\sin(\alpha\pi/2)+(\omega\tau_0)^{2(1-\alpha)}}$ or $\frac{1}{2}\cdot\frac{\cos(\alpha\pi/2)}{(\cosh[(1-\alpha)\ln(\omega\tau_0)]+\sin(\alpha\pi/2))}$	$(\cos\phi)^\gamma\sin(\phi\gamma)$ $\phi=\arctan(\omega\tau_0)$

Note: Extreme caution is required in that α and γ in this table, also in the Havriliak-Negami model, are sometimes written as $1-\alpha$. In those cases, all the interpretations regarding the trends of parameter values should be made in the reverse way. Also the equations take rather different forms than what is obtained from the direct substitution of $1-\alpha$ or $1-\gamma$ into the equations in this table.

function of relaxation times (DFRT) respectively. These three properties are dependent on each other through integral transforms as shown in Figure 7. As such, the knowledge of one property determines the other two, at least in principle.

2.3.2 Cole-Cole model.

The DFRT of the Cole-Cole model[22] was first derived by Cole and Cole using the method of Fuoss and Kirkwood.[23] Later Davidson and Cole found the Stieltjes transform to be convenient in deriving the DFRT of their model.[24] The Stieltjes transform[25, 26] is quite straightforward once the form of complex dielectric constant is given.

Eq.(2.1.6-6) can be reorganized for the Stieltjes transform

$$\left(\frac{\varepsilon^* - \varepsilon_\infty}{\varepsilon_s - \varepsilon_\infty}\right)\cdot(i\omega) = \int_0^\infty \frac{\left(\frac{1}{\tau}F(\frac{\tau}{\tau_0})\right)}{\frac{1}{i\omega\tau_0} + \frac{\tau}{\tau_0}} d\left(\frac{\tau}{\tau_0}\right) \qquad \text{Eq.(2.3.2-1)}$$

with

$$F(\frac{\tau}{\tau_0}) = \tau\rho(\tau) \qquad \text{Eq.(2.3.2-2)}$$

For Eq.(2.3.2-1), the Stieltjes transform applies as follows

By substitution of

$$s = \frac{1}{i\omega\tau_0}$$

$$x = \frac{\tau}{\tau_0}$$

$$S(s) = \left(\frac{\varepsilon^* - \varepsilon_\infty}{\varepsilon_s - \varepsilon_\infty}\right)\cdot(i\omega)$$

$$f(x) = \frac{1}{\tau}\cdot F(\frac{\tau}{\tau_0}) = \frac{1}{\tau_0 x}\cdot F(x)$$

Transform

$$S(s) = \int_0^\infty \frac{f(x)}{s + x} dx \qquad \text{Eq.(2.3.2-3)}$$

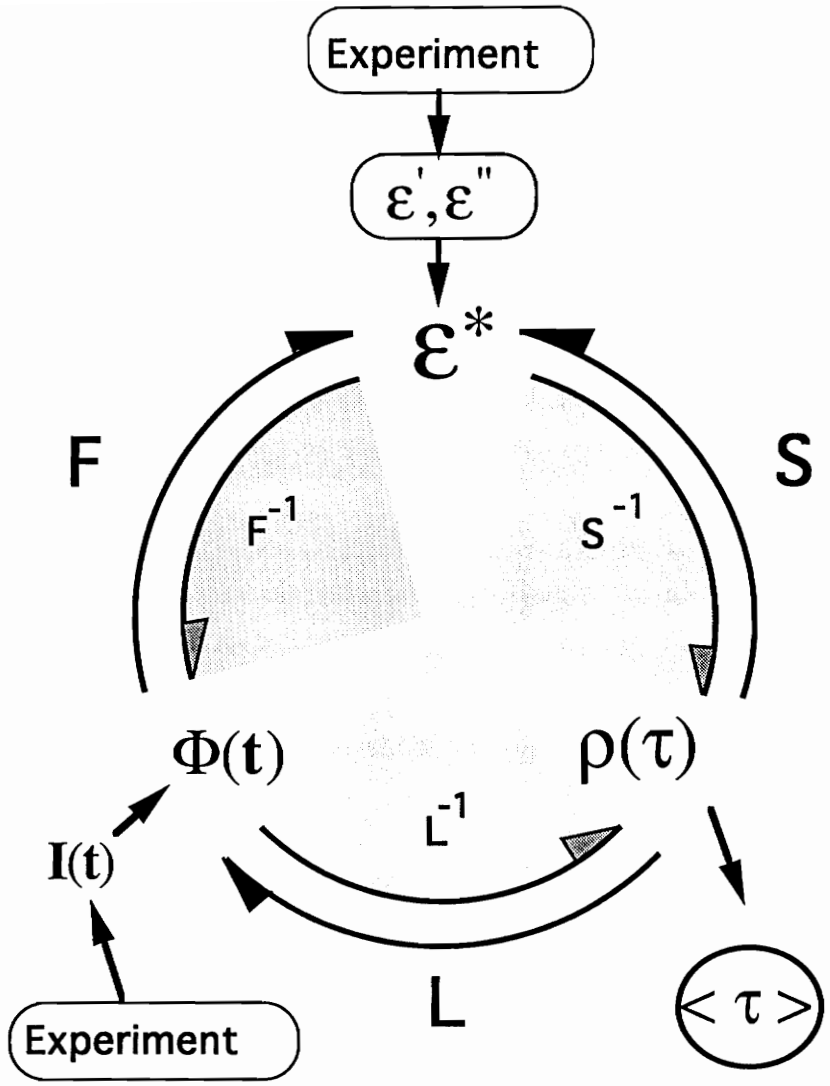

Figure 7. **Integral transform relationships where S and L stands or Stieltjes and Laplace transform respectively and F for Fourier transform or pure imaginary Laplace transform**

and Inverse Transform

$$f(x) = \frac{i}{2\pi} [S(xe^{i\pi}) - S(xe^{-i\pi})] \qquad \text{Eq.(2.3.2-4)}$$

yields the DFRT of the Cole-Cole model as

$$F(\frac{\tau}{\tau_0}) = \frac{1}{\pi} \cdot \frac{\sin \pi\alpha \cdot (\frac{\tau}{\tau_0})^{1-\alpha}}{[\,1 + (\frac{\tau}{\tau_0})^{1-\alpha} \cdot e^{-i\pi(1-\alpha)}\,][\,1 + (\frac{\tau}{\tau_0})^{1-\alpha} \cdot e^{i\pi(1-\alpha)}]} \qquad \text{Eq.(2.3.2-5)}$$

Eq.(2.3.2-5) can be shown to be exactly the same as one which Cole and Cole derived originally by introducing $m = \ln(\tau/\tau_0)$. Then Eq.(2.3.2-5) becomes, after unfolding the denominator

$$F(\frac{\tau}{\tau_0}) = \frac{1}{\pi} \cdot \frac{\sin \pi\alpha \cdot e^{-m(1-\alpha)}}{[\,1 + e^{-m(1-\alpha)} \cdot \{\, e^{-i\pi(1-\alpha)} + e^{i\pi(1-\alpha)} \,\} + e^{i\pi(1-\alpha)}]}$$

Substituting

$$e^{-i\pi(1-\alpha)} + e^{i\pi(1-\alpha)} = -2\cos \alpha\pi$$

and dividing both the numerator and denominator by $e^{-m(1-\alpha)}$ gives the final result.

$$F(\frac{\tau}{\tau_0}) = \frac{1}{2\pi} \cdot \frac{\sin \pi\alpha}{\cosh[\,(1-\alpha)\ln(\tau/\tau_0)\,] - \cos \alpha\pi} \qquad \text{Eq.(2.3.2-6)}$$

It is to be noted that since cosine hyperbolic is an even function, Eq.(2.3.2-6) is symmetric about $\tau = \tau_0$ when the abscissa is $\ln(\tau/\tau_0)$, which shows the symmetric distribution of relaxation times for this model.

TDF , $\Phi(t)$, for the Cole-Cole model is originally derived from the expression of transient current I(t) which is obtained by applying unit potential difference at time t = 0 to a condenser of unit geometrical capacitance.[27] Then using the relation between I(t) and $-d\Phi(t)/dt$

$$I(t) = \frac{1}{(\varepsilon_s - \varepsilon_\infty)} [- \frac{d\Phi(t)}{dt}] \qquad \text{Eq.(2.3.2-7)}$$

$- d\Phi(t)/dt$ is obtained as

$$- \frac{d\Phi(t)}{dt} = \frac{1}{\tau_0} (1-\alpha) (\frac{t}{\tau_0})^{-\alpha} \sum_{n=1}^{\infty} \frac{(-1)^{n-1} n}{\Gamma[1 + n(1-\alpha)]} (\frac{t}{\tau_0})^{(n-1)(1-\alpha)} \qquad \text{Eq.(2.3.2-8)}$$

This equation is reduced into simpler form when $t << \tau_0$ by the leading term of the series.

$$- \frac{d\Phi(t)}{dt} = \frac{1}{\tau_0 \Gamma(1-\alpha)} (\frac{t}{\tau_0})^{-\alpha} \qquad \text{Eq.(2.3.2-9)}$$

When Eq.(2.3.2-7) is reorganized in asymptotic expansion in negative powers of t / τ_0,

$$- \frac{d\Phi(t)}{dt} = \frac{1}{\tau_0} (1-\alpha) (\frac{t}{\tau_0})^{-(2-\alpha)} \sum_{n=1}^{\infty} \frac{(-1)^{n-1} n}{\Gamma[1 - n(1-\alpha)]} (\frac{t}{\tau_0})^{-(n-1)(1-\alpha)} \qquad \text{Eq.(2.3.2-10)}$$

This reduces into the following when $t >> \tau_0$,

$$- \frac{d\Phi(t)}{dt} = \frac{(1-\alpha)}{\tau_0 \Gamma(\alpha)} (\frac{t}{\tau_0})^{-(2-\alpha)} \qquad \text{Eq.(2.3.2-11)}$$

It may be worthwhile to check whether Eq.(2.3.2-9) reverts to the complex form of the Cole-Cole model using the Fourier transform Eq.(2.1.3-9). In order to do that, the complex form of the definition of the Γ function is useful.[28]

$$\Gamma(z) = k^z \int_0^{\infty} t^{z-1} e^{-kt} dt \qquad \text{Eq.(2.3.2-12)}$$

$$\text{Re}[z] > 0 , \text{Re}[k] > 0$$

Then

$$\frac{\varepsilon^* - \varepsilon_\infty}{\varepsilon_S - \varepsilon_\infty} = \int_0^\infty e^{-i\omega t} \frac{1}{\tau_0 \Gamma(1-\alpha)} \left(\frac{t}{\tau_0}\right)^{-\alpha} dt \qquad \text{Eq.(2.3.2-13)}$$

$$= \frac{1}{\tau_0^{1-\alpha}\, \Gamma(1-\alpha)} \int_0^\infty t^{(1-\alpha)-1} e^{-i\omega t}\, dt$$

$$= \frac{1}{(i\omega\tau)^{1-\alpha}}$$

The "1" in the denominator drops out because of the approximation $t << \tau_0$ in Eq.(2.3.2-8). The Fourier transform of Eq.(2.3.2-8) and Eq.(2.3.2-10) does not seem obvious.

2.3.3 Davidson-Cole Model.

In the same way as described in the previous section, the Stieltjes transform yields the DFRT of the Davidson-Cole model as

$$F\left(\frac{\tau}{\tau_0}\right) = -\frac{i}{2\pi} \left[\left(1 + \frac{\tau_0}{\tau} e^{-i\pi}\right)^{-\gamma} - \left(1 + \frac{\tau_0}{\tau} e^{i\pi}\right)^{-\gamma}\right] \qquad \text{Eq.(2.3.3-1)}$$

In order to proceed further from this equation, it is necessary to discriminate between the two cases $\tau_0 > \tau$ and $\tau_0 < \tau$, since the amplitude and argument of the complex number z are affected.

$$z = \left(1 + \frac{\tau_0}{\tau} e^{i\pi}\right)$$

When $\tau_0 > \tau$

$$|z| = \sqrt{\left(\frac{\tau - \tau_0}{\tau}\right)^2} = \left|\frac{\tau - \tau_0}{\tau}\right| = \left(\frac{\tau_0 - \tau}{\tau}\right)$$

$$\arg(z) = \pi$$

Using DeMoivre's theorem, Eq.(2.3.3-1) becomes

$$F\left(\frac{\tau}{\tau_0}\right) = \frac{\sin \gamma\pi}{\pi} \left(\frac{\tau}{\tau_0 - \tau}\right)^{\gamma} \qquad \text{Eq.(2.3.3-2)}$$

When $\tau_0 < \tau$, $\arg(z) = 0$, then

$$F(\frac{\tau}{\tau_0}) = 0 \qquad \text{Eq.(2.3.3-3)}$$

The implication of Eq.(2.3.3-2) and Eq.(2.3.3-3) is that any relaxation time τ which is bigger than τ_0 does not exist in the Davidson-Cole model.

For TDF , $\Phi(t)$, Davidson and Cole[29] derived

$$-\frac{d\Phi(t)}{dt} = \frac{1}{\tau_0\Gamma(\gamma)}(\frac{t}{\tau_0})^{\gamma-1} e^{-t/\tau_0} \qquad \text{Eq.(2.3.3-4)}$$

Since this form is not in the series form, unlike the Cole-Cole model, Eq.(2.3.3-4) readily yields the complex form of the dielectric constant, Eq.(2.2.2-1) when the Fourier transform is used using Eq.(2.3.2-12) and Eq.(2.1.3-9).

2.3.4 Havriliak-Negami Model.

At this moment, the use of $\Phi(t)$ and $\rho(\tau)$ of Havriliak-Negami might seem to have been omitted. The reason might be the practicality of such a derivation, let alone the mathematical difficulty of the derivation in the case of $\Phi(t)$. For the record, here, $\rho(\tau)$ in the form of $F(\tau / \tau_0)$ is derived using the Stieltjes transform.

$$F(\frac{\tau}{\tau_0}) = \frac{\sin\gamma\delta}{\pi}\ |z|^{-\gamma} \qquad \text{Eq.(2.3.4-1)}$$

where

$$\delta = \arctan\left[\frac{(\frac{\tau_0}{\tau})^{1-\alpha}\cdot \sin\pi(1-\alpha)}{1+(\frac{\tau_0}{\tau})^{1-\alpha}\cdot \cos\pi(1-\alpha)}\right]$$

$$|z| = \left[\left(1+(\frac{\tau_0}{\tau})^{1-\alpha}\cdot \cos\pi(1-\alpha)\right)^2 + \left((\frac{\tau_0}{\tau})^{1-\alpha}\cdot \sin\pi(1-\alpha)\right)^2\right]^{1/2}$$

2.3.5 Kohlrausch-Williams-Watts Model

The Kohlrausch-Williams-Watts (KWW) function is an empirical equation which can model the non-exponential time decaying behavior of many normalized physical properties in the form of

$$\Phi(t) = e^{-(t/\tau_0)^{\beta}} \qquad \text{Eq.(2.3.5-1)}$$

where τ_0 is the time at which $\Phi(t)$ becomes 1 / e. On record, this equation was used as early as 1863 by F. Kohlrausch to describe the after-effect of the torsion on glass fibers.[30] His father, R. Kohlrausch used similar expressions for dielectric study. Also this equation is used in fitting light scattering data[31] and the creep behavior of glassy polymers.[32]

For the study of dielectric relaxation, Eq.(2.3.5-1) was studied systematically first by Williams and Watts. As shown in Figure 7, it is possible to have the idea of both ε^* and $\rho(\tau)$ once $\Phi(t)$ of Eq.(2.3.5-1) is chosen. In 1969, Williams and Watts[33] first derived the complex form of the dielectric constant through the Laplace transform for the special case of $\beta = 1/2$ and later they derived the general case[34] as in Eq.(2.3.5-2).

$$\frac{\varepsilon^*-\varepsilon_\infty}{\varepsilon_s-\varepsilon_\infty} = \sum_{n=1}^{\infty} (-1)^{n-1} \cdot \frac{1}{(\omega\tau_0)^{n\beta}} \cdot \frac{\Gamma(n\beta + 1)}{\Gamma(n + 1)} \cdot \left(\cos(\frac{\beta n\pi}{2}) - i \sin(\frac{\beta n\pi}{2})\right) \qquad \text{Eq.(2.3.5-2)}$$

Also, the DFRT of KWW has been derived by Lindsey and Patterson[35] in 1980.

$$\rho(\tau) = - \frac{\tau}{\pi\tau^2} \sum_{k=0}^{\infty} \frac{(-1)^k}{k!} \sin(\pi\beta k)\ \Gamma(\beta k + 1)\ \left(\frac{\tau}{\tau_0}\right)^{\beta k + 1} \qquad \text{Eq.(2.3.5-3)}$$

Lindsey and Patterson performed painstaking numerical calculations of Eq.(2.3.5-3) to find out that as β increases from near zero to near one, $\rho(\tau)$ shows a broad nearly symmetric distribution to sharp asymmetric distribution when $\rho(\tau)$ is plotted over $\log(\tau/\tau_0)$.

2.3.6 Discussions

There have been other forms of TDF and DFRT in both empirical and molecular level models. For example, the following empirical TDF

$$\Phi(t) = A\, t^{-n} \qquad \text{Eq.(2.3.6-1)}$$

where A and n are parameters, has been proposed by Curies and has been found to hold over a range of times by several workers.[36] Recently Matsuoka[37] proposed a TDF of the form

$$\Phi(t) = e^{\left[\beta / \ln(\tau/\tau_0)\right]} \qquad \text{Eq.(2.3.6-2)}$$

This equation has been derived from a semi-molecular model based on intermolecular cooperativity.[38] It is claimed that Eq.(2.3.6-2) decays less than the KWW model in early stages of relaxation and fits experimental data better in this region. It is to be noted that this function is sharply declining around $t = t_{1/e}$ and undefined at $t = \tau_0$.

The concept of the distribution of relaxation times is said to have been introduced, first, by Schweidler[39], as early as 1907. Later Wagner[40] proposed the use of a logarithmic Gaussian distribution of the form

$$F(m) = \frac{b}{\sqrt{\pi}} e^{\left[-b^2 m^2\right]} \qquad \text{Eq.(2.3.6-3)}$$

where $m = \ln(\tau / \tau_0)$ and the parameter b determines the breadth of the distribution. This equation yielded its place to the many other distribution functions which have been explained in section 2.3 due to the high ideality embedded in it.

2.4 Mean Relaxation Time

If one takes macroscopic theory and accepts the distribution of relaxation times for the understanding of dielectric relaxation, mean relaxation time as defined by Eq.(2.4-1) might be the one meaningful parameter which explains the relaxation behavior on average.

$$\begin{aligned} <\tau> &= \int_{-\infty}^{\infty} \tau \; F(\frac{\tau}{\tau_0}) \, d\ln(\frac{\tau}{\tau_0}) \\ &= \int_{0}^{\infty} \tau_0 \; F(\frac{\tau}{\tau_0}) \, d(\frac{\tau}{\tau_0}) \\ &= \int_{0}^{\infty} \tau \, \rho(\tau) \, d\tau \end{aligned} \qquad \text{Eq.(2.4-1)}$$

For the Davidson-Cole and the KWW models, the exact analytic form for $<\tau>$ has been derived. For other models, numerical integration might be possible.

For the Davidson-Cole model, Eq.(2.3.3-2) into Eq.(2.4-1) with the fact that τ can have the value of τ_0 in the limit, gives

$$<\tau> = \int_{0}^{1} \tau_0 \frac{\sin\gamma\pi}{\pi} \cdot \left(\frac{\tau}{\tau_0}\right)^{(1+\gamma)-1} \cdot \left(1 - \frac{\tau}{\tau_0}\right)^{(1-\gamma)-1} d\left(\frac{\tau}{\tau_0}\right)$$

$$= \tau_0 \frac{\sin\gamma\pi}{\pi} \cdot B(\, 1+\gamma, \, 1-\gamma \,) \qquad \text{Eq.(2.4-2)}$$

where B is the Beta function of the following identity among others[41]

$$B(m, n) = \frac{\Gamma(m)\Gamma(n)}{\Gamma(m+n)} \qquad \text{Eq.(2.4-3)}$$

$$\Gamma(m)\Gamma(1-m) = \frac{\pi}{\sin(m\pi)} \qquad \text{Eq.(2.4-4)}$$

Then with the Gamma function property, $\Gamma(1+m) = m\Gamma(m)$,that is

$B(1+\gamma, 1-\gamma) = \gamma B(\gamma,1-\gamma)$, Mean relaxation time for Davidson-Cole model becomes

$$\langle\tau\rangle = \tau_0\gamma \qquad \text{Eq.(2.4-5)}$$

Lindsey and Patterson[42] derived general n-th moments of the average relaxation time $\langle\tau^n\rangle$ as

$$\langle\tau^n\rangle = \int_0^\infty \tau^n \rho(\tau) d\tau = \frac{1}{\Gamma(n)} \int_0^\infty t^{n-1}\, \Phi(t)\, dt \qquad \text{Eq.(2.4-6)}$$

Eq.(2.4-6) can be retro-confirmed by substitution of Eq.(2.1.6-4) into Eq.(2.4-6). Then

$$\langle\tau^n\rangle = \frac{1}{\Gamma(n)} \int_0^\infty t^{n-1} \left[\int_0^\infty e^{-t/\tau} \rho(\tau)\, d\tau \right] dt$$

$$= \frac{1}{\Gamma(n)} \int_0^\infty \rho(\tau) \left[\int_0^\infty t^{n-1} e^{-t/\tau}\, dt \right] d\tau$$

With the following Gamma function identity,

$$\int_0^\infty x^n e^{-\alpha x} dx = \frac{\Gamma(n+1)}{\alpha^{n+1}}$$

N-th moment of the average relaxation time is obtained as

$$<\tau^n> = \frac{1}{\Gamma(n)} \int_0^\infty \rho(\tau) \; [\, \Gamma(n)\, \tau^n] \; d\tau$$

which proves the starting equation Eq.(2.4-6).

As such, for the KWW equation, the first moment of relaxation time comes with the substitution of Eq.(2.3.5-1) into Eq.(2.4-6) with n = 1.

$$<\tau> = \int_0^\infty e^{-(t/\tau_0)^\beta} dt$$

By replacing $(t/\tau_0)^\beta$ with x

$$<\tau> = \frac{\tau_0}{\beta} \int_0^\infty e^{-x}\, X^{(1/\beta)-1}\, dx \qquad \text{Eq.(2.4-7)}$$

The integral part of Eq.(2.4-6) is the case where k = 1 and z = 1/β in Eq.(2.3.2-12). Thus, it follows

$$<\tau> = \frac{\tau_0}{\beta}\, \Gamma(\frac{1}{\beta}) \qquad \text{Eq.(2.4-8)}$$

As a comprehensive map of what has been done in the macroscopic theory of dielectric relaxation, Table 2 has been prepared. In recapitulation, the following major characteristics may be stated for each model in Table 2.

i) The Cole-Cole model implies perfect symmetric distribution of relaxation times. Its time decaying functions are obtained in series form but its DFRT is derived in

Table 2.

Summary of equations for various models based on macroscopic theory

model	ε^*	$\Phi(t)$	$\rho(\tau)$	$\langle\tau\rangle$
Cole-Cole	A	As	A	-
Davidson-Cole	A	A	Ac	A
Havriliak-Negami	A	-	A*	-
KWW	As	A	As	A

Notes:

A : Analytic form, Closed
As: Analytic form, in Series
Ac: Analytic form with constraint
A*: Analytic form (Derived in this paper)

$\Phi(t)$ means $-d\Phi(t)/dt$ whenever necessary.
$\rho(\tau)$ means $F(\tau/\tau_0)$ whenever necessary.

model	ε^*	$\Phi(t)$	$\rho(\tau)$	$\langle\tau\rangle$
Cole-Cole	2.2.1-2	2.3.2.-8	2.3.2-6	-
Davidson-Cole	2.2.2-1	2.3.3-4	2.3.3-3	2.4-5
Havriliak-Negami	2.2.3-1	-	2.3.4-1	-
KWW	2.3.5-2	2.3.5-1	2.3.5-3	2.4-8

Notes:

Numbers correspond to equation numbers in Chapter 2.

$\Phi(t)$ means $-d\Phi(t)/dt$ whenever necessary.
$\rho(\tau)$ means $F(\tau/\tau_0)$ whenever necessary.

closed analytic form. For the mean relaxation time, numerical integration can be used where

τ can take any value from zero to infinity.

ii) The Davidson-Cole model presumes skew-symmetric distribution of relaxation times and possesses a well defined time decaying function. Its distribution function dictates that there exists no relaxation time which is bigger than τ_0, which seems to lack a little bit of generality. Mean relaxation time is most simply defined.

iii) The Havriliak-Negami model is the general model which provides the most freedom in the data fitting of experimental data. TDF and mean relaxation time may be evaluated using numerical integration. Attempts to derive analytic expressions of TDF and mean relaxation time seem not to be of much practical use not to mention the mathematical difficulty.

iv) The KWW model is very difficult to use in the data fitting of experimental $\varepsilon'(\omega)$ and $\varepsilon''(\omega)$, although it is very convenient for transient type experiments. Mean relaxation time is derived in closed analytic form and DFRT can cover from a broad almost symmetric distribution to a sharp asymmetric distribution with a single parameter β.

Chapter 3. Interpretation of Dielectric Processes in Bulk Polymer

3.1 Dipole Moment Autocorrelation Function

The autocorrelation function C(t) of a physical property A is generally defined as[43]

$$C(t) = \frac{\langle A(0) \cdot A(t) \rangle}{\langle A(0) \cdot A(0) \rangle} \qquad \text{Eq.(3.1-1)}$$

where A is a dynamic function of the variables of a given system. The average is taken over an ensemble of systems at the reference time t = 0.

In dielectric analysis, A is $\tilde{M}$, which is the vectorial sum of both permanent and induced moments of all the dipoles existing in the system to be studied.[46] If the system to be studied is a polymer solution, $\tilde{M}(t)$ is the sum of $Q_i(t)$, the permanent dipole moment of the i-th chain q_{ij}, the induced dipole moment of the j-th repeating unit in i-th chain, and q_S, the dipole moment of the solvent.

$$\tilde{M}(t) = \sum_i Q_i(t) + \sum_{ij} q_{ij} + \sum q_s$$

In the study of the dipole orientation of bulk polymeric systems q_S and q_{ij} which are time independent, are unnecessary. Since Q_i is the vector sum of the dipole moment μ_j of the repeating units, it can be decomposed into the components parallel, μ^p, and perpendicular, μ^v, to the chain contour (superscript v meaning "vertical" is used to avoid confusion with p meaning "parallel")

$$Q_i(t) = \sum_j [\mu_{ij}^p(t) + \mu_{ij}^v(t)]$$

where μ_{ij} denotes the dipole moment of the j-th repeating unit in the i-th chain. Hence,

$$<Q_i(0)\cdot Q_i(t)> = \sum_j \sum_k <\mu_{ij}^p(0)\cdot\mu_{ik}^p(t)> + \sum_j \sum_k <\mu_{ij}^p(0)\cdot\mu_{ik}^v(t)>$$
$$+ \sum_j \sum_k <\mu_{ij}^v(0)\cdot\mu_{ik}^p(t)> + \sum_j \sum_k <\mu_{ij}^v(0)\cdot\mu_{ik}^v(t)> \qquad \text{Eq.(3.1-2)}$$

Let $b_{ij}(t)$ be the bond vector of the j-th repeat unit of the i-th molecule, then $\mu_{ij}^p(t)$ may be written as

$$\mu_{ij}^p(t) = \mu b_{ij}(t)$$

where μ is a constant having the meaning of the parallel dipole moment per unit contour length. Then,

$$\sum_j \sum_k <\mu_{ij}^p(0)\cdot\mu_{ik}^p(t)> = \mu^2 \sum_j \sum_k <b_{ij}(0)\cdot b_{ik}(t)>$$
$$= \mu^2 <r_i(0)\cdot r_i(t)>$$

since the end-to-end vector $r_i(t)$ is equal to the vector sum of the bond vectors.

If the cross-terms are assumed to be negligible,

$$C(t) = \frac{\mu^2 <r_i(0)\cdot r_i(t)> + \sum_j \sum_k <\mu_{ij}^v(0)\cdot\mu_{ik}^v(t)>}{\mu^2 <r_i(0)\cdot r_i(0)> + \sum_j \sum_k <\mu_{ij}^v(0)\cdot\mu_{ik}^v(0)>} \qquad \text{Eq.(3.1-3)}$$

The first term of Eq.(3.1-3) is the autocorrelation function for the normal mode process and the second is the autocorrelation function of the perpendicular component dipole moment representing segmental motions. Since the relaxation times for these two components are well separated, C(t) may be evaluated from Eq(2.1.3-10) for each process once C(t) is equated to $\Phi(t)$.[46]

The basis of equating macroscopic time decaying function to molecular level autocorrelation function originates from Glarum, whose work was the development of the Kubo method for the dielectric relaxation of rigid dipoles. His result for a liquid containing only one type of dipole is expressed as[47]

$$\frac{\varepsilon^*(\omega) - \varepsilon_\infty}{\varepsilon_s - \varepsilon_\infty} = [1 + \frac{3\varepsilon_s}{2\varepsilon_s + \varepsilon_\infty}\{[G(\omega)]^{-1} - 1\}]^{-1}$$

$$G(\omega) = \int_0^\infty [-\frac{d\Gamma(t)}{dt}]e^{-i\omega t}\ dt \qquad \text{Eq.(3.1-4)}$$

where $\Gamma(t)$ is the dipole correlation function defined as

$$\Gamma(t) = \frac{<\mu(0)\cdot\mu(t)>}{\mu^2}$$

The factor $3\varepsilon_s / (2\varepsilon_s + \varepsilon_\infty)$, which lies between 1.0 to 1.5, is due to local field effects. If $\Gamma(t)$ is given by

$$\Gamma(t) = \exp[-t/\tau_{micro}] \qquad \text{Eq.(3.1-5)}$$

Eq.(3.1-4) turns into a familiar single relaxation time model

$$\frac{\varepsilon^*(\omega) - \varepsilon_\infty}{\varepsilon_s - \varepsilon_\infty} = \frac{1}{1+i\omega\tau_{macro}}$$

where $\tau_{macro} = [3\varepsilon_s / (2\varepsilon_s - \varepsilon_\infty)]\tau_{micro}$. This is the relationship between macroscopic and microscopic relaxation time. Also, if the internal field factor is set equal to unity, Eq.(3.1-4) becomes

$$\frac{\varepsilon^*(\omega) - \varepsilon_\infty}{\varepsilon_s - \varepsilon_\infty} = \int_0^\infty [-\frac{d\Gamma(t)}{dt}]e^{-i\omega t}\ dt \qquad \text{Eq.(3.1-6)}$$

Comparison of Eq.(3.1-4) and Eq.(2.1.3-9) results in $\Gamma(t) = \Phi(t)$ and the macroscopic time decaying function or response function is the same as the molecular level dipole moment autocorrelation function. If the internal field factor is considered, the relation between $\Gamma(t)$ and $\Phi(t)$ becomes complicated. However, for approximate work, it may be assumed again that in this case $\Gamma(t) \approx \Phi(t)$.

As a summary, two assumptions should be made for $\Phi(t)$, the macroscopic time decaying function, to be equated to the molecular level dipole moment autocorrelation function C(t) for the chain-like molecule. First, local field effects should be neglected and second, cross interactions between dipoles in the repeating unit are assumed to be absent. One representative example of the autocorrelation function approach is the study of bulk polyisoprene where the normal mode and the segmental mode were separable and the autocorrelation function could be calculated separately for each mode.[48] Conceptually, the autocorrelation function is a mathematical expression of the time-evolution of the perturbation arising from an initial disturbance of a dipole from its equilibrium orientation. In other words, the dipole moment autocorrelation function describes the decrease of the projection of the average dipole moment to an original direction as time passes .[44,45] The significance of the autocorrelation function approach is that it relates molecular level relaxation parameters to macroscopic relaxation parameters.

3.2 Frequency Dependent Conductivity

In an actual dielectric experiment, it is practical to consider the sample as a contaminated mixture of polymeric material to be analyzed and unwanted impurities such as conducting ionic species which might come from a catalyst or a minute amount of water which has been incorporated during sample preparation. It is well known that

humid air surrounding the place of an experiment plays a significant role in the acquisition of decent data. As such, the sample might be thought of as a heterogeneous dielectric. For such material, polarization occurs as a result of the accumulation of virtual charge at the interface of two media having different permittivities and/or conductivities. The simplest model of this is a medium having two layers of permittivities ε_1' and ε_2' and conductivities σ_1 and σ_2 respectively. According to van Beek[49], the frequency dependence of the loss permittivity of the composite system is expressed as

$$\varepsilon''(\omega) = \frac{(\bar{\varepsilon}_s - \bar{\varepsilon}_\infty)\omega\tau}{1 + \omega^2\tau^2} + \frac{\bar{\sigma}}{\omega} \qquad \text{Eq.(3.2-1)}$$

where

$$\bar{\varepsilon}_s = \frac{d\,(\varepsilon_1' d_1 \sigma_2^2 + \varepsilon_2' d_2 \sigma_2^2)}{(\sigma_1 d_2 + \sigma_2 d_1)^2}$$

$$\bar{\varepsilon}_s = \frac{d\,\varepsilon_1' \varepsilon_2'}{(\sigma_1 d_2 + \sigma_2 d_1)}$$

$$\tau = \frac{\varepsilon_1' d_2 + \varepsilon_2' d_1}{(\sigma_1 d_2 + \sigma_2 d_1)}$$

$$\bar{\sigma} = \frac{d\,\sigma_1 \sigma_2}{(\sigma_1 d_2 + \sigma_2 d_1)}$$

d_1, d_2 are the thickness for layers 1 and 2. $d = d_1 + d_2$.

In Eq.(3.2-1), the appearance of frequency dependent conductivity is to be noted. Usually this effect is observed in the steep rise of ε'' at low frequencies or at high temperatures.

Also there is a general expression for the frequency dependent conductivity of mobile charge carriers[50]

$$\varepsilon''(\omega) = \frac{\sigma_0}{\varepsilon_0(2\pi f)^s} \qquad \text{Eq.(3.2-2)}$$

where σ_0 and s are fitting parameters.. In certain cases, both Eq.(3.2-1) and Eq.(3.2-2) are considered for the fitting of $\varepsilon''(\omega)$ to the appropriate model of choice,[51] and the basis of such an approach is that the power law behavior over many decades of frequency is typical for a wide variety of different dielectric loss mechanisms.[52]

3.3 Accepted Interpretations

3.3.1 Cooperative Dipolar Relaxation

A major feature of amorphous or partially crystalline polymeric material is the glass transition. It is generally accepted to attribute Tg to a major change in the segmental mobility of polymer chains. Above Tg, there is sufficient chain mobility due to micro-Brownian motion to enable large-scale reorganization of the chains. In other words, an observed Tg is that temperature at which the time constant for a molecular rearrangement process becomes comparable to the time scale of the experiment. At Tg, permanent dipoles attached to the polymer backbone tends to orient themselves in an electric field and the glass transition is accompanied by a major dielectric dispersion. Also free volume increases significantly and this provides a vacant site for the molecular segment to move in. For this free volume driven process, the well known WLF (Williams, Landel, and Ferry) equation is applicable.[53]

$$\log a_T = \log\frac{\tau}{\tau_{Tg}} = -\frac{C_1(T-Tg)}{C_2 + T - Tg} \qquad \text{Eq.(3.3-1)}$$

where C_1 and C_2 are universal constants and a_T is the shift factor.

3.3.2 Secondary Dipolar Relaxation

When dielectric loss is scanned from low to high temperature, molecular mobilities of various types become successively energized and available for dipolar orientation. By convention the dielectric relaxation processes are labeled as α, β.. and so on, beginning from the high temperature end. The same relaxation processes are generally responsible for dispersions in mechanical properties, too, although a particular molecular rearrangement process may produce a stronger dielectric effect than mechanical effect, or vice versa. One good example is water. The strong dielectric loss due to the presence of water in dielectric thermal analysis does not contribute to the absorption of mechanical energy.

Some polymers are wholly amorphous and there is only one phase present in the bulk material. In such cases there might be at least one low temperature subsidiary (β, γ, etc.) relaxation. For the β process, the following mechanisms have been postulated.

(a) Rotation of a side group about a C-C bond

(b) Conformational flip of a cyclic unit

(c) Local motion of a segment of the main chain

For a β process, there is a tendency for the loss intensity to increase with the temperature, implying that the number of dipoles participating in the β-transition becomes greater or that they are less restricted at high temperatures.[54]

3.3.3 Crystalline Phase Associated Transition

As the amorphous and crystalline phases are not as clearly defined in polymers as in small molecules, it is difficult to decide which transitions belong to which phase. It is considered that transitions which are appreciably increased by increasing crystallinity, crystal form or size belong to the crystalline phase. At the surface of the lamellae, the mobility of the chain segments is different from that of the amorphous region. Thus, the transition corresponding to the motion of the surface groups of the lamellae will be

considered as a crystalline transition as it is highly increased by increasing crystallinity. It is believed that mechanical or dielectric transitions are not expected to occur in perfect crystals. The experimental fact that some transitions are strongly dependent on the crystallinity is attributed to local motion at dislocation and defects.[55]

Chapter 4. Modeling of Dielectric Relaxation Processes

4.1 Introduction

Through proper interpretation of dielectric loss permittivity data, important viscoelastic parameters such as the mean relaxation time at given temperature can be readily obtained. So far, most of the theoretical study of relaxation parameters was done by analyzing frequency plane data. By analyzing frequency plane data, interpretation of relaxation parameters could be readily related to a molecular interpretation especially when the system to be studied is monodisperse, an amorphous single phase with a sub-ambient Tg; hence not subject to physical aging at room temperature. However, often the dielectric loss transition is composed of closely associated multiple peaks. Closely associated multiple glass transitions are accepted for certain types of copolymers and blends, yet their appearance in homopolymer samples has been more difficult to explain. Closely associated multiple transitions have been speculated to occur due to segmental cooperation of domain sizes above and below the critical entanglement molecular weight[56], copolymer compositional variances[57], and the simultaneous presence of more than one crystalline form in the sample.[58] When closely associated multiple relaxation peaks are present, it is very hard to observe all multiple transitions within an experimental frequency window available in one type of measuring apparatus. Also, finding the proper isothermal temperature for a frequency sweep experiment becomes difficult if the sample needs a time dependent study with a limited amount of sample. Experimentally when multiple dielectric relaxations are encountered, changing the test frequency to extreme high or low sides often enables one to resolve the multiple curves. However, by that time, the temperature range of an individually resolved relaxation peak shifts out of the

temperature range being investigated and it is not feasible to obtain relaxation parameters at the temperature of interest.

Recently Rotter and Ishida[59] used curve-fitting techniques to resolve multiple peaks in the temperature plane and they found that the Gaussian line shape was intrinsic to the nature of the components which constitute the loss spectrum. This concept was tested in dynamic mechanical, dilatometry, torsion braid, torsion pendulum, and dielectric thermal analysis. They concluded that curve resolving multiple relaxation peaks in the temperature plane with a Gaussian peak was very useful, at least, in an empirical sense, to have qualitative insights into the blending of compatible polymers and the manifestation of crystallinity effects on the glass transition. Based on Rotter and Ishida's work, quantitative analysis which presumes Gaussian type loss peak in the temperature plane of dielectric data can be attempted. This attempt might be useful in understanding the relaxation behavior of binary blends which are miscible or partially miscible as well as closely associated multiple relaxations arising from the homopolymer. Especially, the empirical formalism modeled here provides the mean relaxation time at the temperature of interest and does not introduce new parameters other than what comes from the experiment. From an engineering point of view, toughening brittle plastics with other polymers which possess high chain mobility at / below room temperature is often an attractive route. In this case, closely associated multiple relaxations are often expected and this is the case in which the empirical formalism modeled here could play a small role.

4.2 Basis of Model

The basic idea of curve resolution in the temperature plane can be boiled down to the linear additivity of loss property.[60] In dielectric analysis this means at constant angular frequency ω

$$\varepsilon''_{total}(T) = \varepsilon''_1(T) + \varepsilon''_2(T)$$

where 1 and 2 denote the individual components responsible for the multiple loss peaks overall. For the frequency dependent dielectric loss due to conductivity in the frequency plane, an exponential function in the temperature plane is proposed. This proposition is made based on the general concept that the given loss behavior observed on a log(time) scale can be observed in the temperature plane and these two scales are proportional.

$$\log t \;<\!\!-\!\!>\; T$$

Application of this relation to the power law Eq.(3.2-2) results in an exponential function and Eq.(3.2-2) can be transformed into Eq.(4.2-1) where p and q are fitting parameters.

$$\varepsilon''(T) = e^{p(T-q)} \qquad \text{Eq.(4.2-1)}$$

4.3 Binary Blend- Multiphase

Let $\varepsilon''_1(T)$, $\varepsilon''_2(T)$, and $\varepsilon''_B(T)$ be the dielectric loss permittivity function of pure components 1, 2, and binary blend of 1 and 2 with mole fractions n_1 and n_2. According to Rotter and Ishida, Gaussian type loss permittivity is presumed for $\varepsilon''_1(T)$ and $\varepsilon''_2(T)$. The shape of $\varepsilon''_B(T)$ is considered to be the sum of all loss peaks arising from m multiple phases as shown in Figure 8.

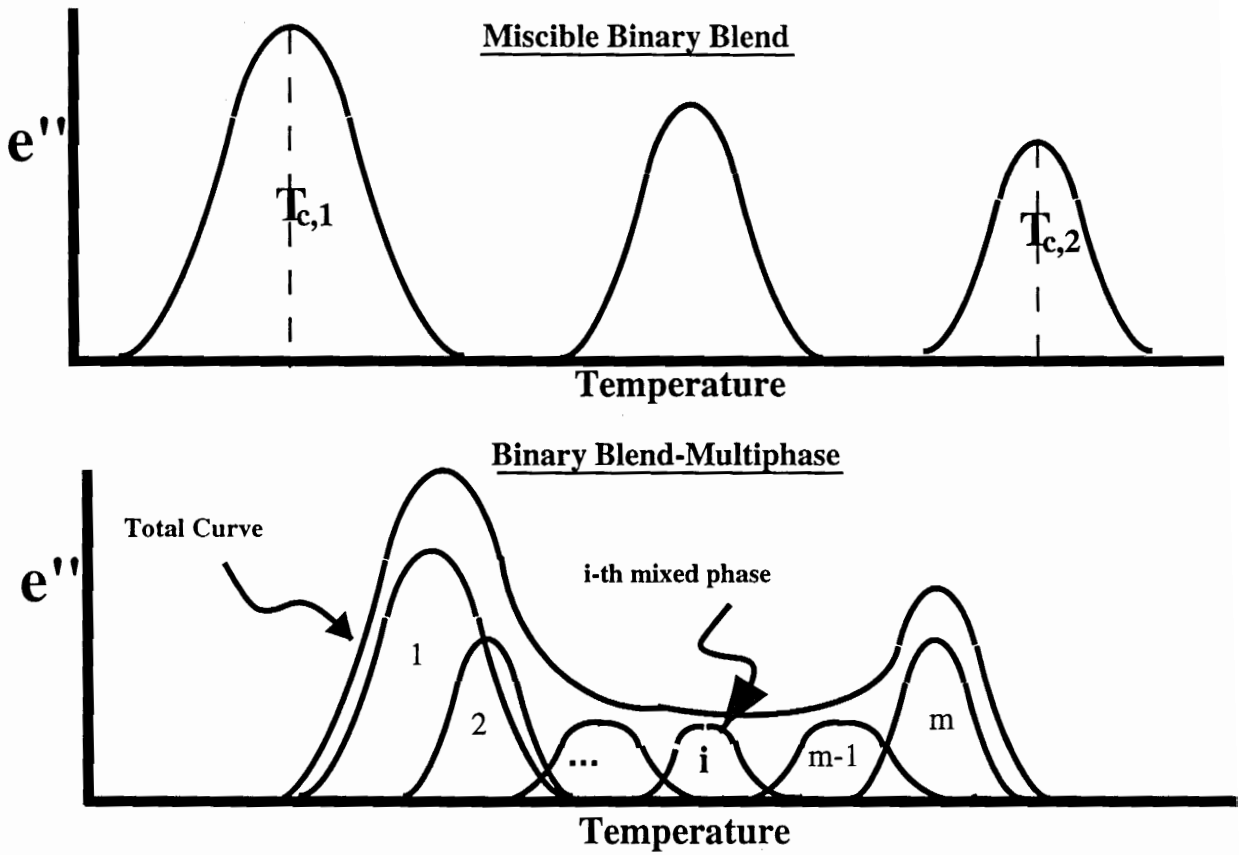

Figure 8. Schematic: Basis of proposed model, top; miscible binary blend, bottom; multiphase binary blend

$$\varepsilon''_B(T) = \sum_{i=1}^{m} \varepsilon''_{B,i}(T) \qquad \text{Eq.(4.3-1)}$$

where $\varepsilon''_{B,i}(T)$ is dielectric loss arising from the i-th mixed phase. The total amount of component 1, expressed in terms of mole fraction as n_1, is supposed to be distributed in various mixed phases as n_{11}, n_{21}, and so on. For component 2, similar reasoning is applied.

$$\sum_{i=1}^{m} n_{ij} = n_j \quad , \quad f_{ij} = n_{ij} / n_j \qquad \text{Eq.(4.3-2)}$$

where i : index of mixed phase

j: blend component i.e. j = 1 or 2

For the i-th mixed phase, linear additivity of loss peaks yields

$$\varepsilon''_{B,i}(T) = n_{i1}\, \varepsilon''_1(T\text{-}T_{i1}) + n_{i2}\, \varepsilon''_2(T\text{-}T_{i2}) \qquad \text{Eq.(4.3-3)}$$

where T_{i1} and T_{i2} are shift scales of the dielectric loss functions of $\varepsilon''_1(T)$ and $\varepsilon''_2(T)$ respectively.

The $\varepsilon''_1(T)$ and $\varepsilon''_2(T)$ can be expressed in terms of oscillator strength and the distribution function of relaxation time which are functions of temperature at given frequency. Then,

$$\begin{aligned} \varepsilon''_{B,i}(T) &= n_{i1}\, \Delta\varepsilon''_1(T\text{-}T_{i1}) \int_0^\infty \frac{\rho_{1,T\text{-}T_{i1}}(\tau)\omega\tau}{1+\omega^2\tau^2} d\tau \\ &\quad + n_{i2}\, \Delta\varepsilon''_2(T\text{-}T_{i2}) \int_0^\infty \frac{\rho_{2,T\text{-}T_{i2}}(\tau)\omega\tau}{1+\omega^2\tau^2} d\tau \\ &= \Delta\varepsilon''_{B,i}(T) \int_0^\infty \frac{\rho_{B,i,T}(\tau)\omega\tau}{1+\omega^2\tau^2} d\tau \end{aligned} \qquad \text{Eq.(4.3-4)}$$

where

$$\Delta\varepsilon''_{B,i}(T) = \sum_j n_j f_{ij} \Delta\varepsilon_j''(T-T_{ij})$$

$$\rho_{B,i,T}(\tau) = \sum_j F_{ij} \rho_{j,T-T_{ij}}(\tau)$$

$$F_{ij} = \frac{n_j f_{ij} \Delta\varepsilon_j''(T-T_{ij})}{\sum_j n_j f_{ij} \Delta\varepsilon_j''(T-T_{ij})}$$

Then from Eq.(4.3-1)

$$\varepsilon''_B(T) = \sum_{i=1}^{m} \varepsilon''_{B,i}(T) = \sum_i \Delta\varepsilon''_{B,i}(T) \int_0^\infty \frac{\rho_{B,i,T}(\tau)\omega\tau}{1+\omega^2\tau^2} d\tau$$
$$= \Delta\varepsilon''_B(T) \int_0^\infty \frac{\rho_{B,T}(\tau)\omega\tau}{1+\omega^2\tau^2} d\tau \qquad \text{Eq.(4.3-5)}$$

where

$$\Delta\varepsilon''_B(T) = \sum_i \Delta\varepsilon''_{B,i}(T) = \sum_i \sum_j n_j f_{ij} \Delta\varepsilon_j''(T-T_{ij})$$

$$\rho_{B,T}(\tau) = \sum_i P_{B,i} \rho_{B,i,T}(\tau)$$

$$P_{B,i} = \frac{\Delta\varepsilon''_{B,i}(T)}{\sum_i \Delta\varepsilon''_{B,i}(T)} = \frac{\sum_j n_j f_{ij} \Delta\varepsilon_j''(T-T_{ij})}{\sum_i \sum_j n_j f_{ij} \Delta\varepsilon_j''(T-T_{ij})}$$

The significance of Eq.(4.3-5) is that if the number of multiple phases is small and if a proper initial guess of fij is chosen, numerical fitting of $\varepsilon''_B(T)$ from $\varepsilon''_1(T)$ and $\varepsilon''_2(T)$ could yield the best least square fitted value of fij as well as oscillator strength and mean relaxation time of each contributing phase to the total loss peak.

4.4 Miscible Binary Blend

Application of Eq.(4.3-5) with a single phase constraint yields

$$\varepsilon''_B(T) = n_1\,\varepsilon''_1(T-T_1) + n_2\,\varepsilon''_2(T-T_2) \qquad \text{Eq.(4.4-1)}$$

where T_1 and T_2 are the shift scales tentatively determined by the lever rule

$$\begin{aligned} T_1 &= n_2(T_{c,2}-T_{c,1}) \\ T_2 &= n_1(T_{c,1}-T_{c,2}) \end{aligned} \qquad \text{Eq.(4.4-2)}$$

where $T_{c,1}$ and $T_{c,2}$ are the temperatures of maximum dielectric loss permittivity of pure components 1 and 2 respectively at a given frequency. Practically $T_{c,1}$ and $T_{c,2}$ can be considered as fitting parameters which gives the best fit of $\varepsilon''_B(T)$ from $\varepsilon''_1(T)$ and $\varepsilon''_2(T)$ according to Eq.(4.4 -1). Then,

$$\begin{aligned} \varepsilon''_B(T) &= n_1\,\Delta\varepsilon''_1(T-T_1)\int_0^\infty \frac{\rho_{1,T-T_1}(\tau)\omega\tau}{1+\omega^2\tau^2}d\tau \\ &\quad + n_2\,\Delta\varepsilon''_2(T-T_2)\int_0^\infty \frac{\rho_{2,T-T_2}(\tau)\omega\tau}{1+\omega^2\tau^2}d\tau \\ &= \Delta\varepsilon''_B(T)\int_0^\infty \frac{\rho_{B,T}(\tau)\omega\tau}{1+\omega^2\tau^2}d\tau \end{aligned} \qquad \text{Eq.(4.4-3)}$$

where

$$\Delta\varepsilon''_B(T) = \sum_i n_i\Delta\varepsilon''_i(T-T_i)$$

$$\rho_{B,T}(\tau) = \sum_i F_i\rho_{i,T-T_i}(\tau)$$

$$F_i = \frac{n_i\Delta\varepsilon''_i(T-T_i)}{\sum_i n_i\Delta\varepsilon''_i(T-T_i)}$$

From Eq.(4.4-3), the oscillator strength and mean relaxation time of the blend can be evaluated and compared with values determined by the experiment since,

$$\begin{aligned} \langle\tau\rangle_{B,T} &= \int_0^\infty \tau\rho_{B,T}(\tau)d\tau = \int_0^\infty \tau[F_1\rho_{1,T-T_1}(\tau) + F_2\rho_{2,T-T_2}(\tau)]d\tau \\ &= F_1\langle\tau\rangle_{1,T-T_1} + F_2\langle\tau\rangle_{2,T-T_2} \end{aligned} \qquad \text{Eq.(4.4-4)}$$

Eq.(4.4-4) tells us that the mean relaxation time of the blend at temperature T can be obtained from the linear sum of individual mean relaxation times at other temperatures with a scaling factor which encompasses two important variables, mole fraction and oscillator strength.

4.5 Closely Associated Multiple Relaxations from Homopolymer

When closely associated multiple relaxations arise from a homopolymer, the pure component behavior is not known a priori as in the case of blending two known polymers. In this case, the mole fraction of an individual peak becomes unnecessary and the dielectric loss of the total peak at temperature T is simply the sum of individual peaks.

$$\varepsilon''_{total}(T) = \varepsilon''_1(T) + \varepsilon''_2(T) \qquad \text{Eq.(4.5-1)}$$

then,

$$\varepsilon''_{total}(T) = \Delta\varepsilon''_1(T) + \Delta\varepsilon''_2(T) \int_0^\infty \frac{[f_1\rho_1(\tau) + f_2\rho_2(\tau)]\omega\tau}{1+\omega^2\tau^2} d\tau$$

$$\text{where} \quad f_i = \frac{\Delta\varepsilon''_i(T)}{\Delta\varepsilon''_1(T) + \Delta\varepsilon''_2(T)} \qquad i = 1 \text{ or } 2 \qquad \text{Eq.(4.5-2)}$$

and

$$\langle\tau\rangle_{total} = f_1\langle\tau\rangle_1 + f_2\langle\tau\rangle_2$$

As the proposed empirical model is linear in nature, the Kramers-Kronig relation should hold for the total curve which has been constructed by this model. In order to show this point, first, it is necessary to derive some relations regarding the total curve from linear viscoelastic theory developed in section 2.1.3.

From Eq.(4.5-1) and Eq.(2.1.3-12) at given ω and T,

$$\varepsilon''_{total}(\omega) = \varepsilon''_{A}(\omega) + \varepsilon''_{B}(\omega)$$

$$= \int_0^\infty \sin\omega t[-\Delta\varepsilon_A \frac{d\Phi_A(t)}{dt}]dt + \int_0^\infty \sin\omega t[-\Delta\varepsilon_B \frac{d\Phi_B(t)}{dt}]dt$$

$$= \int_0^\infty \sin\omega t\,[-(\Delta\varepsilon_A \frac{d\Phi_A(t)}{dt} + \Delta\varepsilon_B \frac{d\Phi_B(t)}{dt})]dt$$

using Eq.(4.5-2) by noting 1, 2 as A, B

$$= \int_0^\infty \sin\omega t\,[-(\Delta\varepsilon_A+\Delta\varepsilon_B)\{ f_A\frac{d\Phi_A(t)}{dt} + f_B\frac{d\Phi_B(t)}{dt}\}]dt$$

$$\varepsilon''_{total} = \int_0^\infty \sin\omega t[-\Delta\varepsilon_{total} \frac{d\Phi_{total}(t)}{dt}]dt$$

This result justifies

$$\Phi_{total}(t) = f_A\Phi_A(t) + f_B\Phi_B(t) \qquad \text{Eq.(4.5-3)}$$

For the storage permittivity of the total curve, Eq.(2.1.3-11) and Eq.(4.5.3) give

$$\frac{\varepsilon'_{total}(\omega) - \varepsilon_{\infty,total}}{\Delta\varepsilon_{total}} = \int_0^\infty \cos\omega t\,[-(f_A\frac{d\Phi_A(t)}{dt} + f_B\frac{d\Phi_B(t)}{dt})]dt$$

$$= f_A\int_0^\infty \cos\omega t\,[-\frac{d\Phi_A(t)}{dt}]dt + f_B\int_0^\infty \cos\omega t\,[-\frac{d\Phi_B(t)}{dt}]dt$$

$$= f_A[\frac{\varepsilon'_A(\omega) - \varepsilon_{\infty,A}}{\Delta\varepsilon_A}] + f_B[\frac{\varepsilon'_B(\omega) - \varepsilon_{\infty,B}}{\Delta\varepsilon_B}]$$

then

$$\varepsilon'_{total}(\omega) - \varepsilon_{\infty,total} = \varepsilon'_A(\omega) - \varepsilon_{\infty,A} + \varepsilon'_B(\omega) - \varepsilon_{\infty,B} \qquad \text{Eq.(4.5-4)}$$

The validity of empirical formalism in the Kramers-Kronig relationship (Eq.(2.1.5-3)) requires that once

$$\frac{\varepsilon'_A(\omega) - \varepsilon_{\infty,A}}{\Delta\varepsilon_A} = \frac{2}{\pi}\int_0^\infty \left[\frac{\varepsilon''_A(\nu)}{\Delta\varepsilon_A}\cdot\frac{\nu}{\nu^2-\omega^2}\right]d\nu$$
$$\frac{\varepsilon'_B(\omega) - \varepsilon_{\infty,B}}{\Delta\varepsilon_B} = \frac{2}{\pi}\int_0^\infty \left[\frac{\varepsilon''_B(\nu)}{\Delta\varepsilon_B}\cdot\frac{\nu}{\nu^2-\omega^2}\right]d\nu \qquad \text{Eq.(4.5-5)}$$

or

$$\frac{\varepsilon''_A(\omega)}{\Delta\varepsilon_A} = \frac{2}{\pi}\int_0^\infty \left[\frac{\varepsilon'_A(\nu) - \varepsilon_{\infty,A}}{\Delta\varepsilon_A}\cdot\frac{\omega}{\omega^2-\nu^2}\right]d\nu$$
$$\frac{\varepsilon''_B(\omega)}{\Delta\varepsilon_B} = \frac{2}{\pi}\int_0^\infty \left[\frac{\varepsilon'_B(\nu) - \varepsilon_{\infty,B}}{\Delta\varepsilon_B}\cdot\frac{\omega}{\omega^2-\nu^2}\right]d\nu \qquad \text{Eq.(4.5-6)}$$

holds for the component, it should hold for the total curve.

Linear additivity of loss says

$$\varepsilon''_{total}(\omega) = \varepsilon''_A(\omega) + \varepsilon''_B(\omega)$$

From Eq.(4.5-6)

$$= \frac{2}{\pi}\int_0^\infty \left[\{\varepsilon'_A(\nu) - \varepsilon_{\infty,A} + \varepsilon'_B(\nu) - \varepsilon_{\infty,B}\}\cdot\frac{\omega}{\omega^2-\nu^2}\right]d\nu$$

The quantity inside the braces has already been found to have the relation of Eq.(4.5-4), thus

$$= \frac{2}{\pi}\int_0^\infty \left[\{\varepsilon'_{total}(\nu) - \varepsilon_{\infty,total}\}\cdot\frac{\omega}{\omega^2-\nu^2}\right]d\nu \qquad \text{Eq.(4.5-7)}$$

Dividing both sides of Eq.(4.5-7) by $\Delta\varepsilon_{total}$ gives the Kramers-Kronig relationship as

$$\frac{\varepsilon''_{total}(\omega)}{\Delta\varepsilon_{total}} = \frac{2}{\pi}\int_0^{\infty}\left[\frac{\varepsilon'_{total}(\nu) - \varepsilon_{\infty,total}}{\Delta\varepsilon_{total}}\cdot\frac{\omega}{\omega^2-\nu^2}\right]d\nu \qquad \text{Eq.(4.5-8)}$$

Note that Eq.(4.5-8) has same form as Eq.(4.5-6). As such, the total loss curve obeys the Kramers-Kronig relation, which is predictable since the empirical model proposed is linear in nature.

Chapter 5. Dielectric Relaxation of Poly(3-hydroxybutyrate)

5.1 Literature Review of Poly(3-hydroxybutyrate)

5.1.1 Introduction

Recently, due to ever increasing environmental awareness, significant efforts have been made to utilize biodegradable polymers in producing disposable products. Poly(3-hydroxybutyrate) (PHB) (Figure 9) is a good candidate for such an approach since it is intrinsically a nutrient for bacteria.[61] It can be attacked by a wide variety of bacteria and its application possibilities are numerous in medical, packaging, and agricultural fields.[62] PHB was first discovered by Lemoigne[63] in 1927. When certain bacteria are placed under poor nutrient conditions, these bacteria produce PHB as an energy storage chemical and use it again when growth resumes in nutritionally favorable conditions. PHB is mass produced usually by a fermentation process.[64] Remarkably, quite recent news reports that when a certain type of weed called mouse-eared cress is implanted with special genes from bacteria, it produces PHB in its tissues.[65] Its implication is that harvesting plastics from plants is not totally impossible. Also it is said that efforts are being made by scientists to produce PHB at a cost which is one hundredth of that of the conventional fermentation process using this biologically engineered plant approach.

PHB is a highly crystalline thermoplastic which is optically active[66] and piezoelectric.[67] Its crystallinity can vary from 60 to 90 % depending on its preparation and physical treatment such as annealing.[68] Glass transition[68] of PHB is reported in the range of -5 to 5°C and its melting point is around 180°C. PHB is polymorphic and exists in α and β crystalline forms.[69] The β form is generated by the orientation process of film so the β form is believed to be a result of strain induced crystallization of the amorphous regions. The biggest problem in utilizing PHB as an industrially useful thermoplastic lies in its brittle mechanical properties which have been ascribed to the

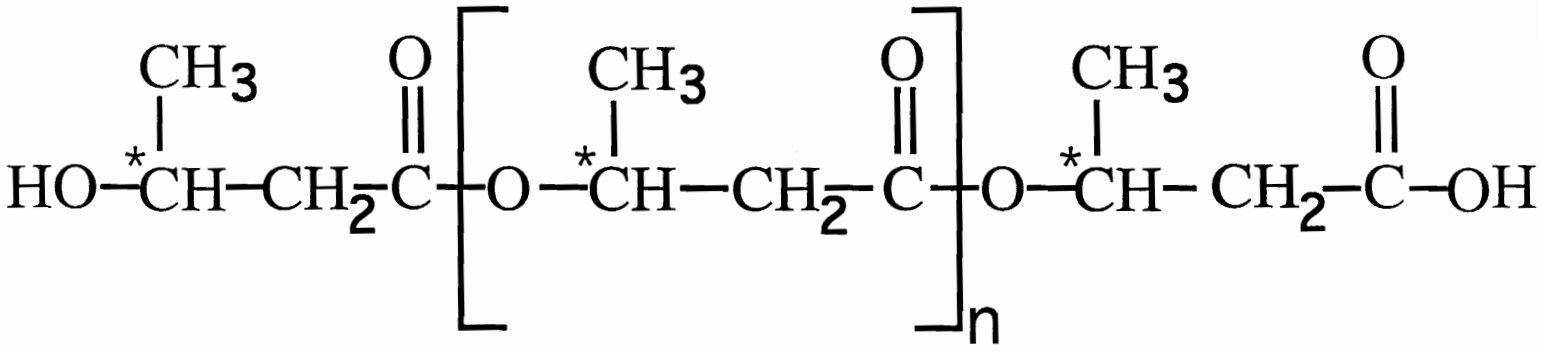

Figure 9. **Structure of Poly(3-Hydroxybutyrate),**
R absolute configuration [D(-) in traditional nomenclature]

cracks already present in its spherulites.[70] There have been numerous research efforts in the hope of overcoming this problem. Notables among them are copolymerization[71-76] and blending PHB with secondary components.[77-85] No matter what type of approach is taken, the cost of production (in the case of the synthetic approach), biodegradability (of the blending alternative), and mechanical toughness obtained out of such efforts should be always balanced and maximized to attain ultimate success.

5.1.2 Characterization of Poly(3-hydroxybutyrate)

In this section, several efforts to characterize PHB which could serve as cross-references for future work are reviewed in chronological order.

In 1981, Marchessault et al[86] measured the melting point of PHB from oligomer size (4 repeating units) to polymer (994 repeating units). Their Small Angle X-ray diffraction experiment revealed that "cold drawn" and "hot drawn" fibers showed distinctively different behavior in the meridional maximum.

Barham[68] carried out a crystallization study of PHB from its molten state. He pointed out PHB's special properties such as its having large spherulites. This was attributed to the high purity of biologically synthesized PHB. Unusual crystal habits, extreme thinness of lamellae, and the possible Regime II to III transition were mentioned in this work. In his next paper[87], Barham, showed that the nucleation behavior of PHB is sporadic and consistent with a homogeneous process. When foreign particles are added the rate of nucleation behavior is found to be modified and this effect is explained in two ways. One is that the local crystal melting point is raised due to the constraints of the actual presence of a surface, and the other is that epitaxial growth occurs on the foreign surface. Also Barham and Keller[70] investigated the relationship between micro-structure and mode of fracture in PHB. The famous brittleness of PHB was attributed to cracks

within the spherulites. They pointed out that these cracks form under conditions of no externally applied stress, hence the cracks were found to arise from thermally induced stress. Based on this observation, they suggested two possible ways of producing ductile PHB sheets: first, by mending the cracks by a cold rolling process; second, by special crystallization conditions.

In 1988, Scandola et al[88] studied the viscoelastic and thermal properties of PHB. It was found from thermogravimetric analysis that unless Mv is lower than $6x10^4$, significant weight loss occurs at temperatures above 230°C. From Differential Scanning Calorimetry, the "room stored" samples' Tm was found to be 177°C and its area increases with annealing. The viscoelastic spectrum obtained from Dynamic Mechanical Thermal Analyzer (frequency 0.33 to 33 Hz) showed three relaxations: a water related low temperature relaxation (-80°C), the glass transition and a broad relaxation in the temperature range between Tg and Tm due to motion in the crystalline phase. They also speculated that the effect of physical aging during storage would affect the solid state properties of PHB. The aging time of their sample was stated as "several weeks" and was not further clarified.

In 1989, Revol et al[89] visualized the lattice planes of PHB, which are highly beam sensitive, using high-resolution electron microscopy. From lattice images having a resolution of 0.35 nm, a simple Fourier averaging performed optically generated an image of the crystal projected along its fiber axis. The lattice image provided a molecular-level picture of the elliptical PHB cross-section with rows of alternating orientation clearly identifiable, as in the X-ray unit cell packing.

For the method of biodegradation, Doi provided a valuable reference.[90]

In 1992, Owen et al[91] studied the crystallization behavior of PHB using optical microscopy, Wide Angle X-ray scattering and calorimetric measurement. It was shown

that subtle changes occur when PHB is heated. They speculated that there was some melting and structural reorganization at temperatures well below the main melting region based on the appearance of melting peaks which were dependent on the heating rate in their Differential Thermal Analysis experiment. On heating PHB, optical polarizing microscopy detected only a gradual decrease of birefringence but distinctive spherulite types were not observed. This work remains to be further researched by the authors.

Burger et al[92] used mass spectrometric analysis based on matrix-assisted laser desorption and ionization to study the molecular weight distribution of PHB whose molecular weight was less than 10,000. This approach allowed the characterization of oligomer distributions obtained by partial depolymerization of PHB through pyrolysis or treatment with bases. Comparison of the results with the data from gel permeation chromatography showed that with some limitations, both methods yielded similar results. The motive of this research was the potential applications of PHB oligomers (a) as plasticizers for high molecular weight PHB, (b) for drug delivery systems or (c) for the synthesis of block copolymers. Although not as effective as gel permeation chromatography when molecular weight distribution is broad, this method has advantages in that its procedure is simple and that it provides chemical structure information together with molecular weight distribution.

5.2 Dielectric Study of Poly(3-hydroxy butyrate)

5.2.1 Sample Preparation

The PHB used in this study was an industrial sample of biological origin. In the final stage of the fermentation process, the PHB was centrifuge dried and had an extremely fine powder form with a diameter less than a micron and it did not show any sign of aggregation to the naked eye. No additives such as fillers, plasticizers, or heat

stabilizers were present in the particular batch provided for this study. Its intrinsic viscosity in chloroform at 30°C was 3.9 (dl/g) which corresponds to a viscosity average molecular weight of about 622 kg/mol.[93]

Neat PHB powder was transformed into a solid chunk using a Brabender melt blender with cam blades and a type-6 measuring head. The operation conditions are specified in Table 3. This melt process is necessary for two reasons. First, it is almost impossible to make self-standing films without micro bubbles directly within the press by consolidating powder when the powder is extremely fine. If a long press time is used, thermal degradation is highly probable. Second, samples prepared in this way can serve as control samples for PHB blends produced by melt process.

PHB film with a diameter of about 20 cm and a thickness of about 0.3 mm was made using a press at 185°C. Even though the press setting temperature was 185°C, due to the thermal gradient between the plates of the press and the ferro-type mold covered with aluminum foil, the actual temperature at the surface of PHB chunk was lower than 185°C. The press work was done such that as soon as the surface of the PHB chunk started to melt, continuous pressure was applied to keep a constant surface renewal process, hence minimizing thermal degradation. When both the upper and bottom plates of the press met, pressure was increased. At that moment, pressure was rapidly increased to 100psi, kept 5 seconds at that pressure, and then the mold was moved into a cooling press. Cooling was done for 5 minutes at 18°C. The PHB film thus prepared had a pancake shape and it was stored in a sealed container for the experiment.

5.2.2 Experimental Conditions

Stress-strain experiment:

After one day of annealing at room temperature, dog bone shaped specimens were prepared using an ASTM-D3368 die. The stress-strain experiment was done with a

Table 3.

Melt processing conditions of poly(3-hydroxybutyrate)

Total Charge Weight (g)	60
Setting Temperature of Blender (°C)	175
Actual Melt Temperature (°C)	min. 175 max. 185
R.P.M. & Blending time charge period blending	 10 for 1 min. 50 for 1 min. 80 for 2 min.

Notes:

Blender:	Brabender Plasticoder
Measuring Head:	Type-6
Mixing Blades:	Cam type

miniature material tester made by Polymer Laboratories. Test conditions and time dependent stress-strain behavior are shown in Table 4 and Figure 10 respectively.

Density measurement:

Density change over time was measured with a density gradient column which used a water-sodium bromide solution.[94] The density gradient of solution ranged from 1.1426 to 1.2672 (g/cc). For each experiment, a PHB chunk out of the melt blender was sliced into two thin samples, one from the skin and the other from the core. The samples were placed in the column and after 14 hours the height was measured and calibrated against the standard density floats. Samples were swollen 0.86% on average. In order to convert density information into %crystallinity, Barham's data for the density of the crystalline and amorphous phases, 1.260 and 1.177 (g/cc) respectively, were used.[68] The results are shown in Figure 11 and Table 5.

Dielectric Measurement:

Two sets of experiments were done.

[Set A]:

One set of experiments was performed during the summer when the relative humidity of the laboratory was 50 +/- 5%. A wide temperature range of -130 to 130°C was used heating at a rate of 1°C/min. The frequency range was from 0.5 to 50kHz and disk electrodes with diameter of 20 mm were used.

[Set B]:

The second set of experiments was done during the winter when the relative humidity was 25 +/- 5 %. The temperature range used was from -60 to 130°C at a heating rate of 0.5°C/min. The frequency range was 0.2 to 28kHz and disk electrodes

Table 4.

Stress-Strain experimental conditions

Cross-head rate (mm/min.)	2
Specimen type	ASTM-D3368
Apparatus	Miniature Material Tester (Polymer Laboratory)

Time dependent Stress-Strain behavior

	2nd day	13th day	34th day
Maximum Stress at break (MPa)	72(3.4)	80(6.54)	80.4(2.87)
Maximum Strain at break (%)	3.8(0.4)	2.9(0.2)	2.9(0.2)

Note: Values inside the parentheses indicate standard deviation of 5 samples

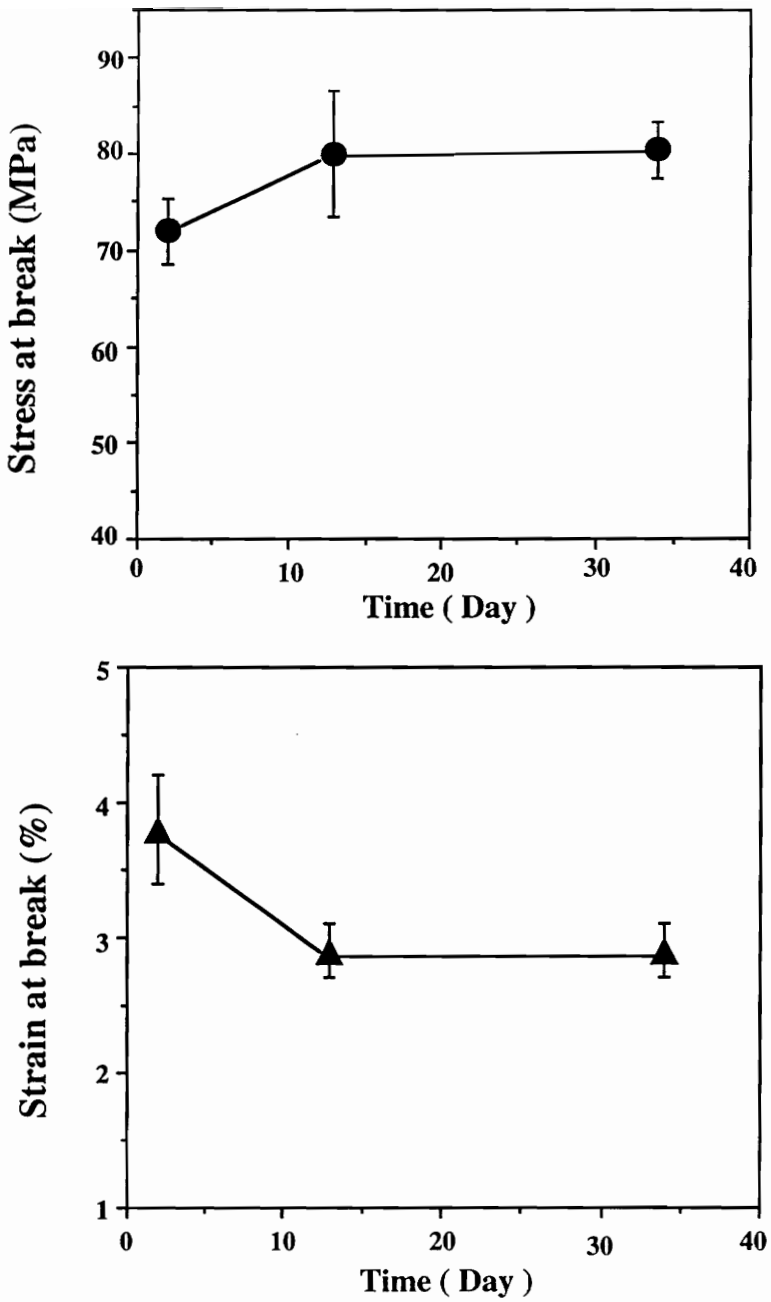

Figure 10. **Time dependent stress-strain behavior of poly(3-hydroxybutyrate)**

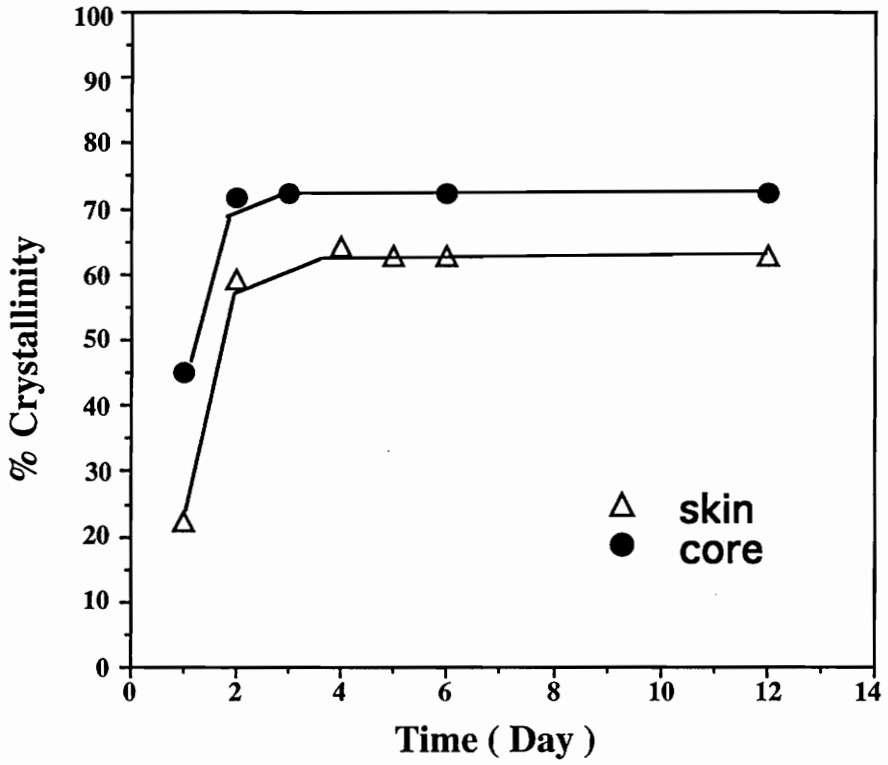

Figure 11. **Time dependent %crystallinity of poly(3-hydroxybutyrate)**

Table 5.

Time dependent density of poly(3-hydroxybutyrate)

Time (day)	PHB skin	PHB core
1	1.1957	1.2144
2	1.2262	1.2304
3		1.2372
4	1.2302	
5	1.2290	
6	1.2290	1.2340
12	1.2340	1.2372

Time dependent %crystallinity poly(3-hydroxybutyrate)

Time (day)	PHB skin	PHB core
1	22.5	45.1
2	59.3	71.6
3		72.5
4	64.1	
5	62.7	
6	62.7	72.5
12	68.7	72.5

with a diameter of 33 mm was used. In the second set of experiments, an accelerated annealing experiment was performed in addition to a room temperature annealing experiment.

Samples for stress -strain and dielectric measurement were cut out of a pancake shaped film in a symmetric fashion as shown in Figure 12.

5.2.3 Data Reduction Procedure

Since storage and loss dielectric properties are related to each other via a Kramers-Kronig relation, data reduction was concentrated on the loss property. The data reduction procedure began with nonlinear curve resolution of dielectric loss permittivity since all data showed multiple relaxation peaks together with d.c. conductivity. For this purpose, a Levenberg-Marquardt algorithm was used (Appendix A). A custom-made program was developed to handle multiple Gaussian peaks with an exponential baseline (Appendix B-1).

Next, evaluation of empirical distribution function parameters was done using the Havriliak-Negami or the Cole-Cole type model whichever yielded lower chi-square values (Appendix B-3). Following the approach of Cook et al,[34] who do not consider the detailed mechanical motions of chains, no special model for chain dynamics or structural relaxation was preferred.

In the third step, the time decaying function or autocorrelation function was calculated. This process was done by half-sided cosine transformation and involved numerical integration of the loss permittivity function. This procedure had the advantage of being able to calculate the autocorrelation function by an analytical and well-known equation (Appendix C).

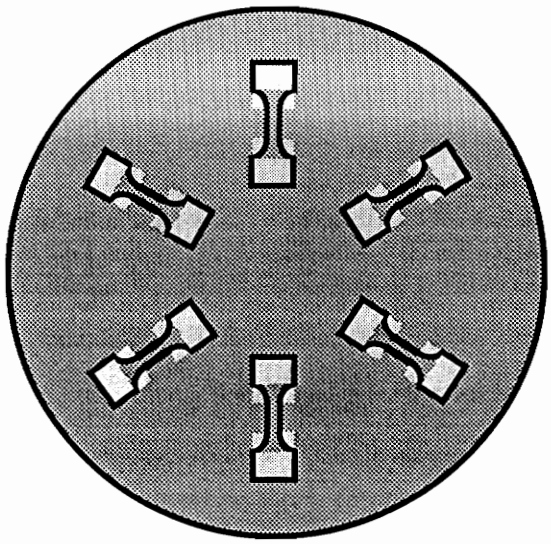

(a)

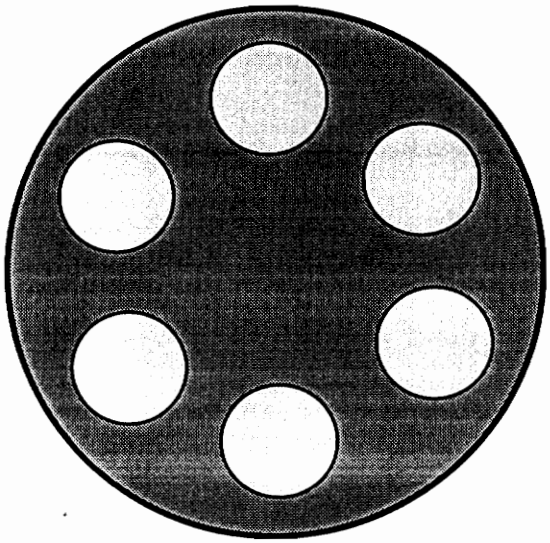

(b)

Figure 12. **Schematic: (a) samples for Stress-Strain experiment, (b) samples for dielectric thermal analysis**

Finally, to the resulting correlation functions, the empirical relation as given by the Kohlrausch-Williams-Watts (KWW) function was fitted (Appendix B-2). From the determined KWW parameters, the mean relaxation time was obtained.

5.3 Results and Discussions

5.3.1 General Considerations for the Interpretations of Data

In this section an attempt at a phenomenological study of the dielectric relaxation behavior of a melt processed PHB bulk sample will be made. After all the phenomenological analysis, the molecular meaning of relaxation peaks will be speculated. When the system to be studied by dielectric analysis has a single component, a single amorphous phase, monodisperse molecular weight distribution, and a sub-ambient glass transition temperature, hence no physical aging effect during the sample storage period (at room temperature) and within the experimental time scale, a molecular level interpretation is readily achieved. However, when the polymeric system of interest has multi-component, multi-phase (crystalline or cross-linked system), polydisperse molecular weight distribution, and an ambient or above room temperature glass transition temperature, hence the possibility of physical aging during the sample storage period and within the experimental time scale, molecular level interpretation can not be straightforward.

The system of present concern, melt processed PHB bulk sample, has a crystalline phase and its glass transition temperature changes during room temperature storage since the temperature range of glass transition and melting temperature encompasses room temperature. Hence, only phenomenological interpretation is suitable at the moment. If one studies kinetically fully developed PHB samples such as fully annealed, long time-stored samples, quite straight forward analysis of dielectric relaxation behavior is readily

achieved.[97] However, when one is interested in the crystallization behavior of PHB as a reference for any toughened PHB blend at a relatively early stage (within two weeks) or if one wants to study the dielectric relaxation behavior of PHB in order to correlate it with mechanical properties which are well known to become progressively brittle during shelf-life (Figure 10), the experimental conditions of a dielectric experiment should be close to "normal conditions", meaning room temperature storage with no exposure to extremely low pressure or high temperature. The thermal degradation behavior of PHB is appreciable, even when the temperature is well below that of degradation onset indicated by thermogravimetry, due to chain scission which is not reflected by a weight change because of the low volatility of oligomeric species.[98] Thermal degradation products, notably crotonic acid, can hinder observation of pure dielectric relaxation behavior of PHB. If samples to undergo dielectric analysis have to be stored at room temperature, water naturally becomes a concern. The effect of water on low temperature relaxations of polymers containing polar groups is already well known.[100-102] Water molecules, inevitably incorporated in the PHB sample used in this study, may have come from two stages of sample preparation. The first stage was when the weighing of PHB powder was followed by melt processing in the blender. The approximate time was a maximum of 5 minutes. In this stage, water molecules from ambient humidity adsorbed to the extremely fine PHB powder particles. When melt processing was performed, some of the water volatilized and escaped, but the majority of water was likely blended with PHB molecules. The second stage was when the sample was taken out of the sealed container to be installed in-between the disk electrodes. The approximate time taken for this stage was a maximum of 2 minutes. In this stage, water molecules from ambient humidity adsorbed on the surface of PHB film and these water molecules may not have desorbed completely during the nitrogen purge time (30 minutes) prior to actual data collection. The pancake shaped film prepared according to the method in section 5.2.1 was stored in

a sealed container which did not contain any active dehumidifying agent. There were three reasons for not using any active drying agent. First many drying agents are inorganic salts, and if PHB films are contaminated by these chemicals, additional or excessive noise in conductivity is possible. Second, if the sample were stored in a desiccator, escape of water molecules from the surface and interior of the PHB film through diffusion would be expected. This would cause difficulty in comparing the data of a freshly prepared sample with that of a long term shelf-life sample. As a third reason, one of the major conditions of sample storage for commercial products would be that drying agent would not be present. Thus, the observed dielectric relaxation behavior under the best conditions of this study would reveal room temperature relaxation of PHB which may be only coupled with the reorganization of water molecules with PHB molecules. The point of using the curve resolution scheme is to decouple this effect of water molecules, inevitably incorporated under the special condition of this study, in the low temperature relaxation behavior as well as the multiple relaxations due to the crystallization process in the glass transition region.

5.3.2 Time Dependent Behavior of Dielectric Loss Property

Initially, the time dependent behavior of dielectric loss property was investigated using a wide temperature range. The test conditions for this experiment are described in Set A (section 5.2.2). From Figure 13 to 17, dielectric loss permittivity over elapsing time is shown for a frequency of 2kHz to illustrate the point. In all these figures, experimental values are expressed with filled circles. After curve resolution, in general, four components of loss permittivity are found; the first one for low temperature relaxation centered ~ -70°C, the second one centered ~ -10°C, the third one centered around 20°C initially then 40°C later, and the fourth one d.c. conductivity. The glass transition region is composed of two relaxation peaks which will be referred to as LTP

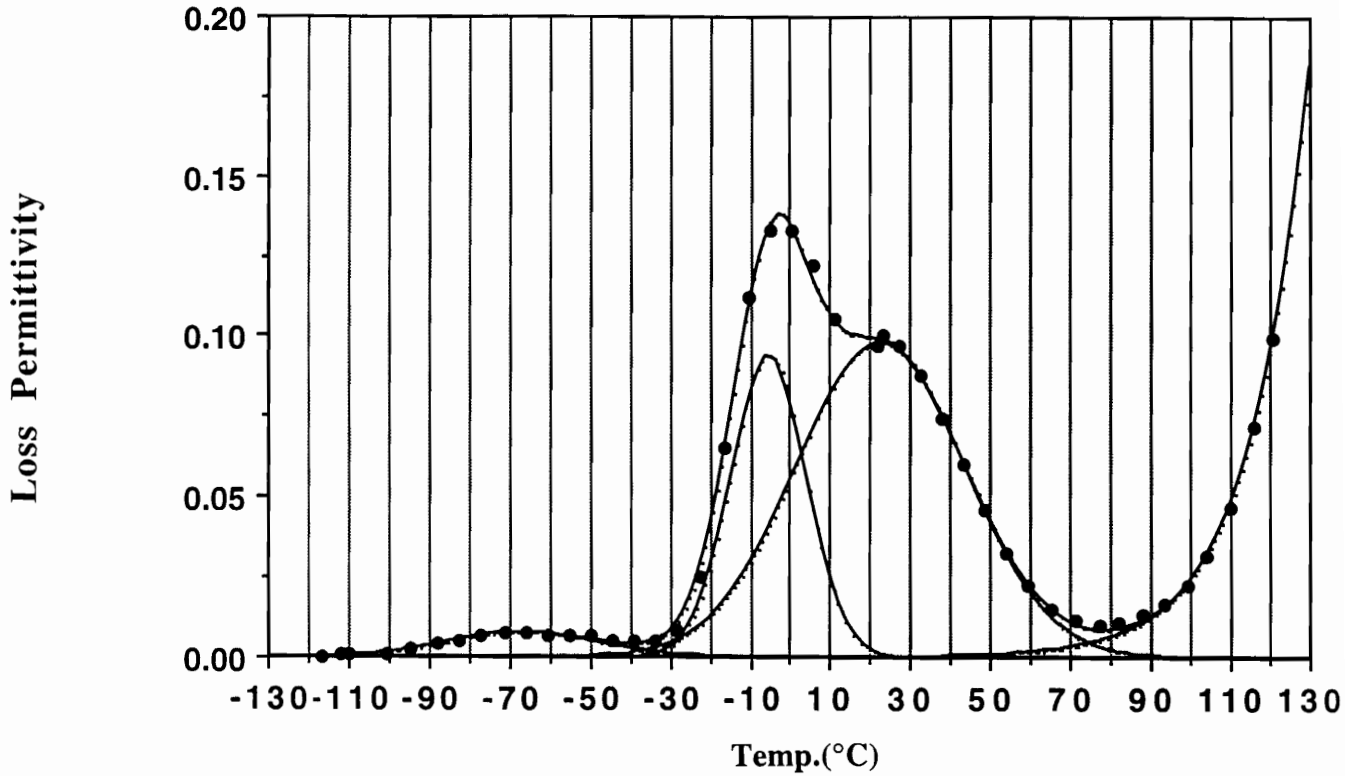

Figure 13. **Loss dielectric constant of PHB (1 hour, 2 kHz); filled circles for experimental data point**

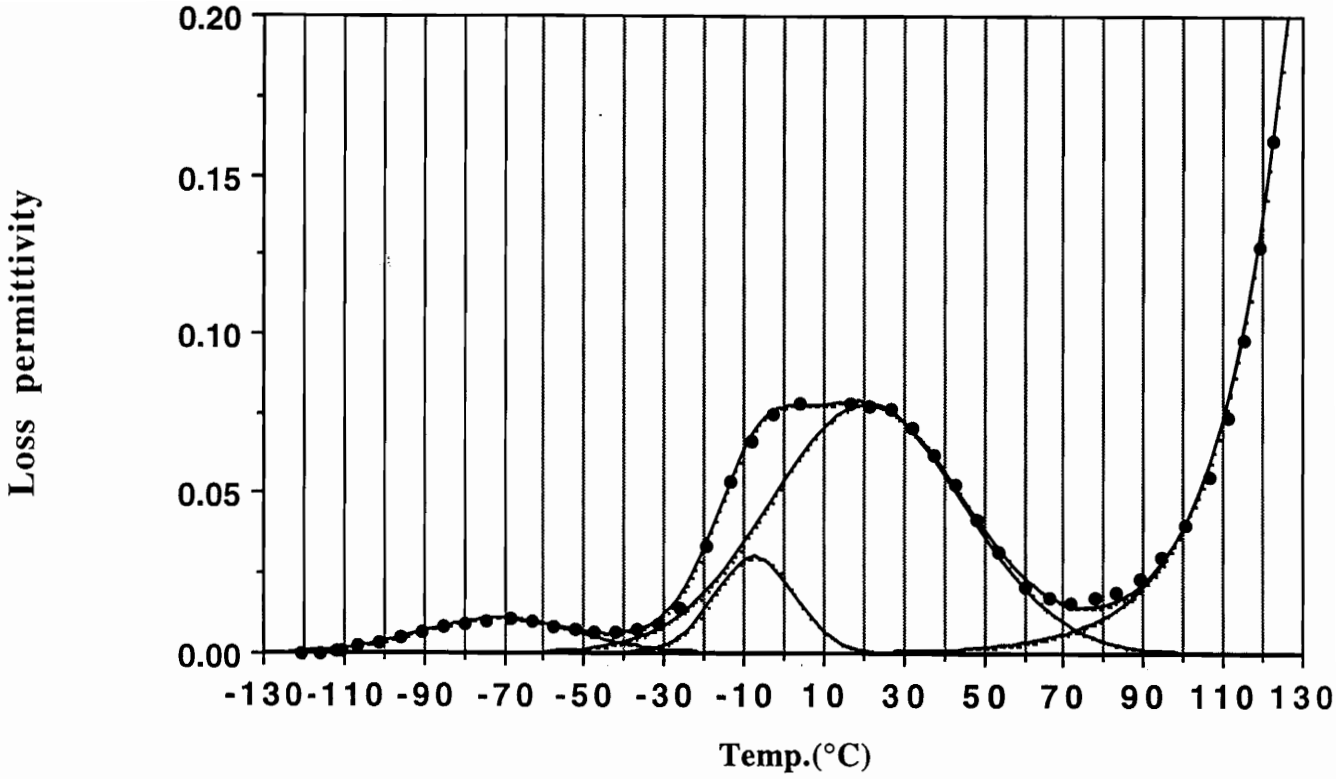

Figure 14. Loss dielectric constant of PHB (24 hours, 2 kHz); filled circles for experimental data point

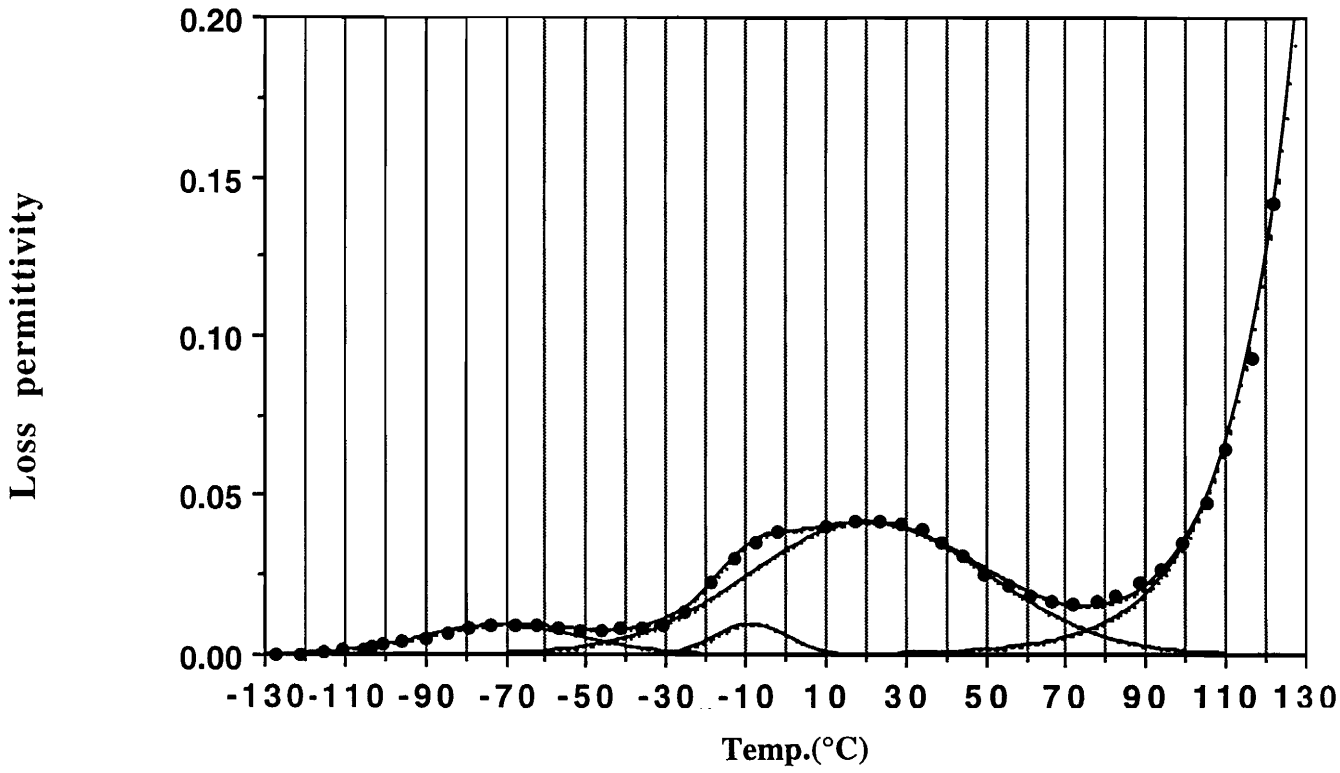

Figure 15. Loss dielectric constant of PHB (168 hours, 2 kHz); filled circles for experimental data point

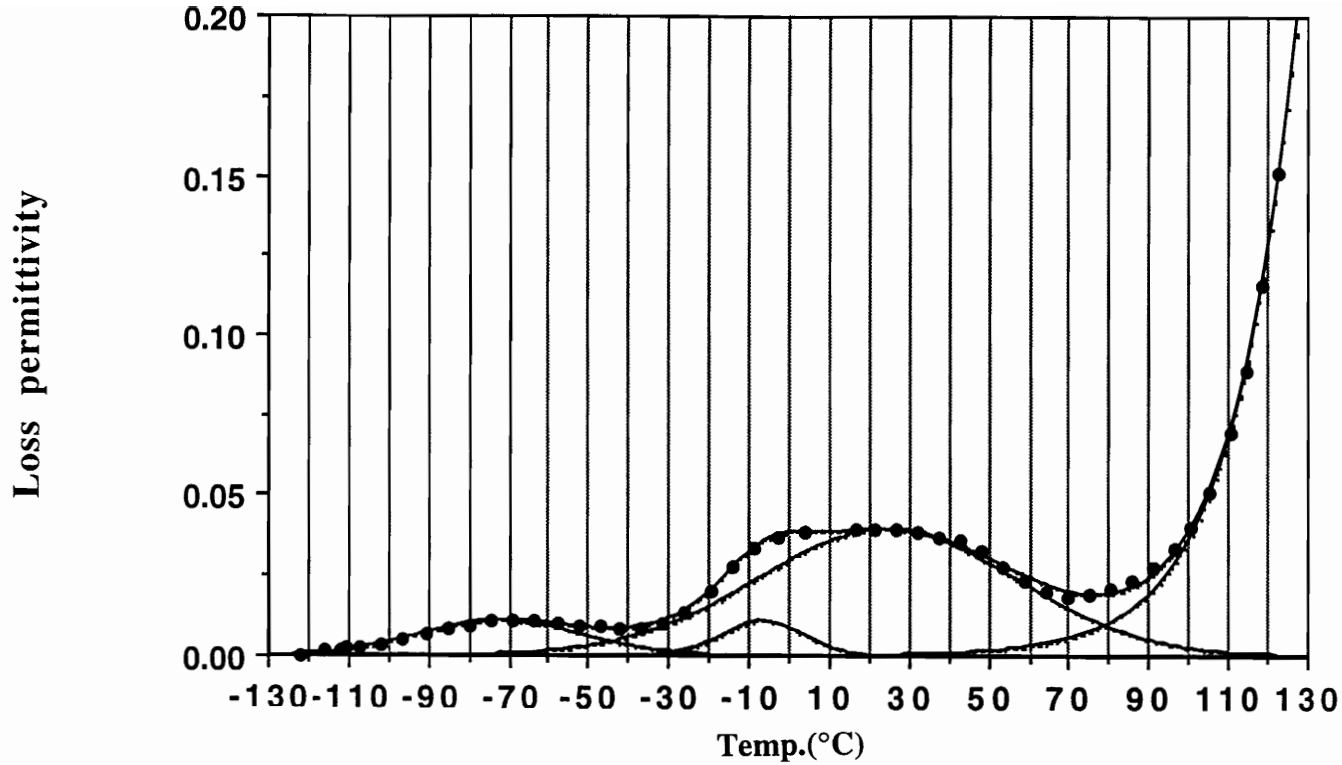

Figure 16. Loss dielectric constant of PHB (2 weeks, 2 kHz); filled circles for experimental data point

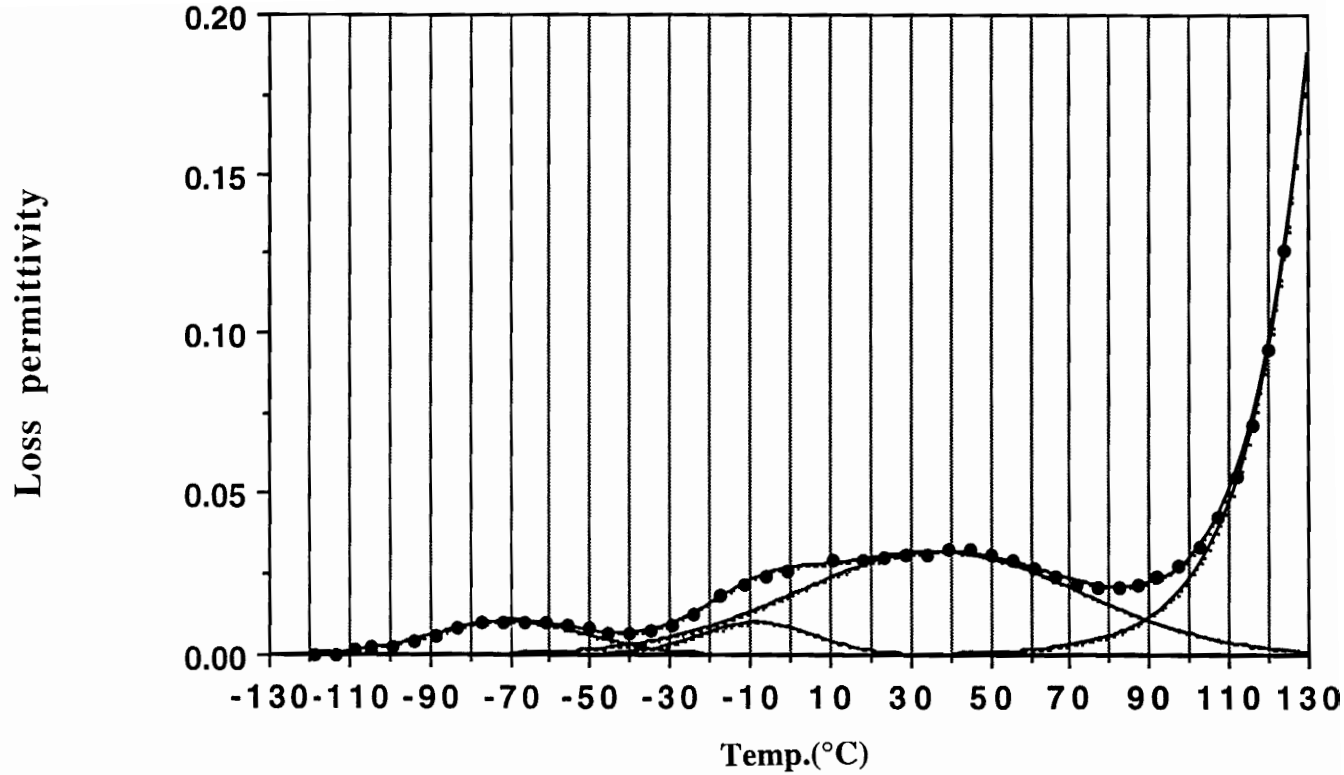

Figure 17. Loss dielectric constant of PHB (17 weeks, 2 kHz); filled circles for experimental data point

(relatively low temperature peak) and HTP (relatively high temperature peak), respectively. Overall, the magnitude of dielectric loss of both LTP and HTP are found to decrease over time. This observation is significant in that it means neither LTP nor HTP represent the relaxation behavior of chain segments directly attached to the surface of lamellae or spherulites. For the chain segments directly attached to the surface of lamellae or spherulites, the magnitude of dielectric loss should increase over time since the extent of crystallization increases over time (Figure 11). For such relaxations directly associated with a crystalline phase, the relaxation time is shorter than that of normal segmental motion and they are usually found at higher temperatures and frequencies.[6] Then, the obvious two peaks at/above the reported glass transition temperature of PHB are quite interesting at first glance since they are reasoned to be related to the amorphous phase, and yet the magnitude of HTP is growing bigger and broader relative to that of the LTP implying that HTP is related to the advancement of crystallization over time. In order to understand this phenomenon, the frequency dependence of dielectric loss permittivity of a fresh sample (whose 2kHz frequency data is as shown in Figure 13) was investigated. In Figure 18, overall loss behavior of the fresh sample is shown in a three dimensional view and frequency goes from low to high as the face of the cubicle goes from front to back. For the temperature range of -30°C to 70°C, the curve resolution results , LTP and HTP, for each frequency are shown in a three dimensional view in Figure 19. As the frequency increases, Figure 19 shows that the magnitude of LTP and HTP decreases and increases in an opposite manner and also crosses each other at around 0°C which is the reported glass transition temperature of PHB. In a magnified two dimensional plot, this observation is more clear (Figure 20). Usually the dielectric loss permittivity shows dispersion behavior in the temperature plane in such a manner that the loss maxima shift toward higher temperatures as the test frequency increases (Figure 21 and 22). Of course, the system depicted in Figure 21 and 22 is stable during the time

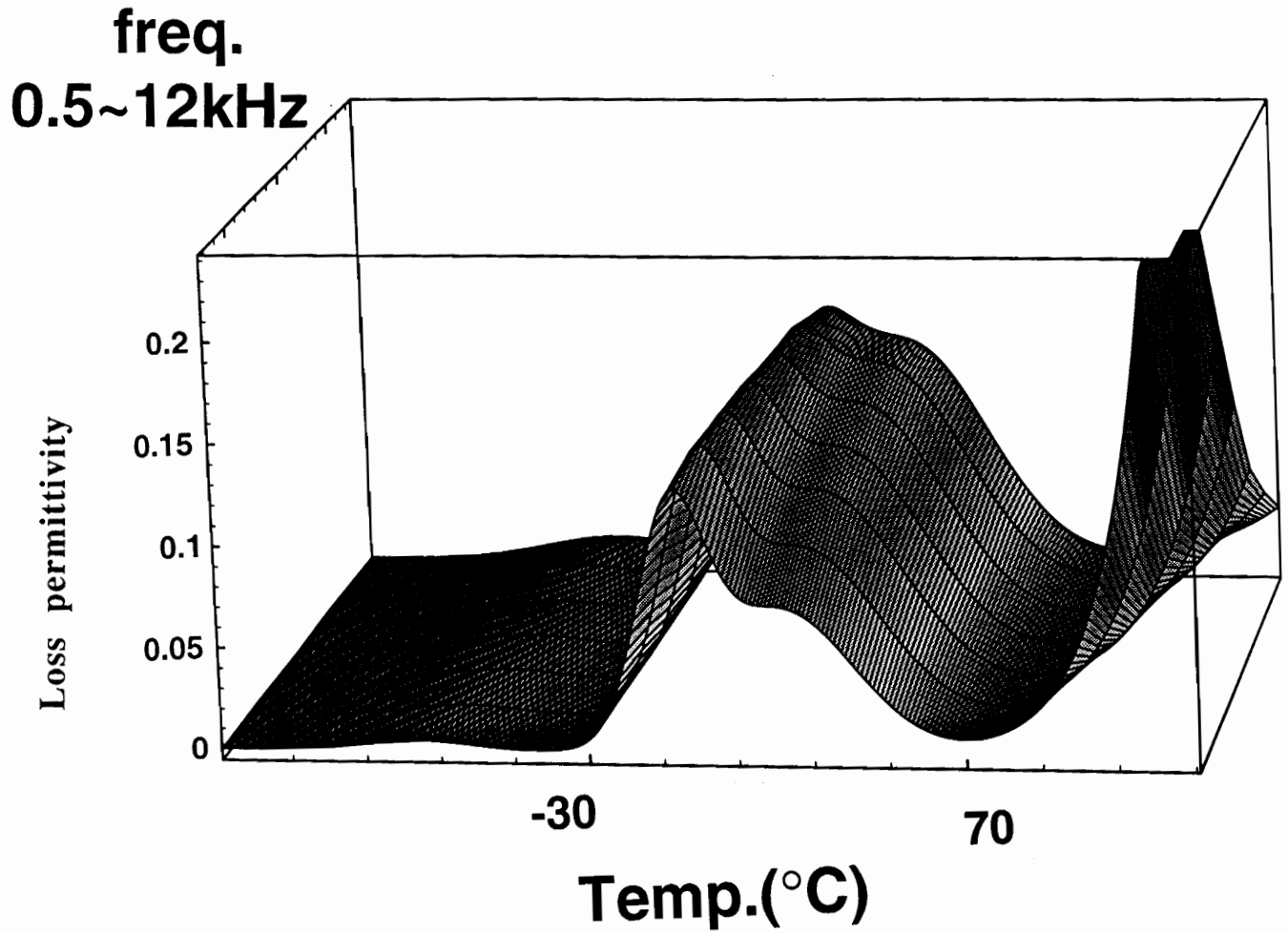

Figure 18. **Overall dielectric loss constant behavior of PHB (fresh sample, Set A), frequencies, 0.5, 1, 2, 3, 5, 7.5, 12 kHz from front to rear face of the cubicle**

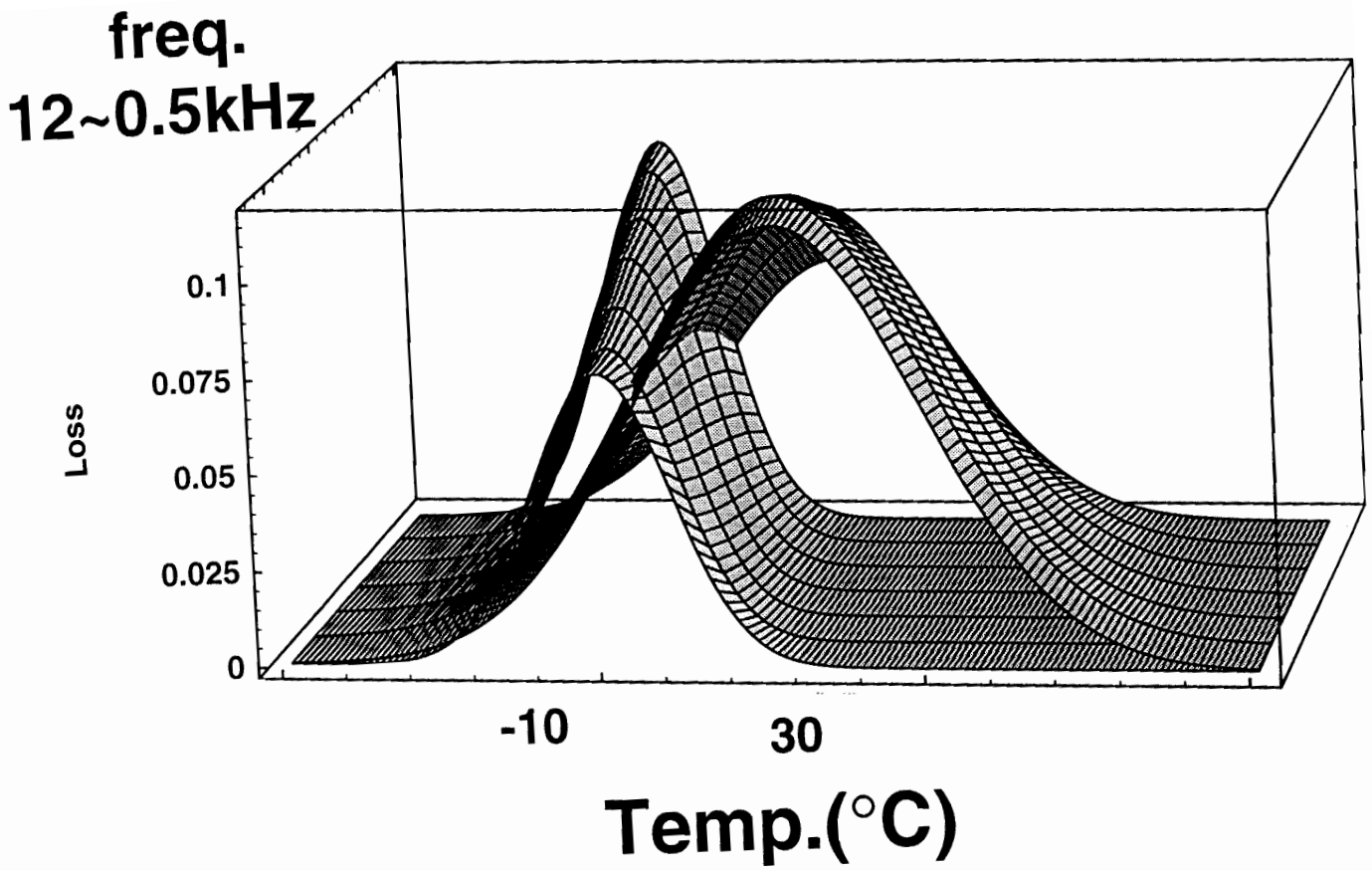

Figure 19. Temperature plane curve resolved 3-D view (fresh sample, Set A), frequencies, 0.5, 1, 2, 3, 5, 7.5, 12 kHz from rear to front face of the cubicle

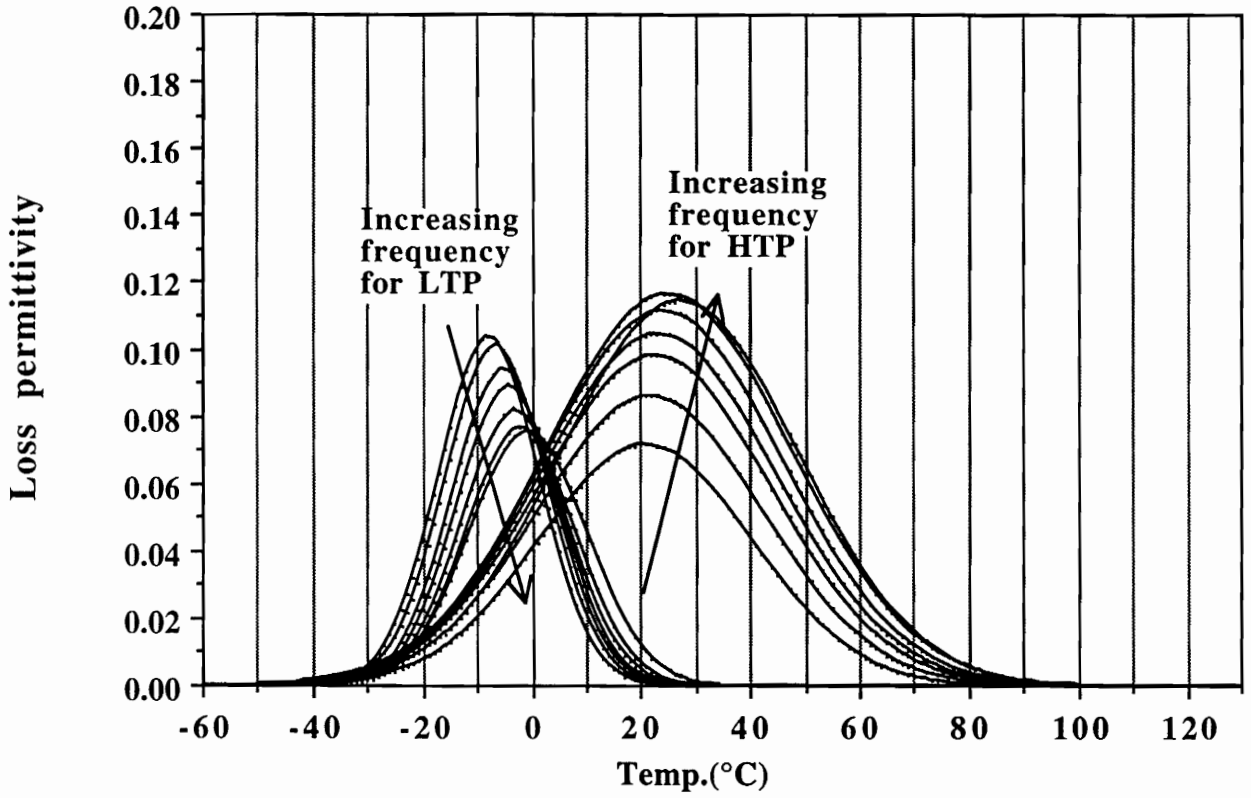

Figure 20. **Temperature plane curve resolved 2-D view (fresh sample, Set A), frequencies, 0.5, 1, 2, 3, 5, 7.5, 12 kHz in advancing T_{max} order for LTP and HTP**

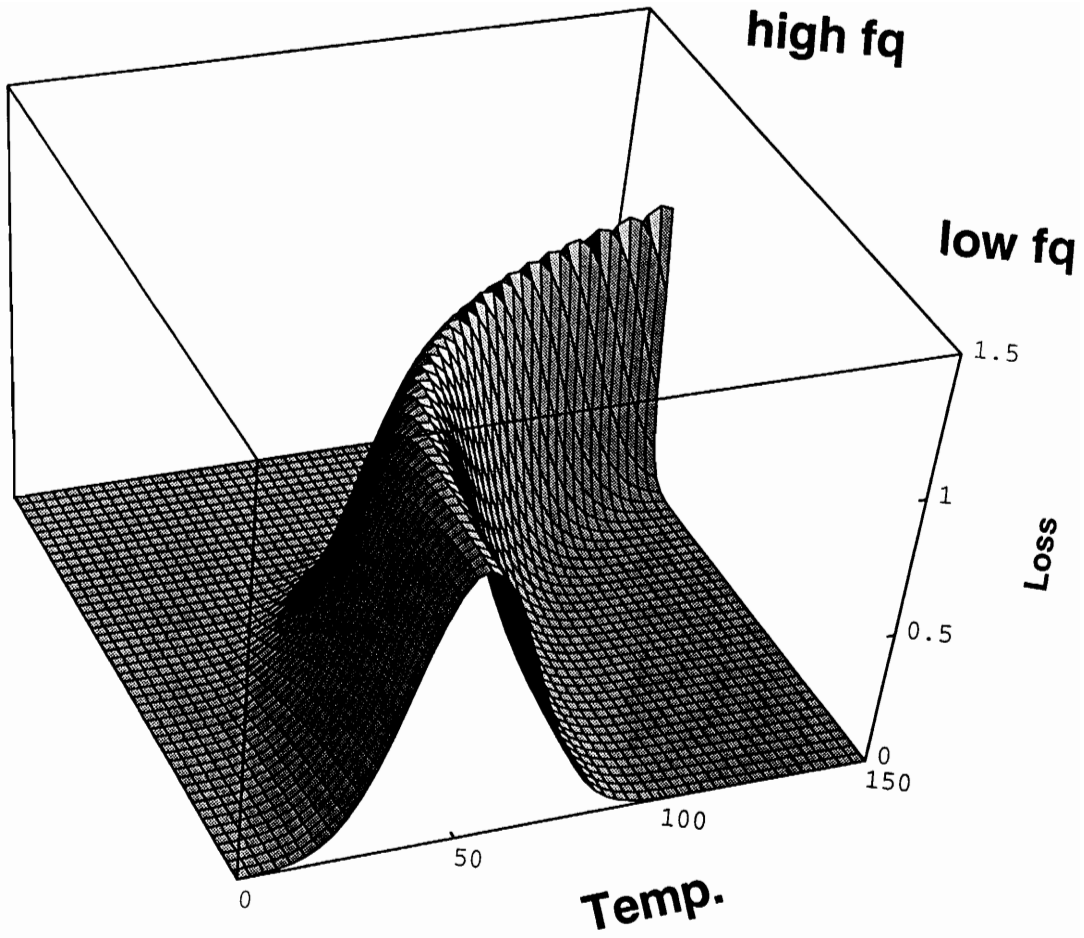

Figure 21. **Schematic: 3-D view of the dispersion of dielectric loss constant in general**

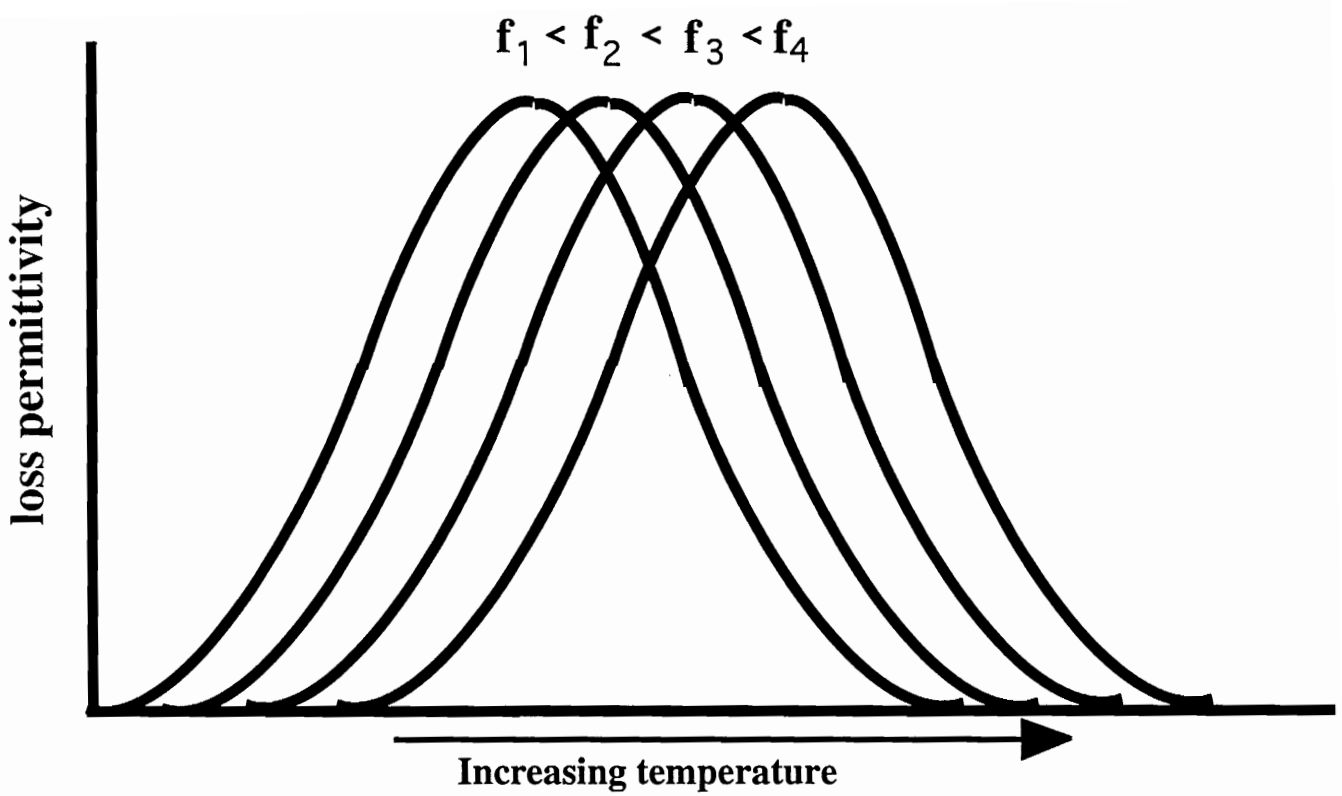

Figure 22. Schematic: 2-D view of the dispersion of dielectric loss constant in general. "f" stands for frequency

scale of the experiment. However, in this experiment (Figure 18 and 19), the system underwent crystallization during the experiment and the following reasoning is not rigorous but is a good enough approximation to show the point.

In a dielectric thermal analysis experiment which is performed dynamically, the analyzer acquires the capacitance of the sample in a sequential manner. While the analyzer is collecting the capacitance for each frequency of a given frequency set according to the pre-determined order set by the operating software, the heater is being controlled to produce linear temperature rise in the oven. If the heating rate is given as r_h, then

$$r_h = \frac{dT}{dt} \qquad \text{Eq.(5.3.2-1)}$$

The total amount of crystalline phase increases during the experiment which is the cause of the decrease in the dielectric loss. Let X_0 and X(t), be the %crystallinity of the sample at the starting time of the experiment and at any time t during the experiment respectively. Since temperature is programmed linearly with time, it is the same as stating that X_0 and X(t) are the %crystallinity of the sample at the starting temperature of experiment and at any temperature T during the experiment respectively. Then,

$$X(t) = \int_{t_0}^{t} \frac{dX(t)}{dt} \cdot dt$$

or

$$X(T) = \int_{T_0}^{T} \left(\frac{dX(t)}{dt}\right) \cdot \frac{dT}{r_h} \qquad \text{Eq.(5.3.2-2)}$$

The exact functional relation of increasing crystallinity with respect to time in this dynamic heating situation under an electric field is not known. However, it is certain that as the temperature of the oven gets closer to the glass transition temperature, the rate of

the crystallization process increases due to the increase in free volume. For example, if the crystallization rate is linear with respect to increasing temperature,

$$r_X = \frac{dX(t)}{dt} = kT, \qquad k = \text{constant}$$

$$X(T) = \int_{T_0}^{T} kT \cdot \frac{dT}{r_h}$$

$$X(T) = \int_{T_0}^{T} kT \cdot \frac{dT}{r_h} = \frac{k}{2r_h}[T^2 - T_0^2] \qquad \text{Eq.(5.3.2-3)}$$

This last equation shows the nonlinear behavior of the extent of crystallization with respect to temperature. In Figure 23, the peaks drawn with the thin and thick lines are those of low frequency and high frequency respectively in ideal measurement. As the temperature is increased, the dielectric loss property decreases due to increasing crystallinity and deviates from ideal measurement. The deviation is of a nonlinear fashion (circles represent the actual situation for ideal low frequency loss behavior in Figure 23). Also, due to the order of measurement in a given frequency set, the analyzer acquires the high frequency data after the low frequency data is obtained. This causes even more deviation of dielectric loss property from the ideal curve for the high frequency data (squares represent the actual situation for ideal high frequency loss behavior in Figure 23). As such, for the peak which corresponds with the relaxation of crystallizing species, the higher frequency data tends to have smaller loss values, and this is basically the situation for the LTP in Figure 20. For the HTP behavior in Figure 20, the reverse situation is applicable if HTP is considered as corresponding to the relaxation of species which are affected by crystallizing species nearby. From Eq.(5.3.2-3), one might think, if r_h, the heating rate of experiment is increased, the system would undergo less crystallization during the time of data acquisition, and may yield loss curves which describe the dynamic crystallization behavior more faithfully. However, practical data

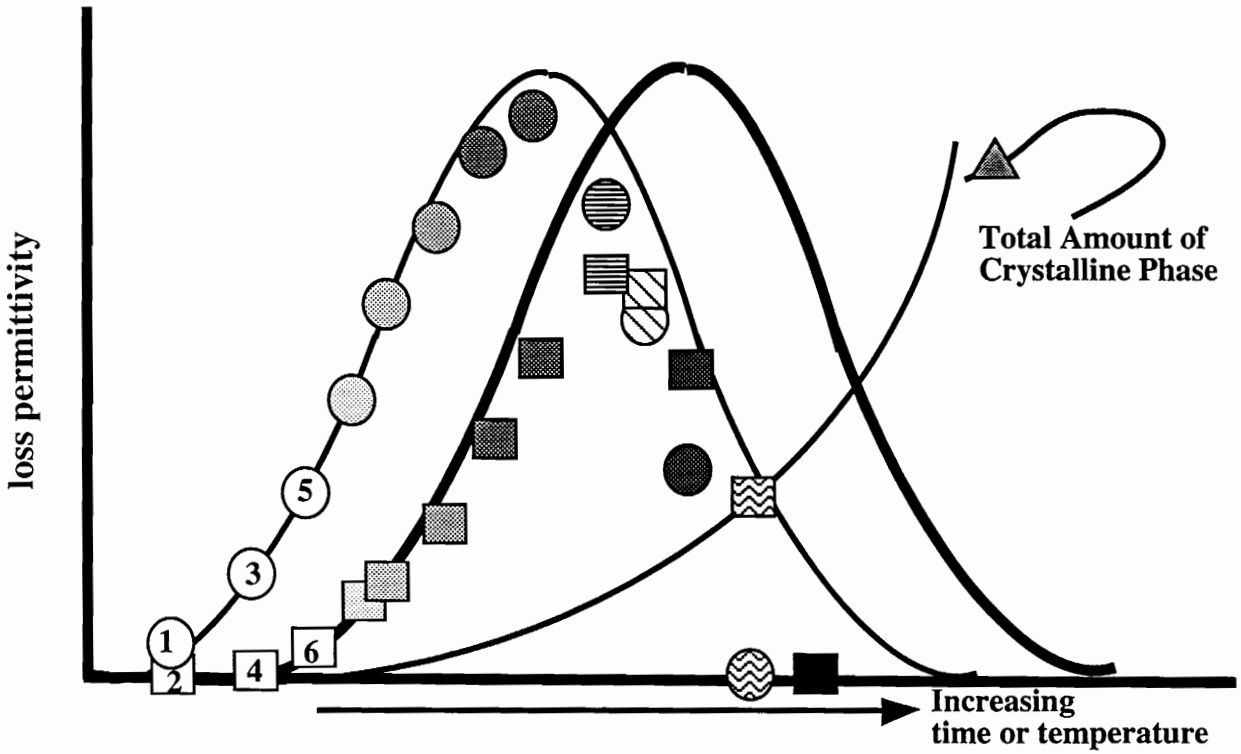

Figure 23. Schematic: Dispersion of dielectric loss constant for two frequencies low and high when the system is undergoing dynamic process and the measurement is made in dynamic temperature sweep. (Numbers indicate the order of measurement)

acquisition might suffer a serious aliasing effect as well as more significant deviation of probe temperatures from actual temperatures which are experienced by the sample.

5.3.3 Temperature Dependent Behavior

As shown in Eq.(5.3.2-2), if a slow heating rate is used, the extent of the crystallization process would be greater by the time the oven reaches a certain temperature than in the case of rapid heating rate. Another set of experiments was done using experimental conditions, Set B (section 5.2.2), which use a slower heating rate than the previous experiment of section 5.3.2. Also this experiment was done over a narrower temperature range of -60 to 130°C, with the same number of data acquisition points. From Figure 24 to 28, time dependent loss permittivity is shown for the glass transition range. As in the previous experiment, dielectric loss of both LTP and HTP are decreasing. For the fresh sample of this set of experiments (Figure 29), curve resolution was performed as in Figure 30 for HTP and Figure 31 for LTP. In order to illustrate the relative magnitudes of LTP and HTP, Figure 32 was prepared. Unlike Figure 20, HTP now shows a familiar dispersion of dielectric loss which permits the evaluation of relaxation parameters. By comparison of Figure 20 and Figure 32, it can be seen that the slower heating rate increased the extent of crystallization at any temperature. As a result, the LTP is now very small and HTPs show decent dispersion behavior. Still LTP is centered around 0°C, which is the average glass transition temperature of reported values (-5 to 5°C). Figure 33, shows the T_{max} of HTP over time at 5kHz. Similar behavior was observed for all the other test frequencies used in the experiment as shown in Figure 34. Figures 35, 36, and 37 show frequency plane plots of dielectric loss for fresh, second day, and fourth day room temperature crystallized samples. While the dielectric loss maximum ε_{max} for the fresh sample shows rather similar values for the given temperature range (20 to 40°C), as the room temperature crystallization proceeds, ε_{max} is highly

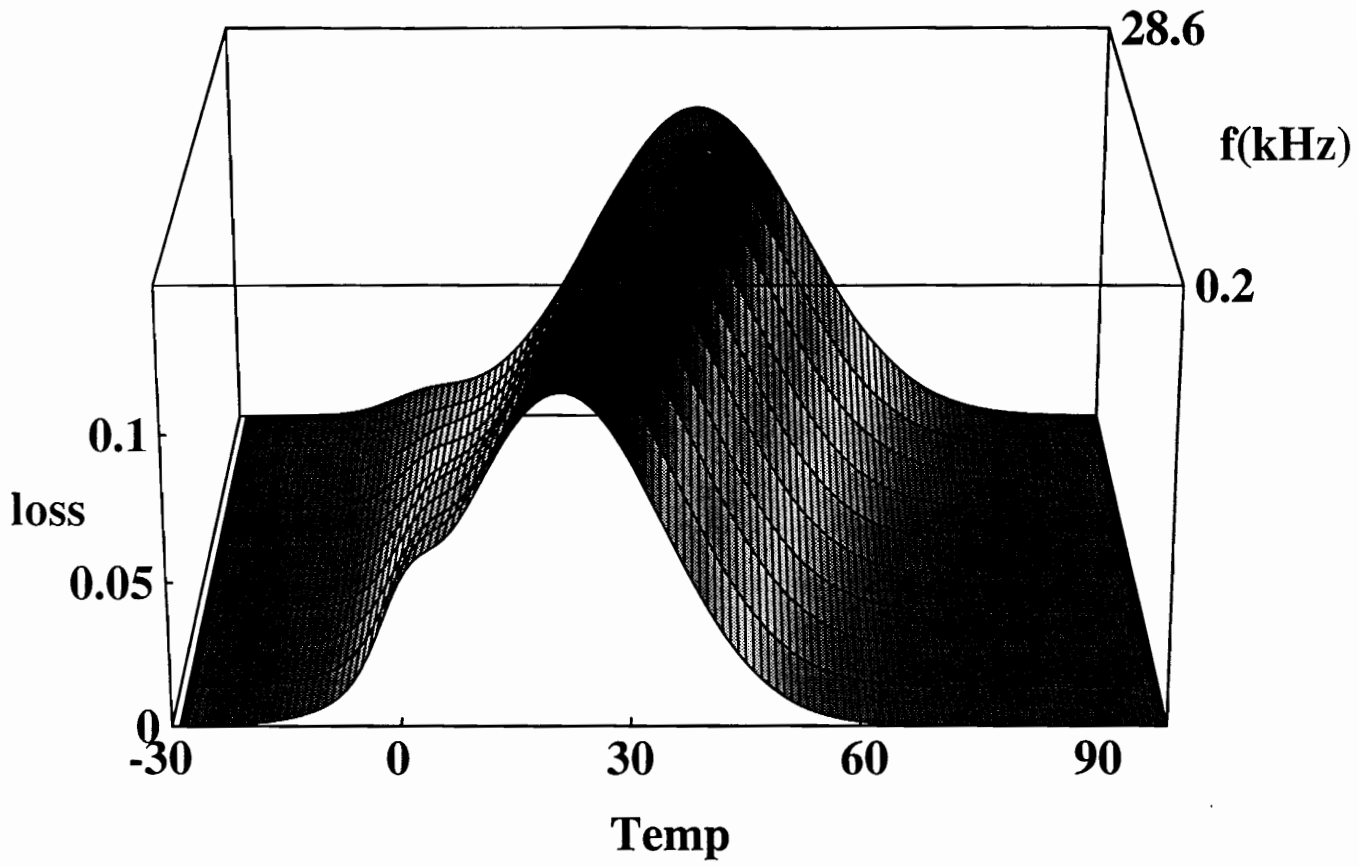

Figure 24. Overall dielectric loss constant behavior of PHB (fresh sample, Set B), frequencies, 0.2, 0.3, 0.6, 1, 1.7, 3, 5, 8.6, 15, 29 kHz from front to rear face of the cubicle

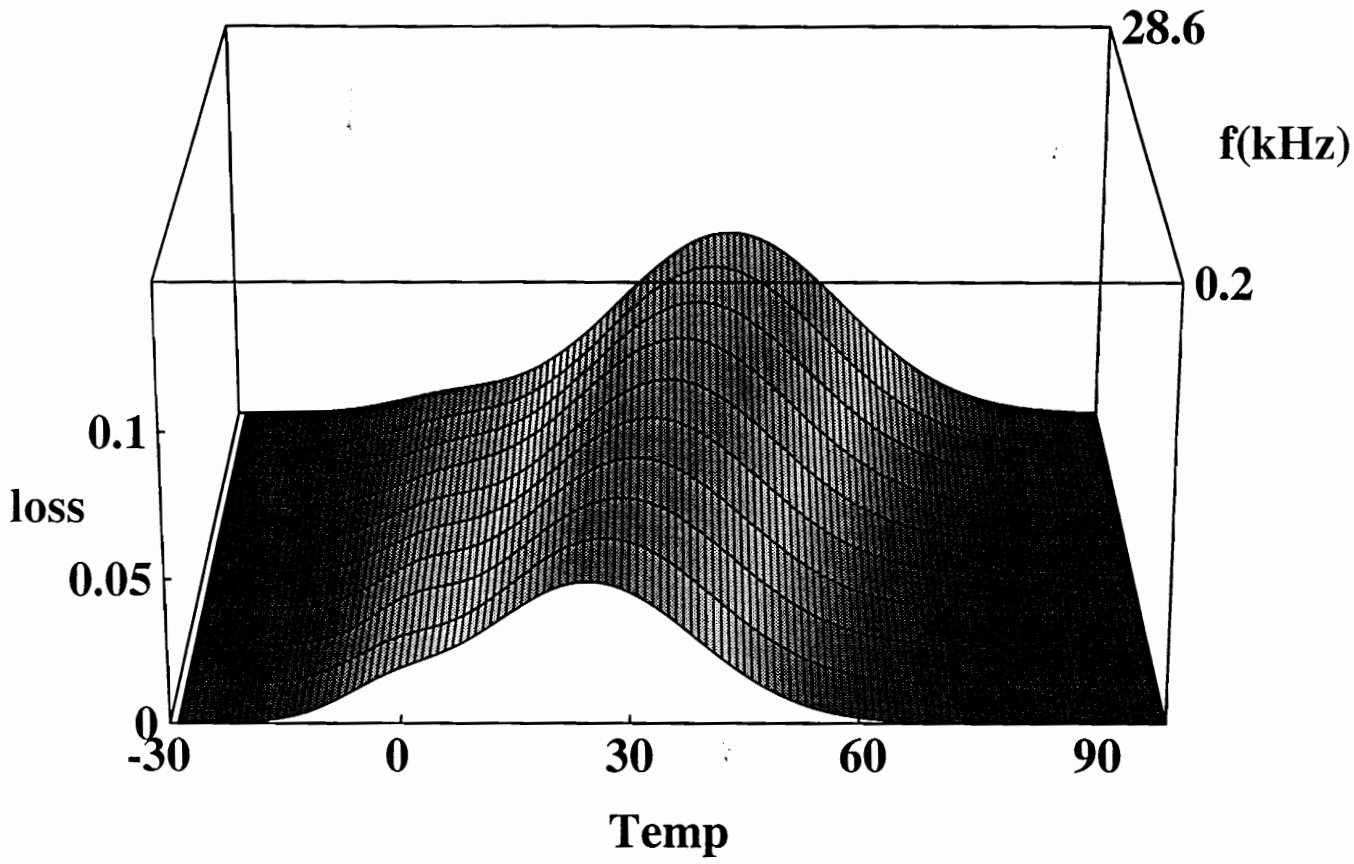

Figure 25. Overall dielectric loss constant behavior of PHB (2nd day sample, Set B), frequencies, 0.2, 0.3, 0.6, 1, 1.7, 3, 5, 8.6, 15, 29 kHz from front to rear face of the cubicle

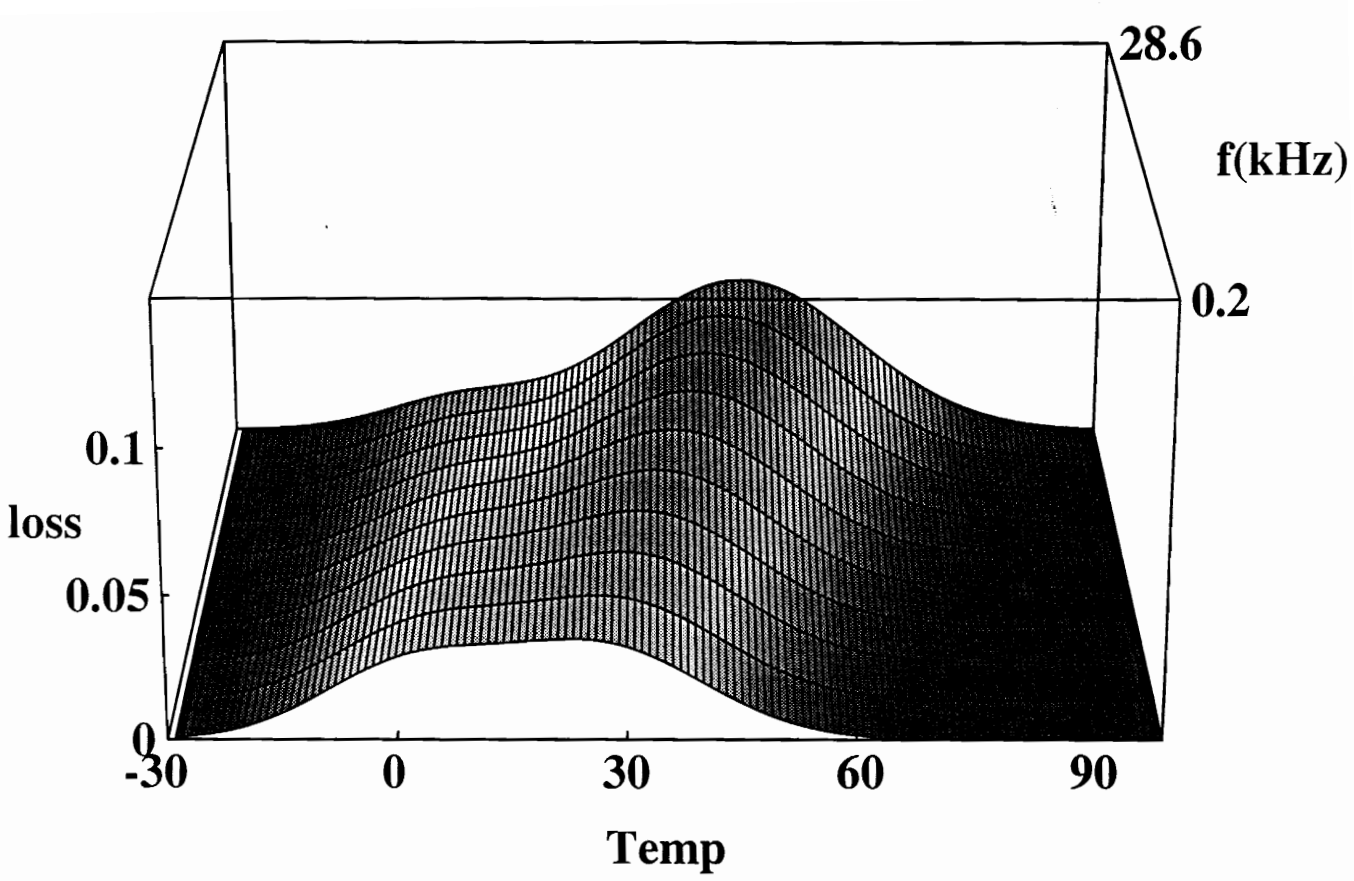

Figure 26. Overall dielectric loss constant behavior of PHB (4th day, Set B), frequencies, 0.2, 0.3, 0.6, 1, 1.7, 3, 5, 8.6, 15, 29 kHz from front to rear face of the cubicle

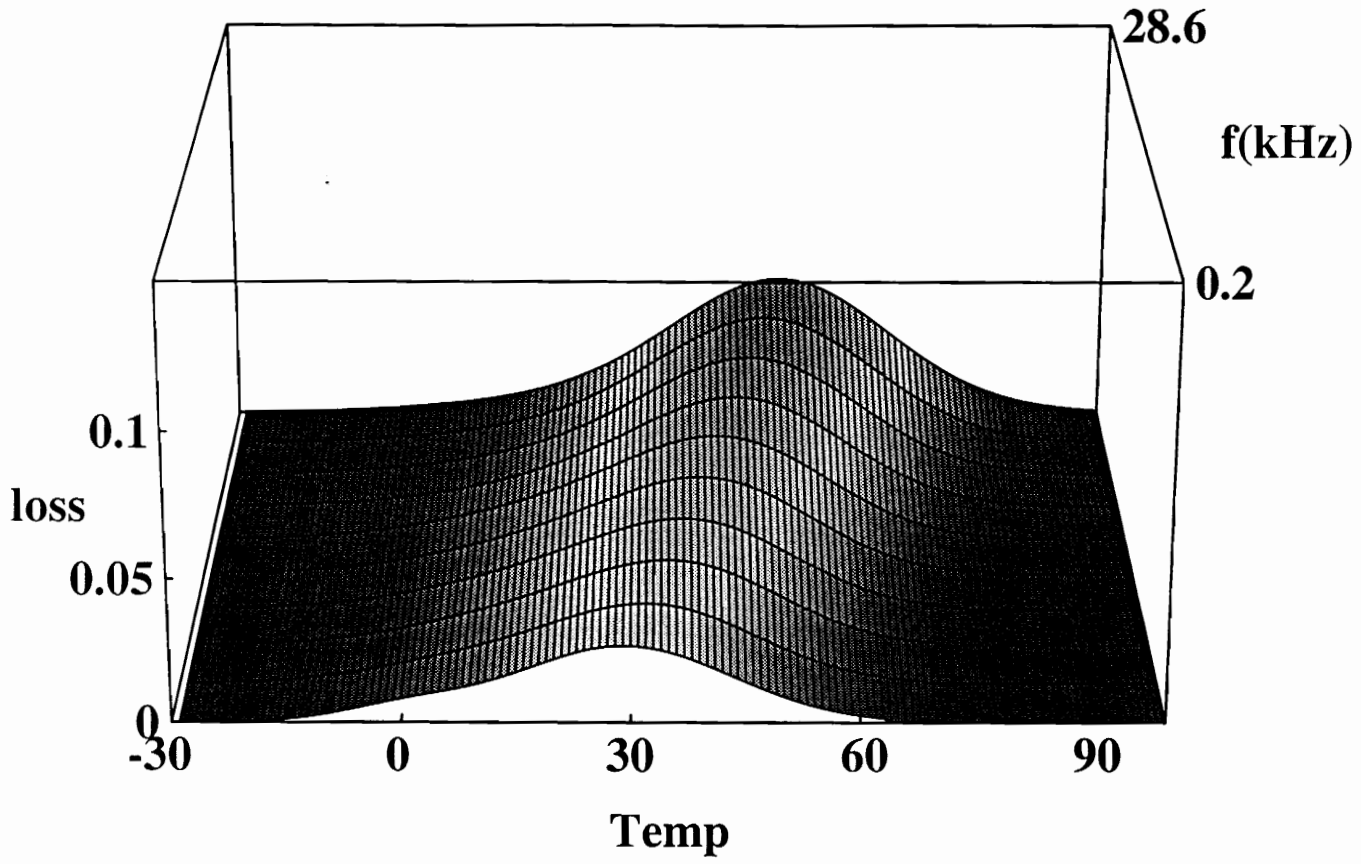

Figure 27. **Overall dielectric loss constant behavior of PHB (8th day, Set B), frequencies, 0.2, 0.3, 0.6, 1, 1.7, 3, 5, 8.6, 15, 29 kHz from front to rear face of the cubicle**

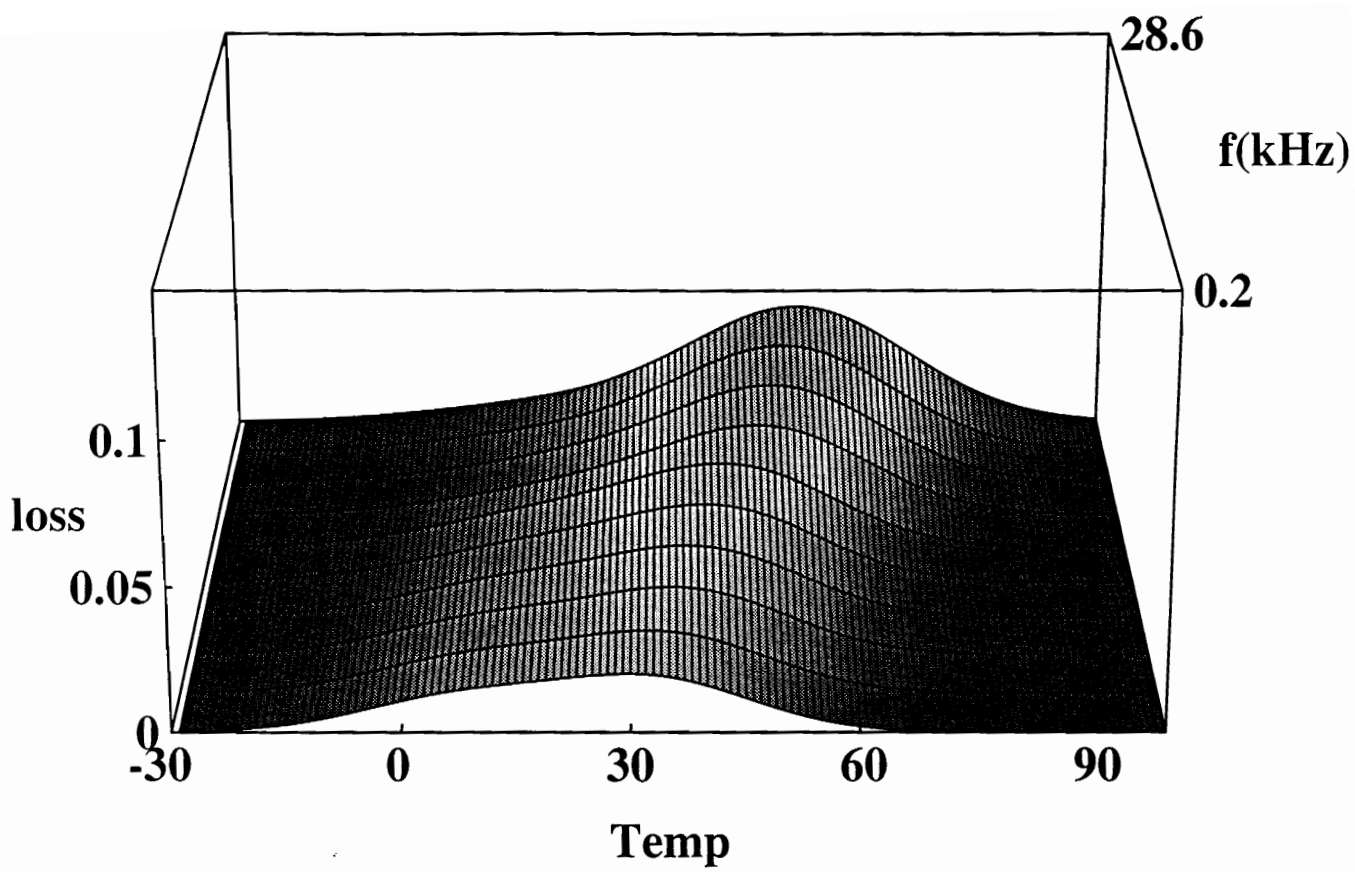

Figure 28. Overall dielectric loss constant behavior of PHB (15th day, Set B), frequencies, 0.2, 0.3, 0.6, 1, 1.7, 3, 5, 8.6, 15, 29 kHz from front to rear face of the cubicle

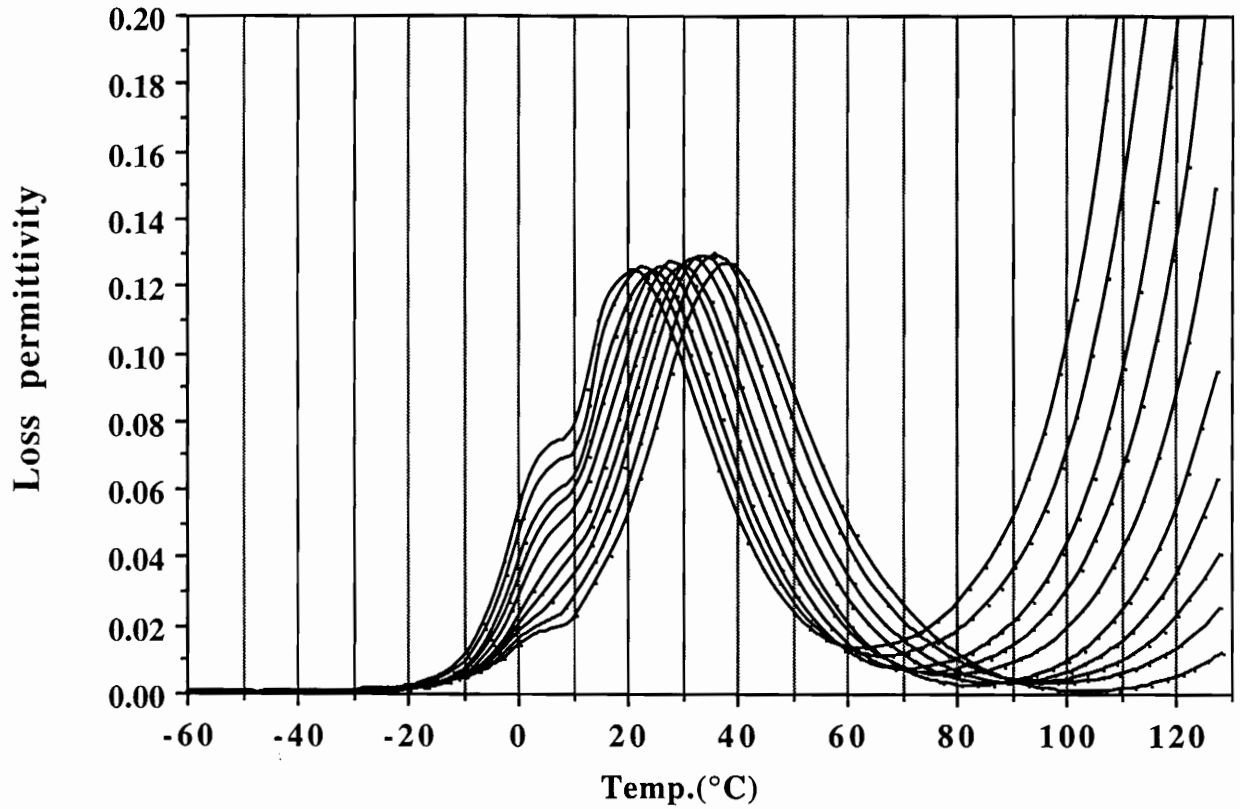

Figure 29. **Dispersion of dielectric loss constant before curve resolution (fresh sample, Set B), frequencies, 0.2, 0.3, 0.6, 1, 1.7, 3, 5, 8.6, 15, 29 kHz in advancing T_{max} order.**

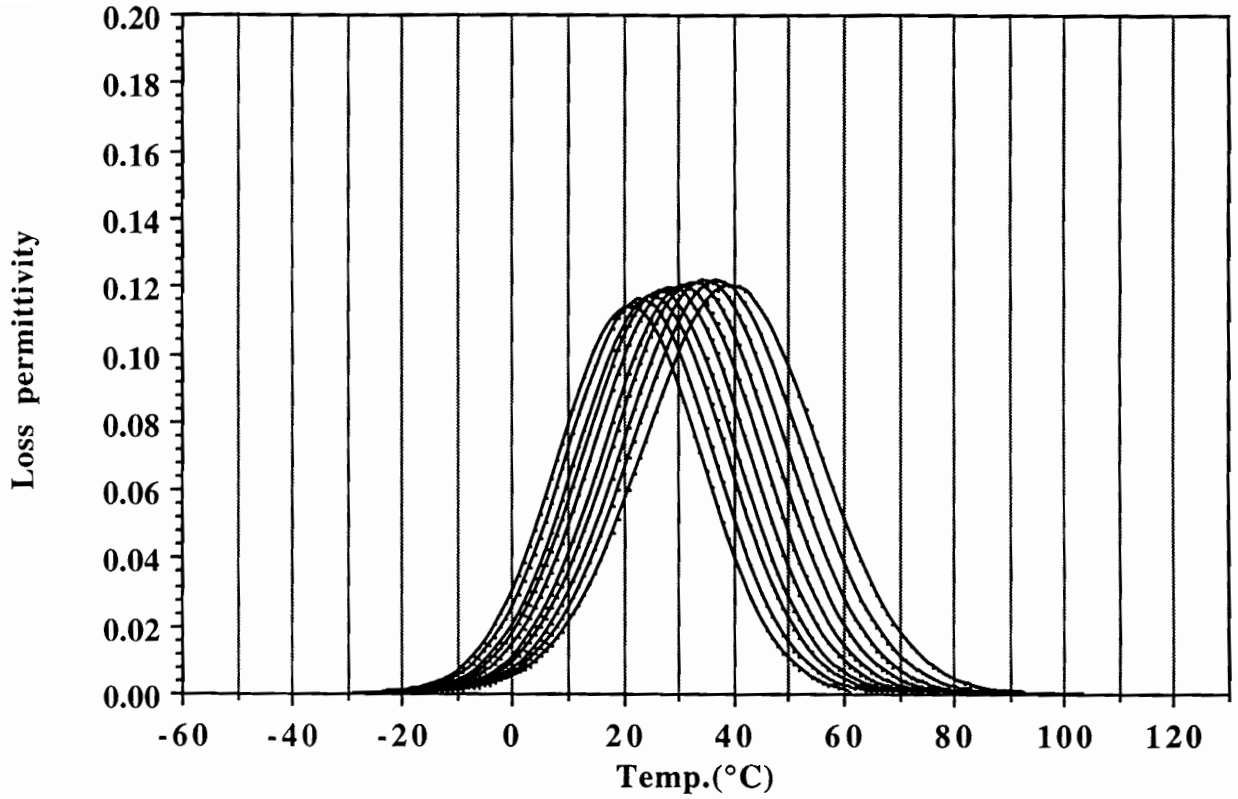

Figure 30. **Temperature plane curve resolved HTP (fresh sample, Set B), frequencies, 0.2, 0.3, 0.6, 1, 1.7, 3, 5, 8.6, 15, 29 kHz in advancing T_{max} order.**

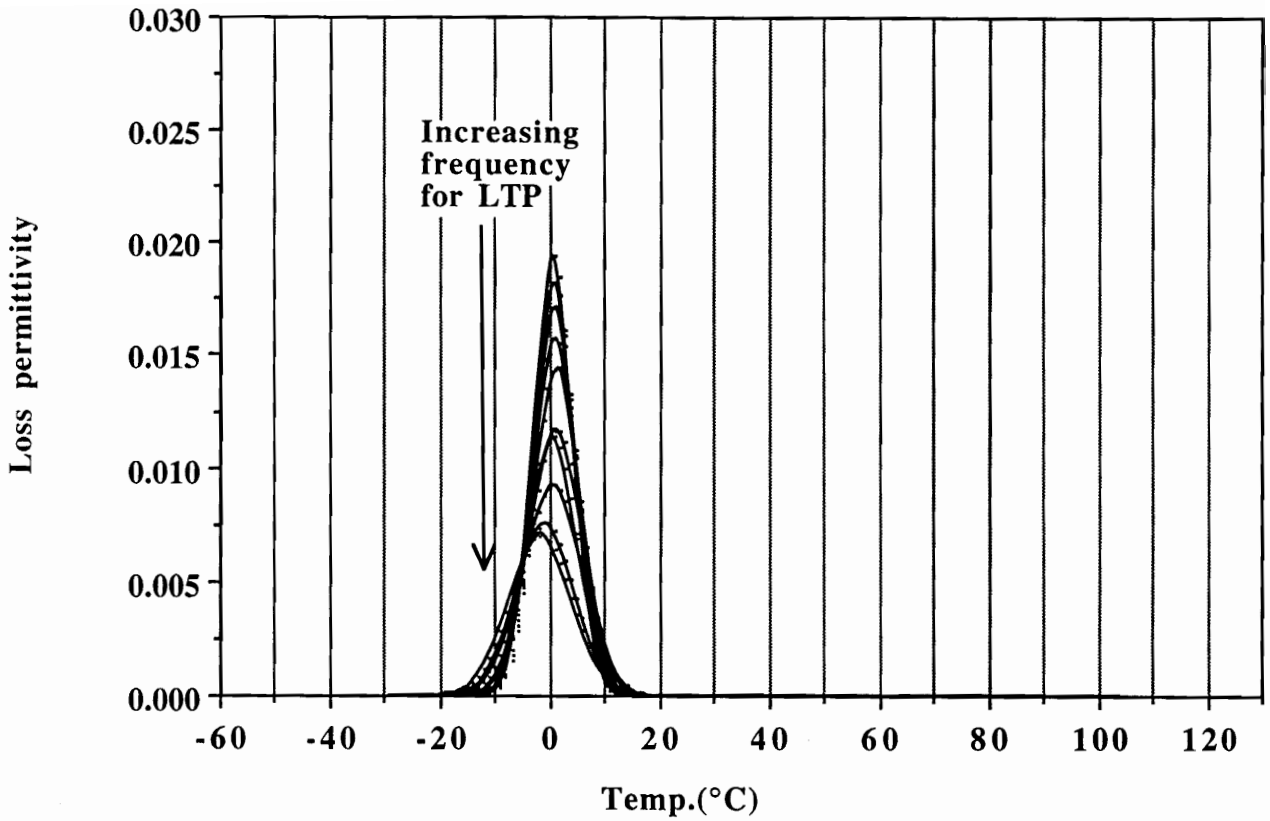

Figure 31. Temperature plane curve resolved LTP (fresh sample, Set B), frequencies, 0.2, 0.3, 0.6, 1, 1.7, 3, 5, 8.6, 15, 29 kHz in the order of decreasing magnitude. Note the disappearance of dispersion behavior due to slow heating rate

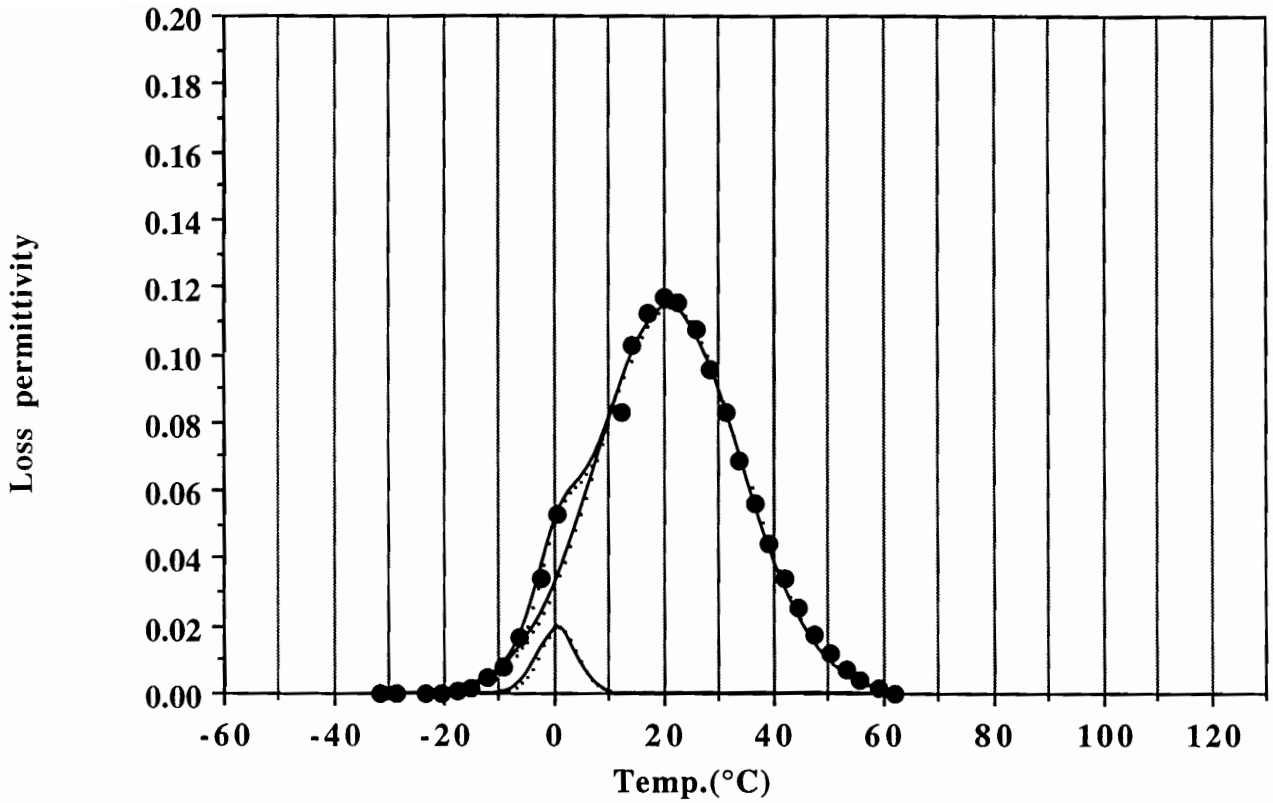

Figure 32. **Relative magnitude of the dielectric loss constant between LTP and HTP (fresh sample, Set B), frequency 0.2 kHz. filled circle and solid line represent experimental data point and composite curve respectively**

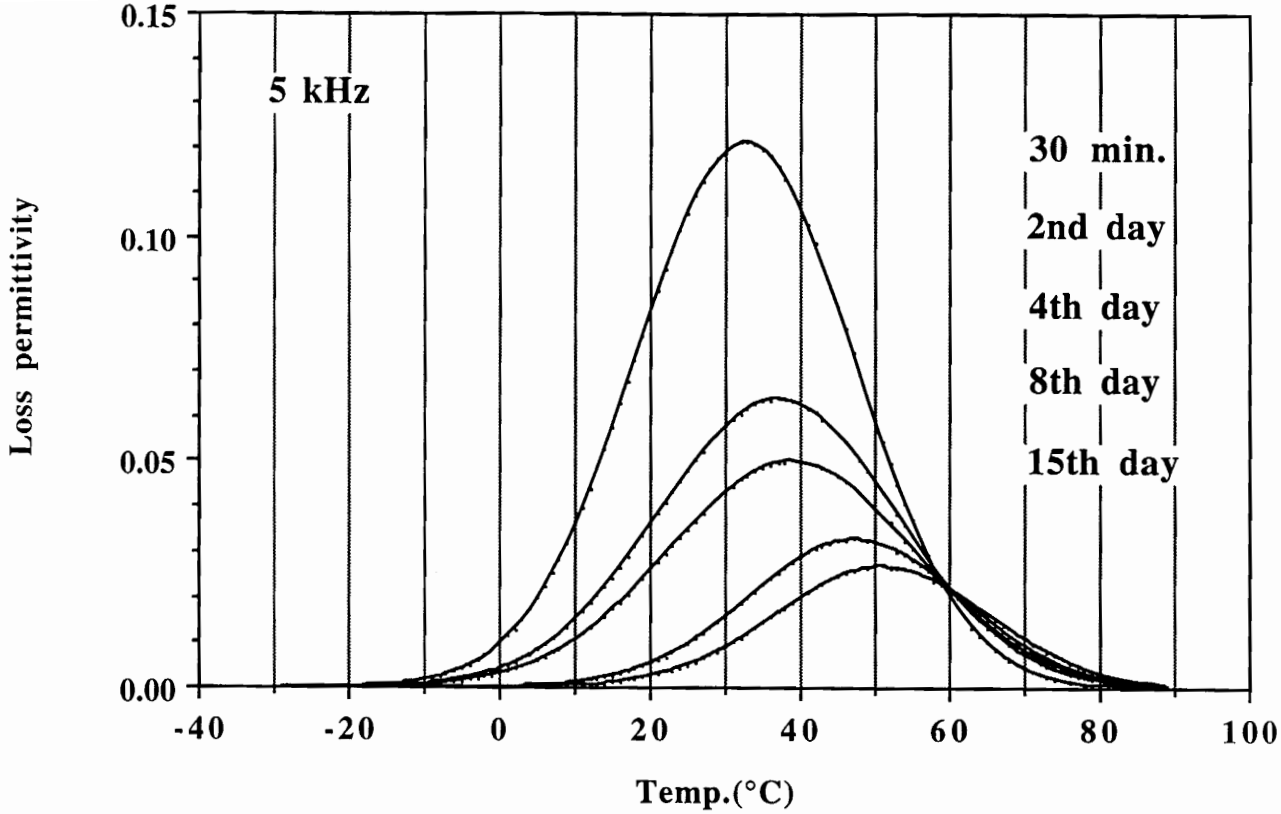

Figure 33. Time dependent variation of dielectric loss constant of HTP (Set B, frequency, 5 kHz)

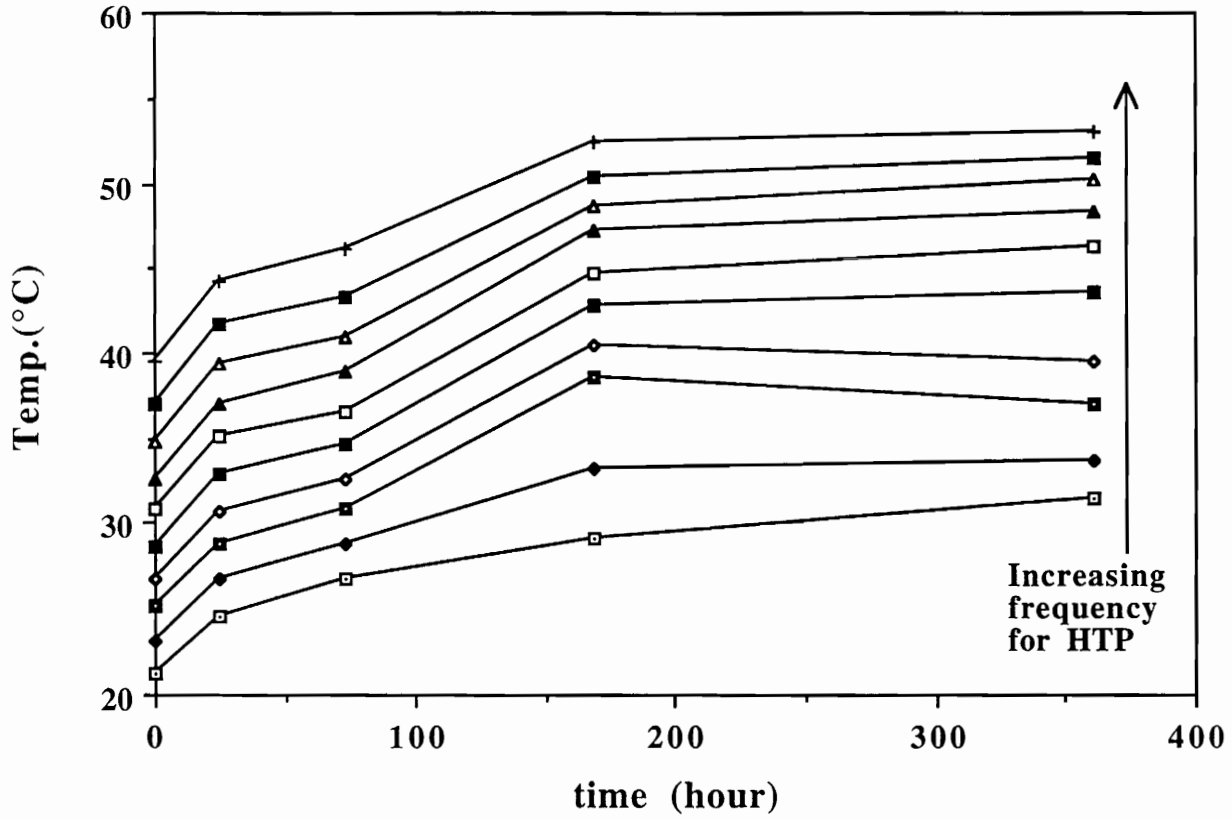

Figure 34 T_{max} variation of HTP over time (frequencies, 0.2, 0.3, 0.6, 1, 1.7, 3, 5, 8.6, 15, 29 kHz from bottom to top)

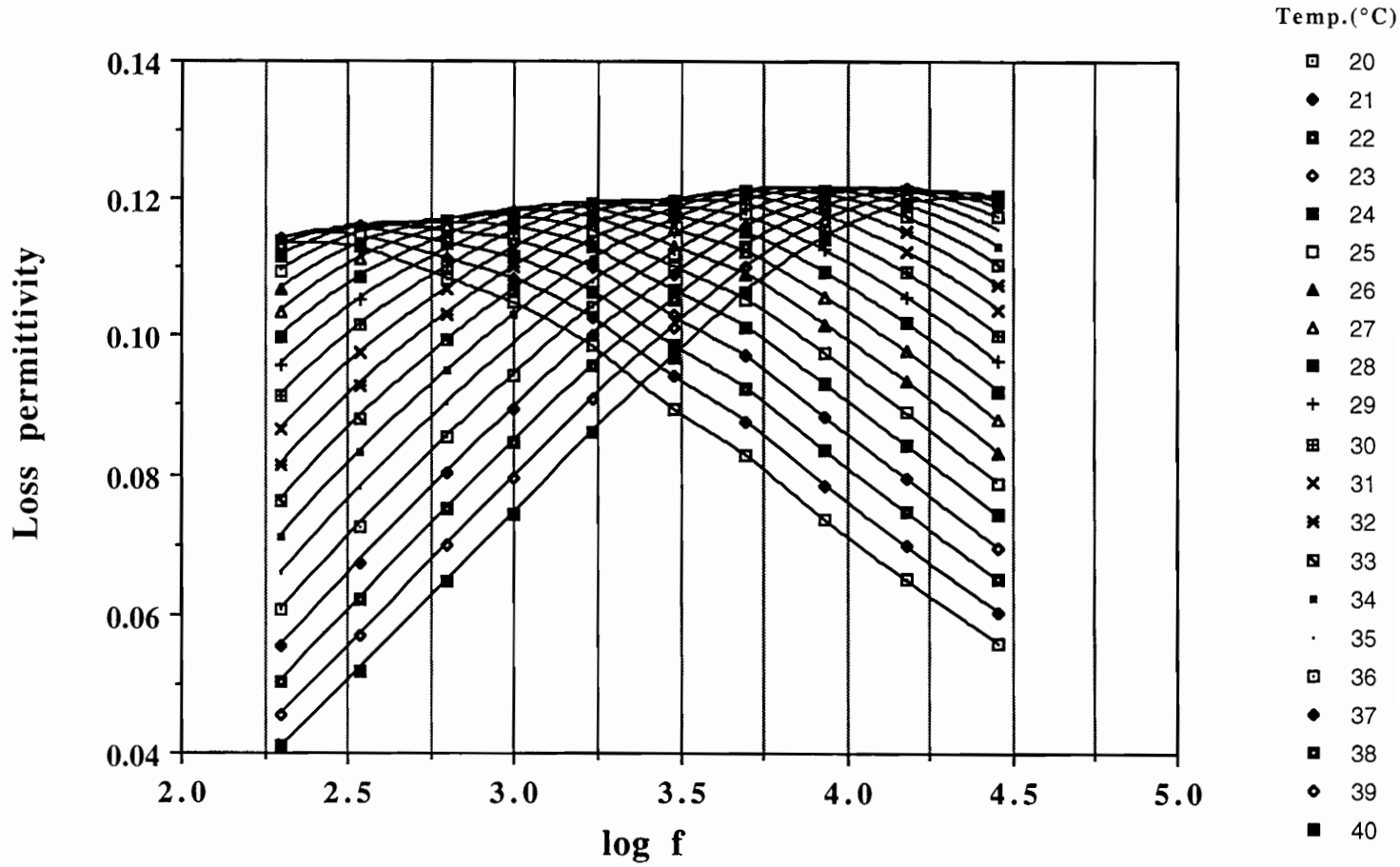

Figure 35. **Frequency plane view of dielectric loss constant of HTP (fresh sample, Set B). f_{max} shifts to higher frequency as the temperature increases from 20 to 40°C in 1 degree step**

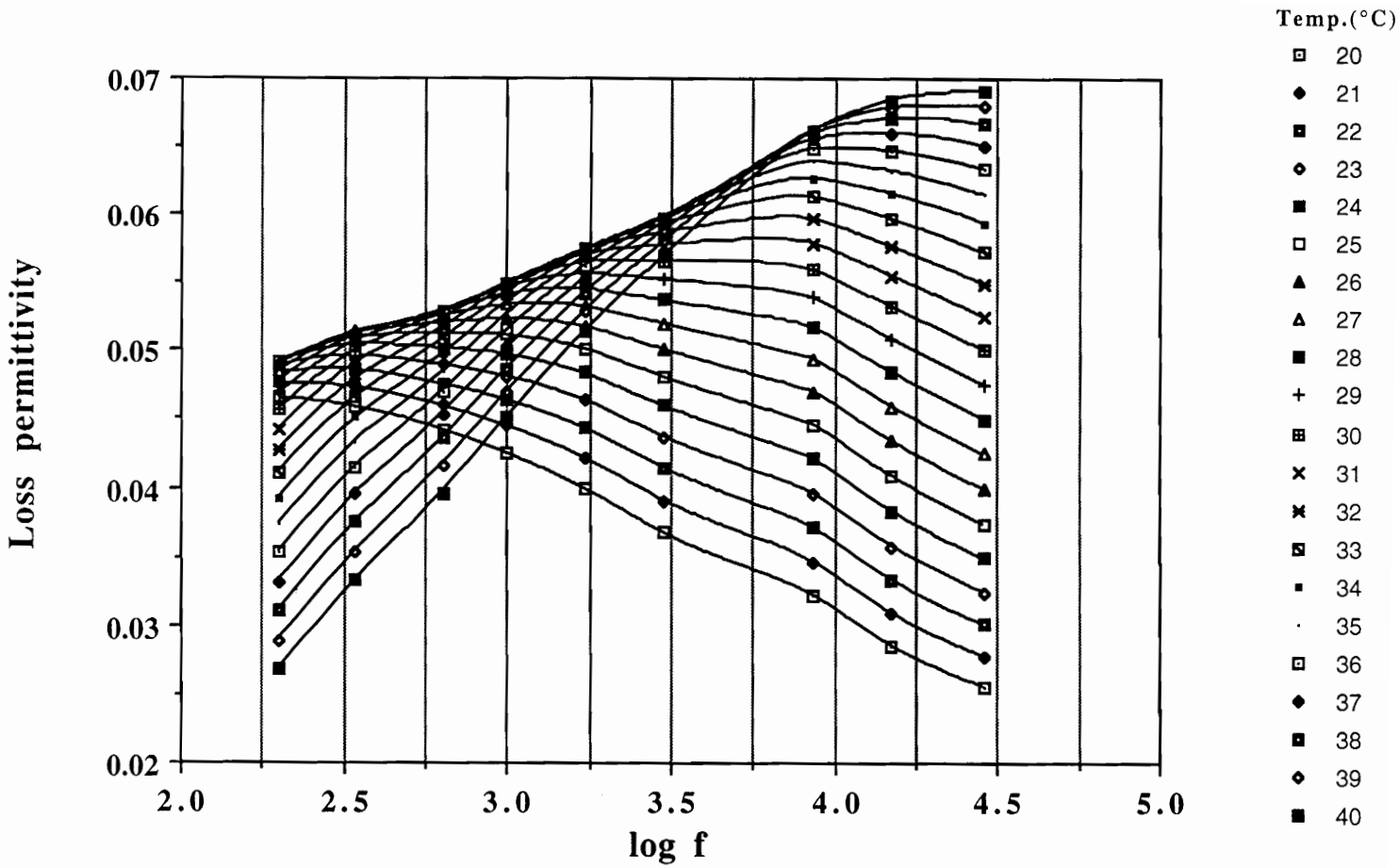

Figure 36. **Frequency plane view of dielectric loss constant of HTP (2nd day, Set B). f_{max} shifts to higher frequency as the temperature increases from 20 to 40°C in 1 degree step**

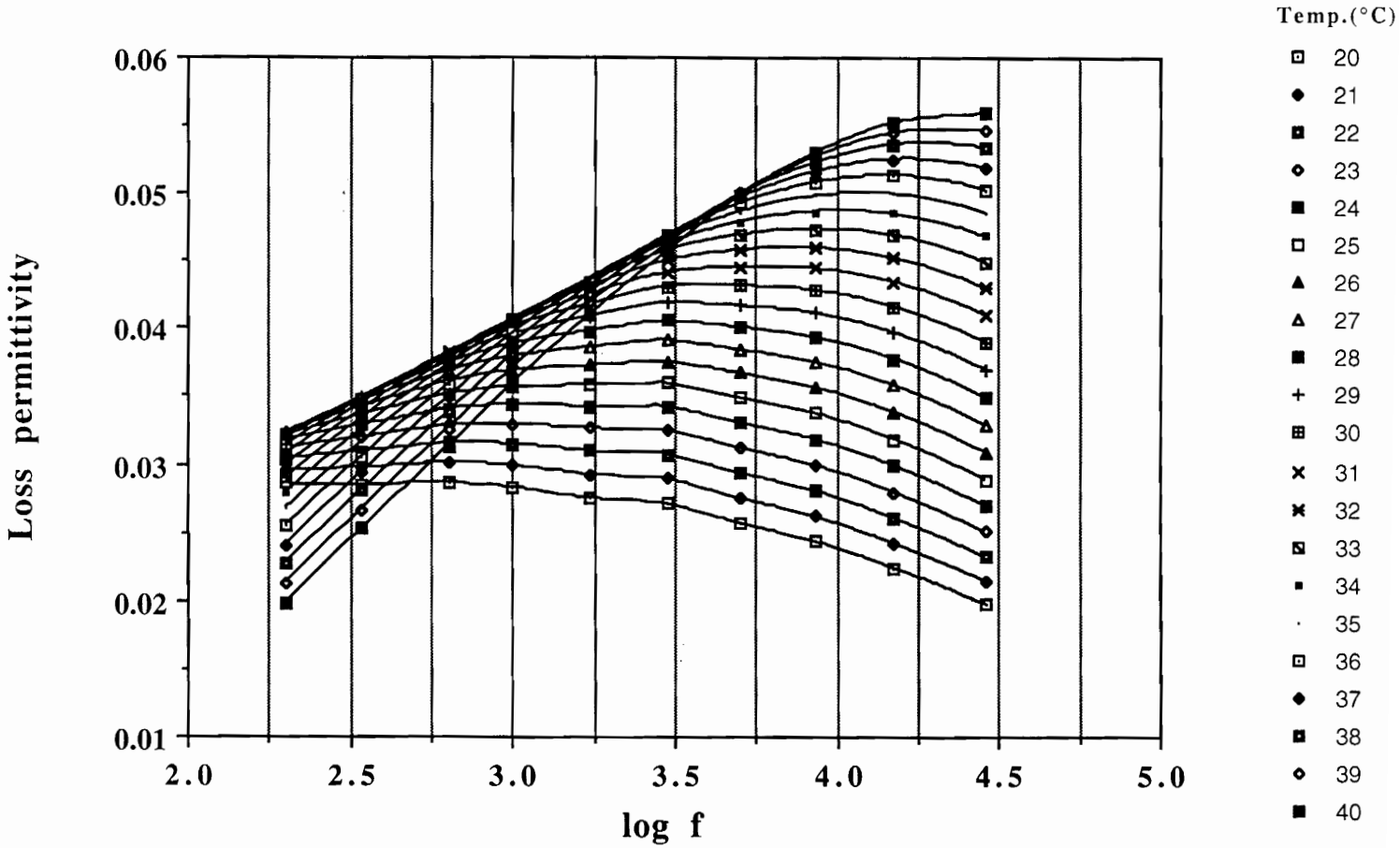

Figure 37. **Frequency plane view of dielectric loss constant of HTP (4th day, Set B). f_{max} shifts to higher frequency as the temperature increases from 20 to 40°C in 1 degree step**

dependent on the temperature, implying that the number of dipoles participating in the relaxation process becomes greater or that they are less restricted at higher temperature.[54] Now, based on the observations made so far, it is proposed that the LTP is caused by the transformation of a specific segment of pure amorphous phase into crystalline phase and HTP is caused by relaxations of chains which are confined by crystalline phase and also which are not directly attached to the surface of lamellae or spherulites. As the HTP is caused by confined chains, its relaxation behavior is significantly dependent on the temperature as the crystallization is going on. In other words, as the extent of crystallization increases, the magnitude of dielectric loss which is dependent on the number of dipoles capable of motion, decreases and the chains, confined in ever narrowing geometry, experience more temperature dependent relaxation.

5.3.4 Accelerated Annealing Experiment

In order to have some idea of the effect of annealing temperature on the relaxation behavior of PHB, another fresh pancake of PHB was made and annealed at 90, 135, and 45°C for twelve hours in a convection drying oven. The dielectric measurement conditions were the same as the conditions of Set B. It is to be noted that the samples studied in this experiment were from one pancake of PHB to reduce sample to sample variation. Also if the sample is annealed at room temperature too much prior to the accelerated annealing experiment, the effect of the accelerated annealing is very hard to detect. On the other hand, if a fresh sample is used every time whenever an annealing experiment has to be done, sample to sample variation becomes of concern. First, variations in the processing temperature and time are a concern. Second, since the initial rate of crystallization is the highest, a small difference in the timing of the start of the experiment might cause appreciable error. As such, samples were subjected to accelerated annealing experiments after one, two, and three days of room temperature

crystallization for 90, 135, and 45°C accelerated annealing experiments. The results are shown in Figures 38, 39, and 40. If there had been no accelerated annealing for these three samples, the dielectric loss of these three sample would have showed gradual decreases in magnitude due to room temperature annealing effects. However, due to accelerated annealing temperature effects, the order of the magnitude of dielectric loss is not sequential. Since the melting temperature of PHB is around 180°C and the glass transition temperature of pure amorphous phase is 0°C, 90°C was close to the temperature of the maximum crystallization rate. In comparing the 135°C and 45°C data, the effect of one additional day of room temperature annealing should be considered since the rate of crystallization at 135°C and 45°C should not be much different. Also the 135°C data shows some signs that degradation occurred, the products of which might act as plasticizers. In Figure 41, the oscillator strength values of the room temperature annealed sample are shown. It can be seen that as the room temperature crystallization proceeds, oscillator strength, which may be interpreted as effective dipole moment, decreases. In Figure 42, the oscillator strength values of the accelerated annealing experiment are shown. The oscillator strength showed the annealed status quantitatively. In Figure 43 and 44, the autocorrelation function of the fresh sample and the most annealed sample of Figure 40 are shown. It is easily noticeable through this analysis that annealed sample relaxes somewhat faster in the initial stage of relaxation and slower in the later stage of relaxation. This effect can be seen in an even more contrasting way when the logarithm is taken for the autocorrelation function as shown in Figures 45, 46. From Table 6 to 9, the parameters of the relaxation function and their chi-square values are tabulated. It was found that while Havriliak-Negami parameters were rather temperature dependent, those of KWW showed rather constant values (Figure 47). In Figures 48 and 49, the center of relaxation time and mean relaxation time is plotted versus 1/T for selected samples. First, there exists a general trend that as temperature

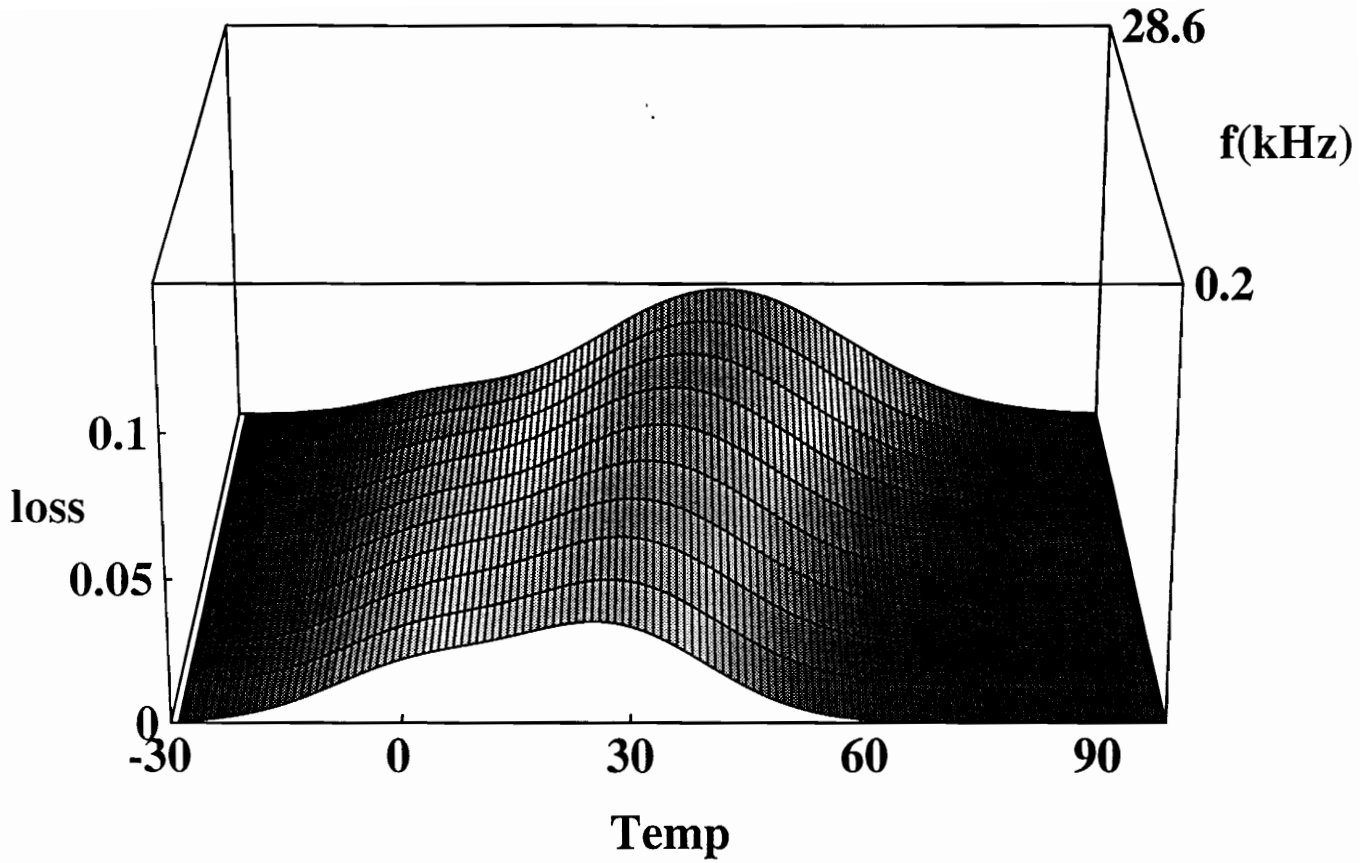

Figure 38. Overall dielectric loss constant behavior of PHB (annealed at 90°C for 12 hours after 1 day room temperature annealing, Set B), frequencies, 0.2, 0.3, 0.6, 1, 1.7, 3, 5, 8.6, 15, 29 kHz from front to rear face of the cubicle

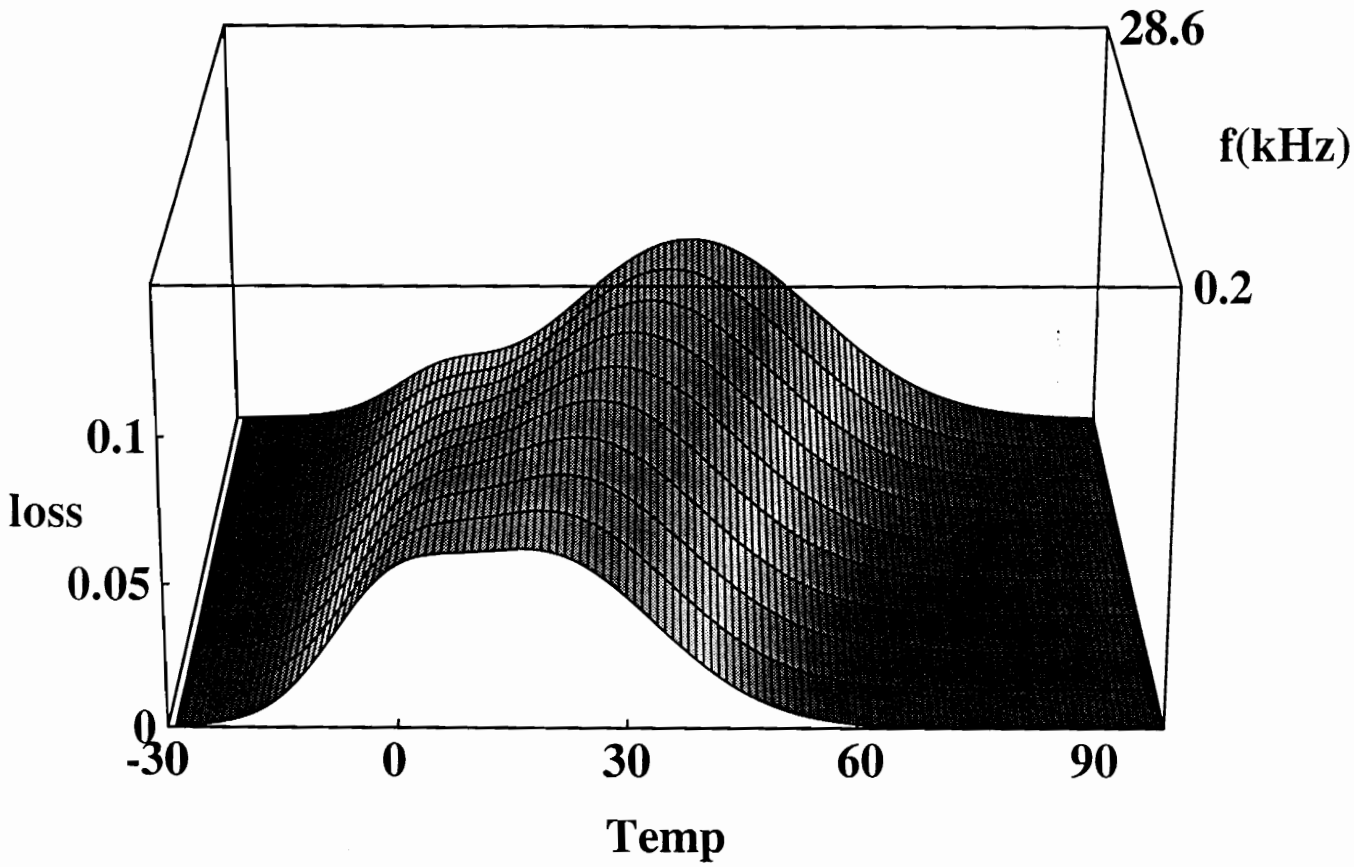

Figure 39. **Overall dielectric loss constant behavior of PHB (annealed at 135°C for 12 hours after 2 day room temperature annealing, Set B), frequencies, 0.2, 0.3, 0.6, 1, 1.7, 3, 5, 8.6, 15, 29 kHz from front to rear face of the cubicle**

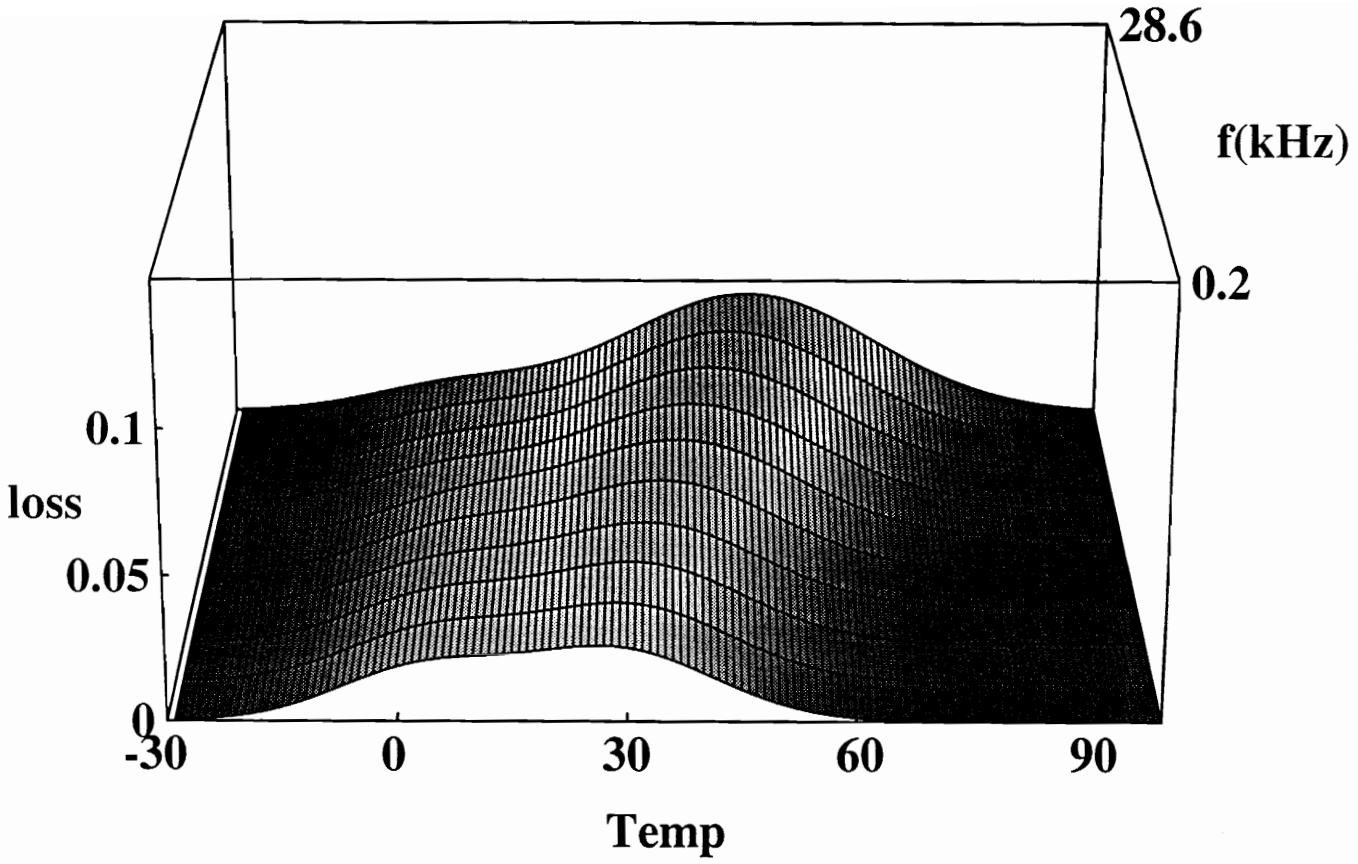

Figure 40. **Overall dielectric loss constant behavior of PHB (annealed at 45°C for 12 hours after 3 day room temperature annealing, Set B), frequencies, 0.2, 0.3, 0.6, 1, 1.7, 3, 5, 8.6, 15, 29 kHz from front to rear face of the cubicle**

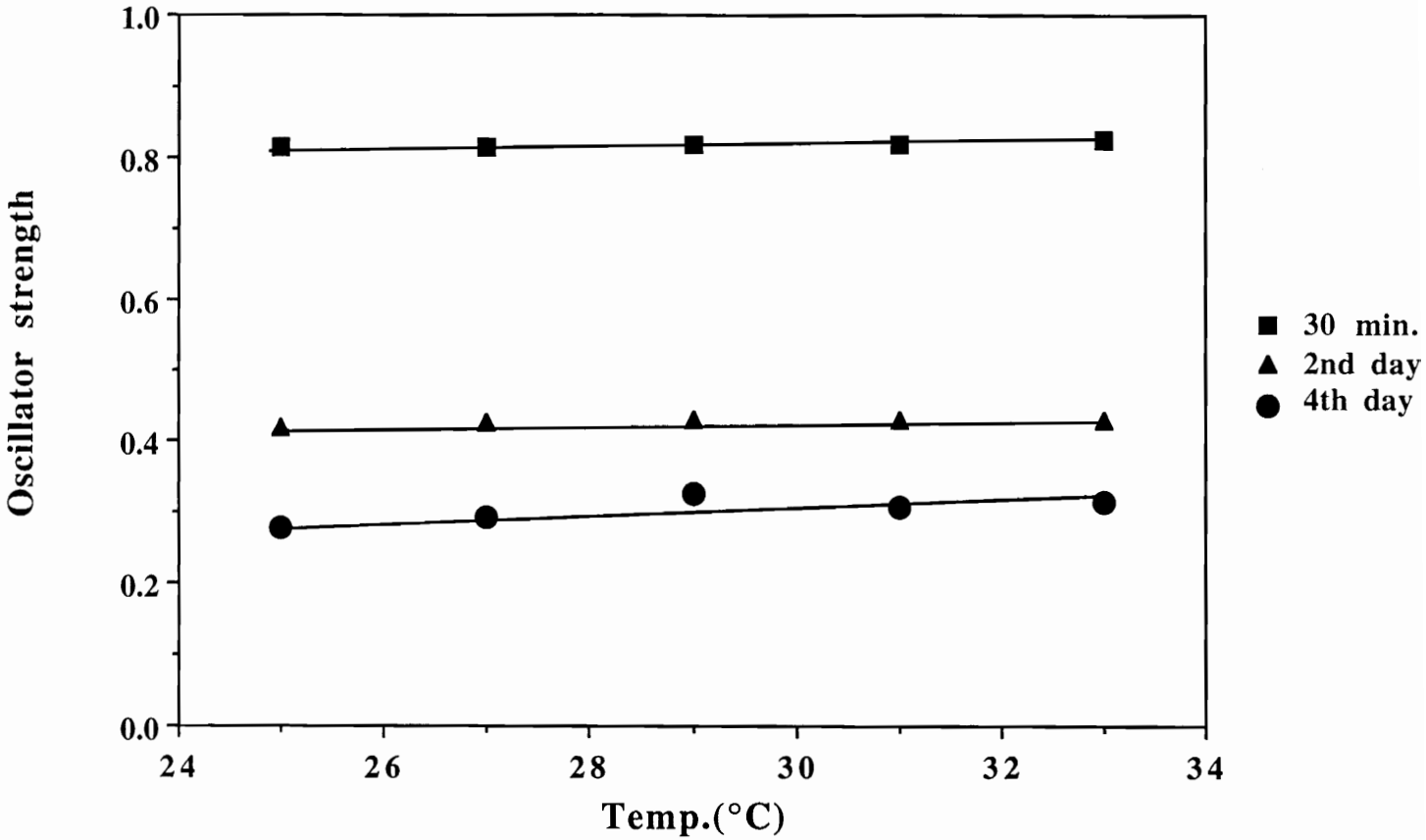

Figure 41. Time and temperature dependence of oscillator strength (HTP, Set B) room temperature annealing

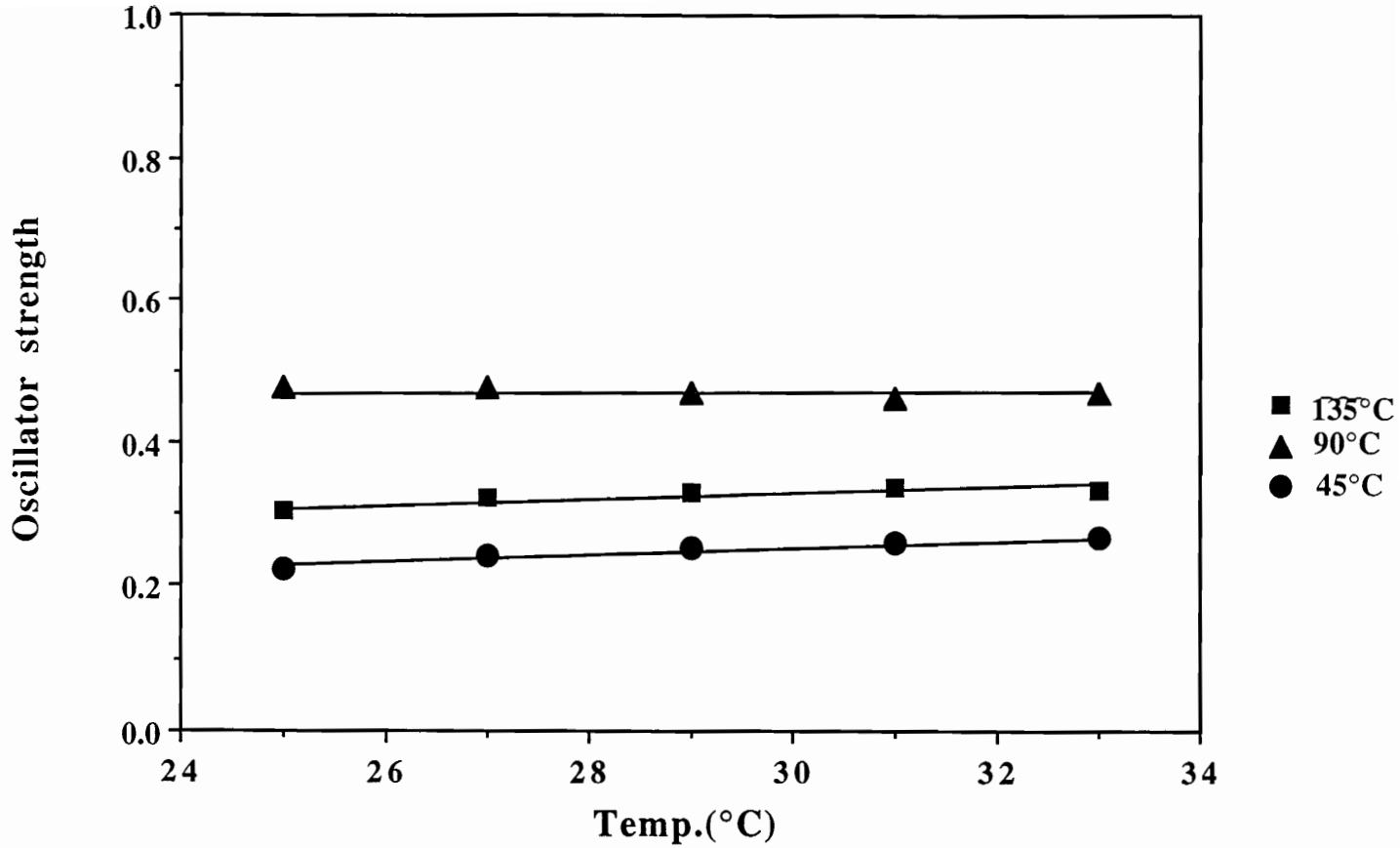

Figure 42. **Time and temperature dependence of oscillator strength (HTP, Set B) accelerated annealing**

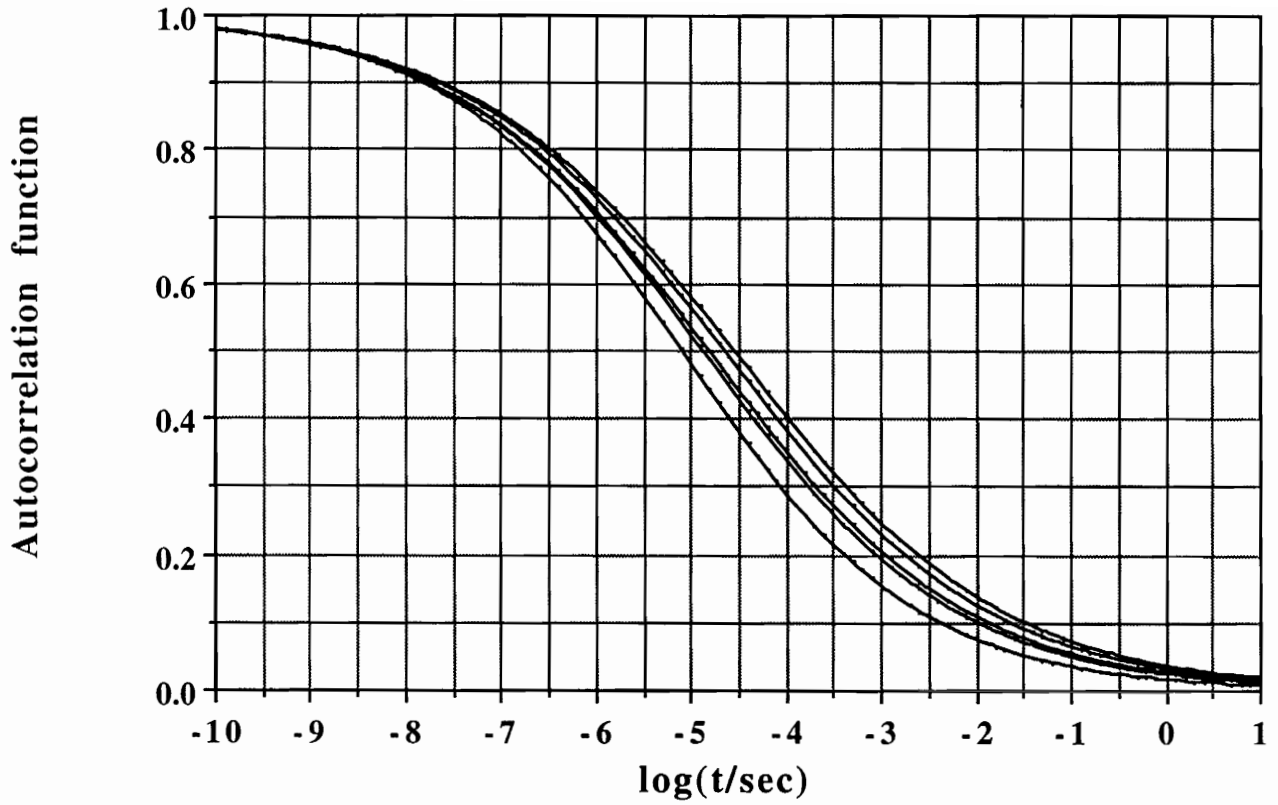

Figure 43. **Autocorrelation function of HTP (annealed at 45°C for 12 hours after 3 day room temperature annealing, Set B), curve shifts to the left hand side as temperature is increasing from 25 to 33°C in 2 degree step**

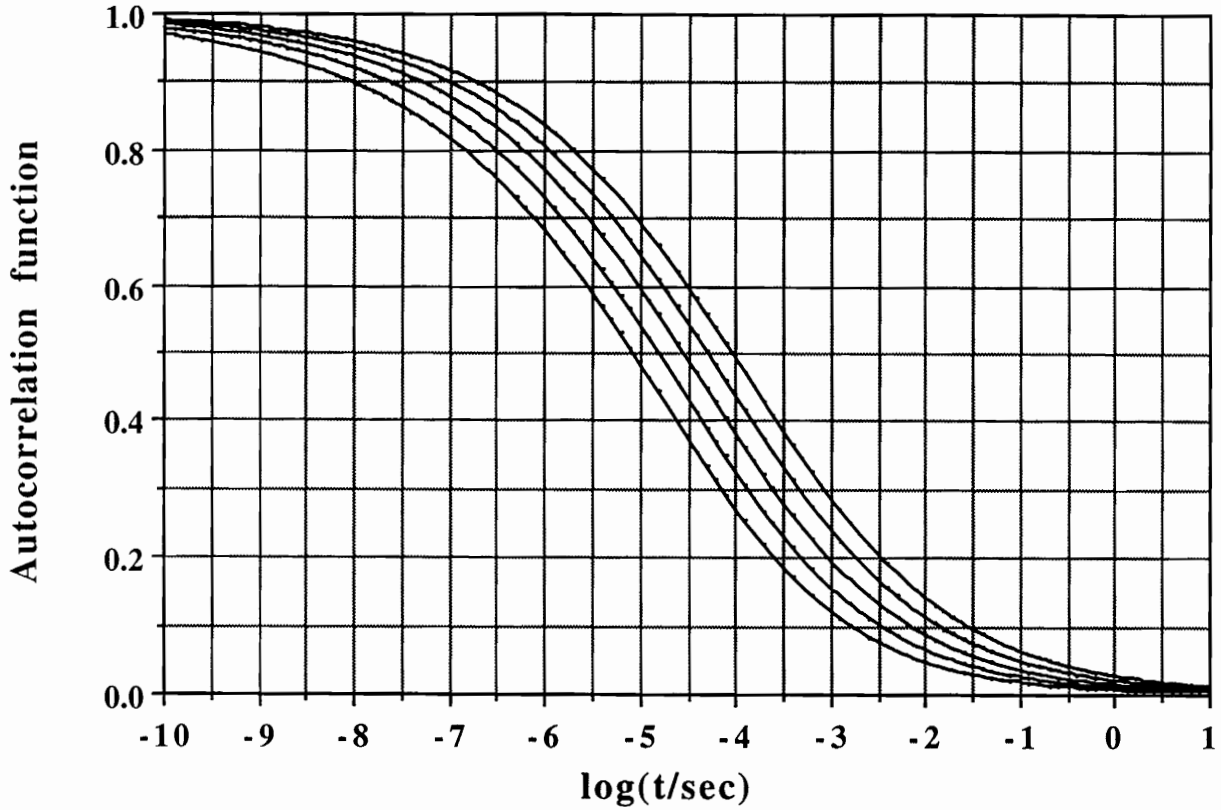

Figure 44. **Autocorrelation function of HTP (fresh sample, Set B), curve shifts to the left hand side as temperature is increasing from 25 to 33°C in 2 degree step**

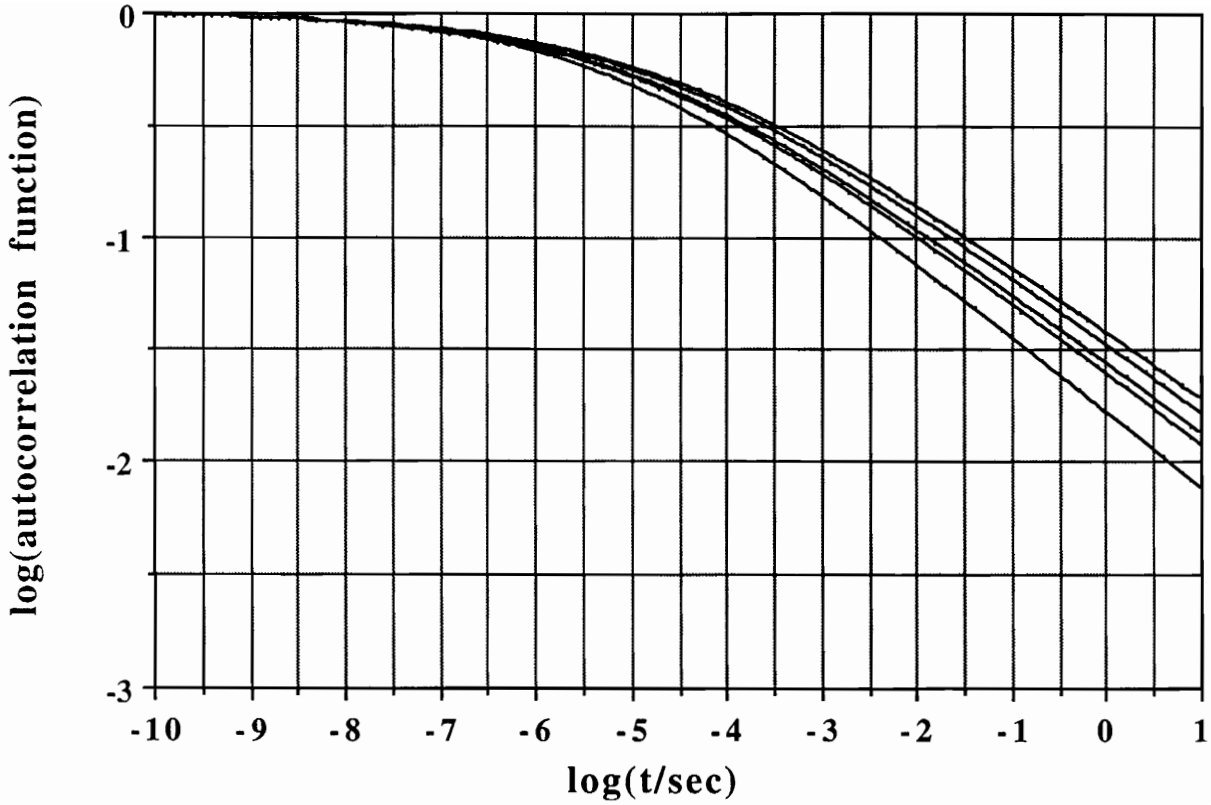

Figure 45. Plot of log(autocorrelation function) versus log(time) of HTP (annealed at 45°C for 12 hours after 3 day room temperature annealing, Set B), curve shifts to the left hand side as temperature is increasing from 25 to 33°C in 2 degree step

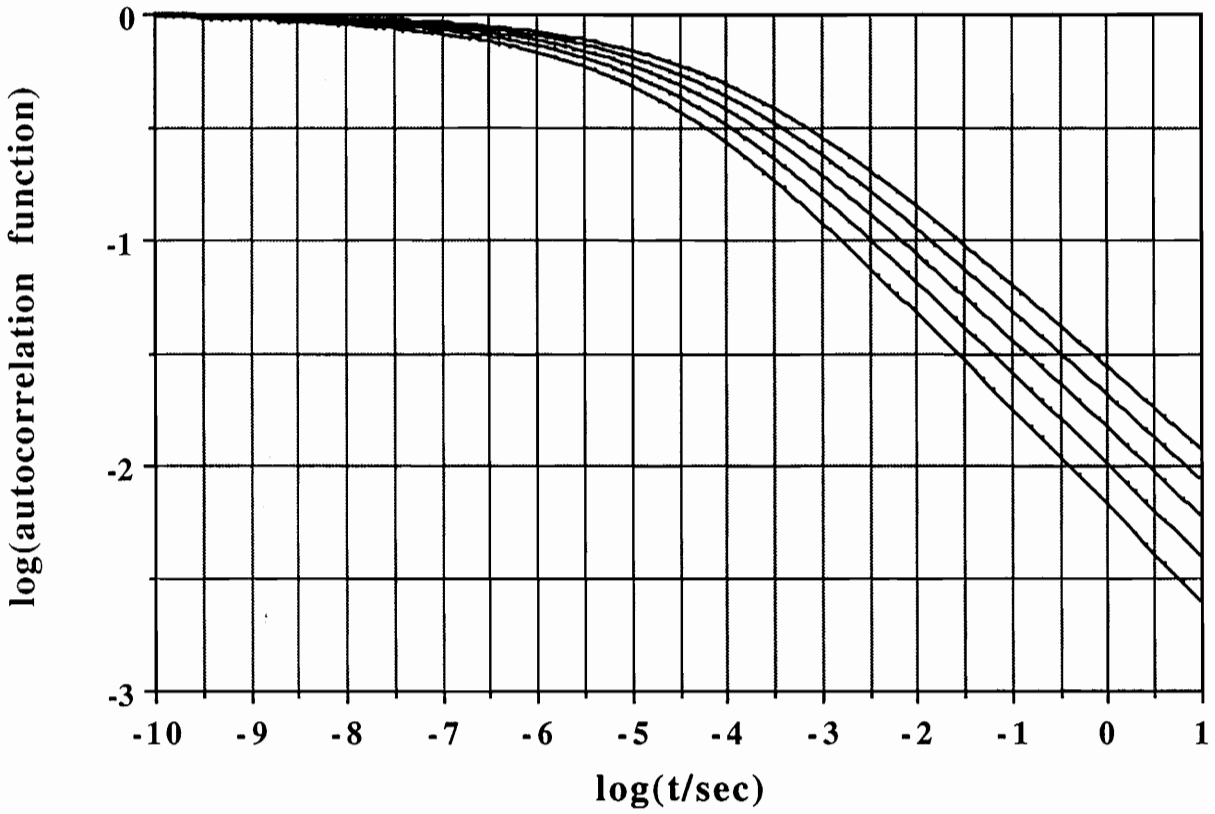

Figure 46. **Plot of log(autocorrelation function) versus log(time) of HTP (fresh sample, Set B), curve shifts to the left hand side as temperature is increasing from 25 to 33°C in 2 degree step**

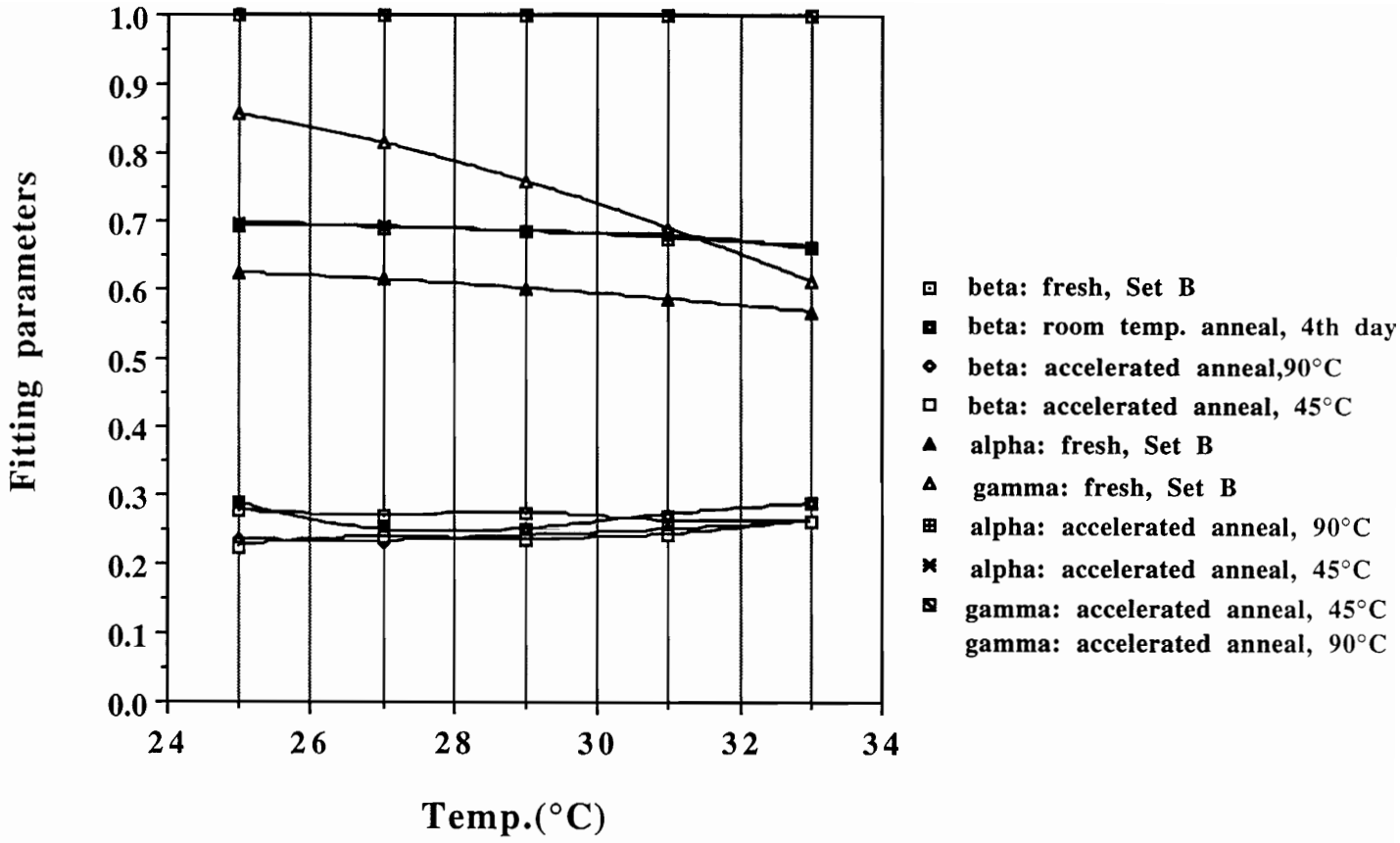

Figure 47. **Temperature dependence of fitting parameters in Havriliak-Negami and KWW model**

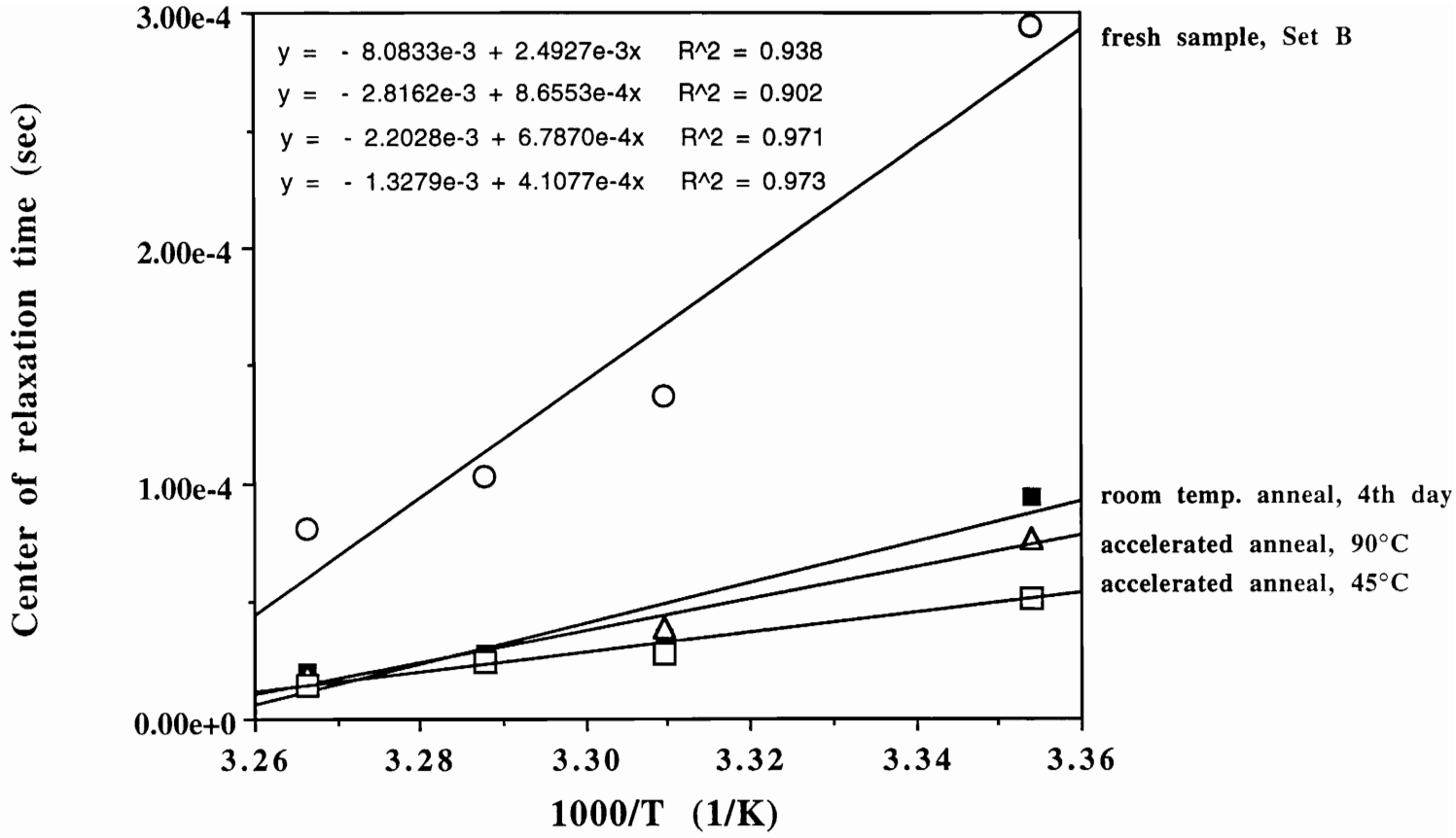

Figure 48. **Temperature and annealed status dependence of center of relaxation time in Havriliak-Negami model**

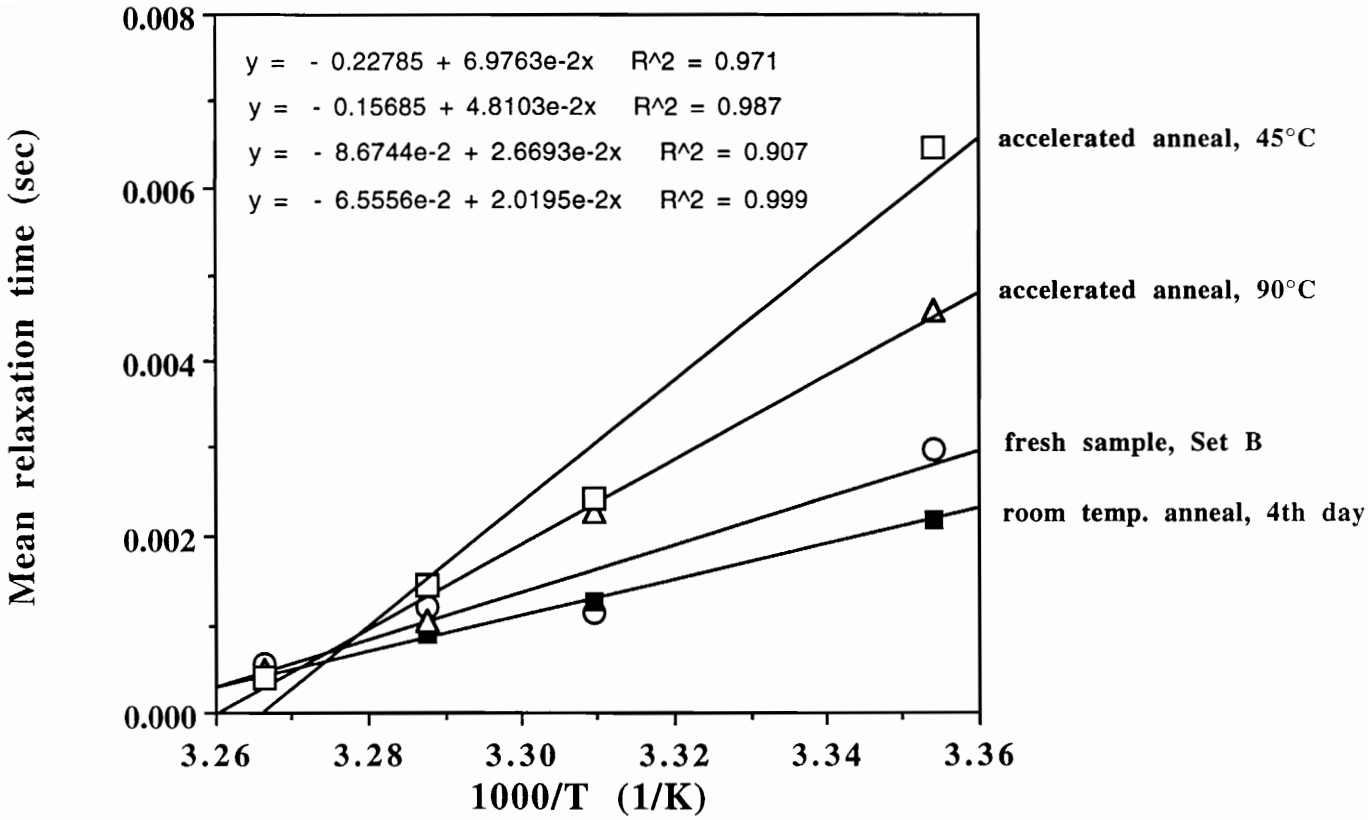

Figure 49. **Temperature and annealed status dependence of mean relaxation time as evaluated from KWW model**

Table 6.

Parameters of Havriliak-Negami and KWW model / Fresh sample, Set B

	Temperature (°C)				
	25	27	29	31	33
Havriliak-Negami					
oscillator strength	0.81	0.82	0.82	0.82	0.83
alpha	0.62	0.62	0.60	0.59	0.57
gamma	0.86	0.82	0.78	0.69	0.61
center of relaxation time $x10^4$	2.9	1.9	1.4	1.0	0.8
chi-square $x10^7$	1.4	1.3	1.4	1.6	1.9
KWW					
beta	0.30	0.28	0.29	0.27	0.27
kww relaxation time $x10^4$	3.2	2.3	1.1	0.78	0.36
mean relaxationtime $x10^3$	3.0	2.8	1.1	1.2	0.54
chi-square $x10^5$	3.8	4.6	1.5	6.5	5.5

Table 7.

Parameters of Havriliak-Negami and KWW model / Room temperature anneal 4 th day, Set B

	Temperature (°C)				
	25	27	29	31	33
Havriliak-Negami					
oscillator strength	0.28	0.29	0.32	0.30	0.31
alpha	0.68	0.67	0.68	0.64	0.63
gamma	1.00	1.00	1.00	1.00	1.00
center of relaxation time $x10^4$	0.94	0.61	0.34	0.28	0.20
chi-square $x10^7$	0.50	0.25	2.3	0.37	0.89
KWW					
beta	0.30	0.26	0.27	0.29	0.30
kww relaxation time $x10^4$	2.4	1.9	8.2	7.5	4.5
mean relaxationtime $x10^3$	2.2	3.5	1.3	0.88	0.38
chi-square $x10^4$	1.4	1.5	0.59	0.13	0.81

Table 8.

Parameters of Havriliak-Negami and KWW model / annealed at 90°C
for 12 hours after 1 day room temperature annealing, Set B

	Temperature (°C)				
	25	27	29	31	33
Havriliak-Negami					
oscillator strength	0.31	0.32	0.33	0.34	0.33
alpha	0.69	0.69	0.69	0.68	0.66
gamma	1.00	1.00	1.00	1.00	1.00
center of relaxation time $x10^4$	0.77	0.55	0.38	0.26	0.18
chi-square $x10^7$	1.5	1.2	1.3	0.84	0.73
KWW					
beta	0.25	0.25	0.26	0.27	0.28
kww relaxation time $x10^4$	2.1	1.9	1.1	0.67	0.41
mean relaxationtime $x10^3$	4.6	5.0	2.3	1.1	0.50
chi-square $x10^4$	0.63	1.3	0.81	0.63	0.59

Table 9.

Parameters of Havriliak-Negami and KWW model / annealed at 45°C
for 12 hours after 3 day room temperature annealing, Set B

	Temperature (°C)				
	25	27	29	31	33
Havriliak-Negami					
oscillator strength	0.23	0.24	0.25	0.26	0.28
alpha	0.70	0.69	0.69	0.68	0.66
gamma	1.00	1.00	1.00	1.00	1.00
center of relaxation time $x10^4$	0.51	0.41	0.28	0.24	0.14
chi-square $x10^7$	3.6	2.2	2.2	1.8	1.5
KWW					
beta	0.24	0.26	0.25	0.26	0.28
kww relaxation time $x10^4$	1.9	1.0	0.96	0.72	0.33
mean relaxationtime $x10^3$	6.4	1.9	2.4	1.4	0.4
chi-square $x10^4$	1.7	0.62	1.6	1.0	0.59

increases, relaxation time decreases. The mean relaxation is bigger than the center of relaxation time by an order of magnitude since it accounts for the distribution of relaxation time. The trends in the slopes of straight lines in Figures 48 and 49 is almost in reverse order signifying that the single parameter, center of relaxation time, is more skewed toward early stage of relaxation while mean relaxation time obtained using KWW model encompasses all relaxation stages and represents the effect of species which relax with difficulty.

Chapter 6. Conclusions and Recommendations

Through the phenomenological study of the dielectric relaxation behavior involving the crystallization process of melt processed PHB which has been annealed at room temperature and also annealed at high temperature in an accelerated fashion, several conclusions can be drawn.

In the glass transition region, two relaxation peaks were found which are coalesced at test frequencies in the kilo Hertz region. Temperature plane curve resolution revealed two separate peaks which are described as LTP and HTP in this study. From the fact that both peaks LTP and HTP, decrease in magnitude as crystallization proceeds, it is concluded that neither peak is related to the mobilities of chains of PHB which are directly attached to the crystalline phases such as lamellae or spherulites. Also, as the magnitude of HTP grows bigger relative to LTP as the extent of crystallization increases, HTP is speculated as representing the relaxation behavior of amorphous chains which are confined in-between the crystalline phases. This speculation was supported in the later part of this study which evaluated the temperature dependence of mean relaxation time constant and in the observation of the strong temperature dependence of maximum loss property when analyzed in the frequency plane. From the two peaks, the relaxation occurring at the lower temperature was found to be related to the loss occurring due to chain mobility of amorphous phase PHB. In the early stage of crystallization, the magnitude of the dielectric loss of the lower peak at given frequency decreases with the test frequency used in data acquisition signifying the PHB under study is still undergoing significant crystallization. At this stage, if PHB chains are activated by an electric field for measurement, some of the amorphous chains will be crystallized and irrecoverably transformed into part of crystalline phases, hence the evaluation of relaxation parameter is thought to be invalid for LTP at this stage of crystallization. However, when the extent

of crystallization is fully achieved, the relaxation behavior of amorphous chains which never crystallize between the lamellae can be studied. The only problem hindering this work is that by the time crystallization is complete, the magnitude of dielectric loss of these amorphous peak is so small that the curve resolution scheme which delineates the shape of amorphous peaks might be affected by other effects caused by small but strong polar impurities such as water. When a relatively slower heating rate was used, LTP showed less frequency dependent dispersion. This meant that LTP was a kinetically affected peak. It also signifies that during the time scale of the experiment, PHB was crystallized to a much larger extent than in the case where a higher heating rate was used. In this latter case, evaluation of the relaxation parameters was attempted for the HTP since HTP no longer showed a significant kinetic controlled effect as LTP did, and the frequency dispersion behavior of this peak was comparable to that of most of the systems usually studied. The mean relaxation time was found to be increase as the extent of crystallization increased, signifying that more and more uncrystallized remaining amorphous chains were relaxing with difficulty. As is easily expected, the oscillator strength, which may be called the effective dipole moment of the system, was found to decrease as the extent of crystallization increased. This can be interpreted simply to mean that the absolute number of dipoles participating in the relaxation process decreased. The trend observed in the time scale of this study was in agreement with the macroscopic measurement of stress-strain property and high precision gradient column density measurement. Also, it was found after the evaluation of autocorrelation function that the center of relaxation time in the Havriliak-Negami model is skewed toward short time scale of relaxation, while the mean relaxation time reflects the relaxation time on average and explains the crystallization behavior in a more persuasive manner. The test of temperature plane curve resolution was found to yield meaningful results even when subjected to quantitative analysis as shown in this study. However, this does not

necessarily mean that this approach is valid as a way to measure relaxation parameters absolutely at this moment. At least, in an empirical sense, where it is concerned with trends and relative scale, temperature plane curve resolution with Gaussian curves is considered to be satisfactory. Also the exponential baseline used for the decoupling of d.c. conductivity from meaningful relaxation seems to work at least in an empirical way. For the future development of dielectric analysis of blends, empirical formalism which can evaluate the dielectric mean relaxation time is proposed. The strong point of this kind of modeling is that it is rooted in the well accepted pre-existing theory of linear viscoelasticity and all the parameters can be evaluated from experiments.

As a by-product of my research, most of the empirical relaxation models currently used by many researchers in this field have been reviewed with worked out derivations which are often considered to be trivial in respected journals. Several computer programs were written and tested from scratch, notably using the Levenberg-Marquardt algorithm with constrained parameters.

There are several recommendations which can be made with regard to this research. First, the study of dielectric relaxation behavior which does not change kinetically benefits from the mechanical tools developed during this research. In such cases, as the system to be studied is not undergoing significant change during the time scale of the experiment, an isothermal scan followed by usual data reduction scheme is the only thing required. Binary blends with varying composition can be studied using temperature plane curve resolution in case the practical frequency window of the measuring device is limited. The effect of plasticizers, curing agents, heat stabilizers, and impact modifiers on the relaxation behavior of matrix polymers may be re-visited since the test of KWW model and the concept of mean relaxation time have not been prevalent in these types of research so far. If a system showing a well established physical aging effect is available with reliable experimental values describing the physical aging effect,

mean relaxation time analysis as well as conventional dielectric analysis could be correlated with those experimental values even though the success might depend heavily on the frequency window of the apparatus. All types of modifications to chemical structures, such as the introduction of spacers and polar groups and bulky side groups, might be characterized in a more quantitative manner.

REFERENCES

(1) Manning, M.F.; Bell, M.E. *Rev. Mod. Phys.* **1940**, 12, 215.

(2) Scaife, B.K.P. *Progr. Dielect.* **1963**, 5, 143.

(3) Fuoss, R.M. *J. Am. Chem. Soc.* **1941**, 63, 369

(4) Reitz, J.R.; Milford, F.J.; Christy, R.W. *Foundations of Electromagnetic Theory*; Addison-Wesley: Massachusetts, 1993.

(5) Wylie, C.R. *Advanced Enginnering Mathematics*; McGraw-Hill: New York, 1975.

(6) Jonscher, A.K. *Dielectric Relaxation in Solids*; Chelsea Dielectric Press: London, 1983.

(7) Ref.(4), p 613.

(8) Landau, L.D.; Lifshiftz, E.E. *Statistical Physics*; Addison-Wesley: Massachusetts, 1969, p 385.

(9) McQuarrie, D.A. *Statistical Mechanics*; Harper & Row: New York, 1973, p 498.

(10) Debye, P. *Polar Molecules*; Dover: New York, 1929.

(11) Blythe, A.R. *Electrical Properties of polymers*; Cambridge University Press: Cambridge, 1979.

(12) Cole, K.S.; Cole, R.S. *J. Chem. Phys.* **1941**, 9, 341.

(13) Davidson, D.W.; Cole, R.H. *J. Chem. Phys.* **1951**,19,1484.

(14) McCrum, N.G.; Read, B.E.; Williams, G. *Anelastic and Dielectric Effects in Polymeric Solids;* Dover: New York, 1991.

(15) Glarum, S.H. *J. Chem. Phys.* **1960**, 33, 639.

(16) ibid, p 1371

(17) Fuoss, R.M.; Kirkwood, J.G. *J. Am. Chem. Soc.*, **1941**, 63, 385.

(18) Havriliak, S.; Negami, S. *J. Polym. Sci., Part C* **1966**, 14, 99.

(19) Havriliak, S.; Negami, S. *Polymer* **1967**, 8, 161.

(20) Hedvig, P. *Dielectric Spectroscopy of Polymers*; Adam Hilger: Bristol, U.K., 1977, p 62.

(21) Williams, G. *Chem. Rev.* **1972**, 72, 55.

(22) Ref.(12), p 350.

(23) Formalism established in Ref.(17)

(24) Ref.(13), p 1489.

(25) Tschoegl, N.W. The *Phenomenological Theory of Linear Viscoelastic Behavior*; Springer-Verlag: Berlin, 1989.

(26) Cochran, J.A. *Applied Mathematics*; Wadsworth: Belmont, California, 1982.

(27) Cole, K.S.; Cole, R.S. *J. Chem. Phys.* **1942**, 10, 98.

(28) Abramowitz, M.; Stegun, I.A. *Handbook of Mathematical Functions with Formulas, Graphs and Mathematical Tables*; Dover: New York, 1966.

(29) Davidson, D.W. *Can. J. Chem.* **1961**, 39, 571.

(30) Kohlrausch, F. *Pogg. Ann. Physik* **1863**, 29, 337.

(31) Patterson, G.D.; Lindsey, C.P. *Macromolecules* **1981**, 14, 83.

(32) Struik, L.C.E. *Physical Aging in Amorphous Polymers and other Materials, TNO Communication No.565;* Delft: Netherlands, 1977.

(33) Williams, G.; Watts, D.C. *Trans. Faraday Soc.* **1970**, 66, 80.

(34) Cook, M.; Watts, D.C.; Williams, G. *Trans. Faraday Soc.* **1970**, 66, 2503.

(35) Lindsey, C.P.; Patterson, G.D. *J. Chem. Phys.* **1980**, 73, 3348.

(36) Ref(1), p 234.

(37) Matsuoka, S. *Relaxation Phenomena in Polymers*; Hanser: Munich, 1992.

(38) Matsuoka, S.; Quan, X. *Macromolecules* **1991**, 24, 2770.

(39) Schweidler, E.von *Ann. d. Physik* **1907**, 24, 711.

(40) Wagner, K.W. *Ann. d. Physik* **1913**, 40, 817

(41) Boas, L.M. *Mathematical Methods in the Physical Sciences*; Wiley: New York, 1983, p 609.

(42) Ref.(31), p 3356.

(43) Reed, T. M.; Gubbins, K. E. *Applied Statistical Mechanics*; McGraw-Hill : New York, 1973.

(44) Boon, J. P.; Rice, S. A. *J.Chem.Phys.* **1967**, 47, 2480.

(45) Resibois, P. *J.Chem. Phys*. **1964**, 41, 2979.

(46) Adachi, K.; Kotaka, T. *Macromolecules* **1988**, 22, 157.

(47) Ref.(20), p 40.

(48) Boese, D.; Kremer, F. *Macromolecules* **1990**, 23, 829.

(49) van Beek, L.K.H. *J. Appl.Polym.Sci.* **1964**, 8, 843.

(50) Mott, N.F.; Davis, E.A. *Electronic Processes in Non Crystalline Materials*; Clarendon Press: Oxford, U.K., 1979.

(51) Kohler, W.; Robello, D.R.; Williard, C.S.; Williams, D.J. *Macromolecules* **1991**, 24, 4859.

(52) Ref.(6), p 89.

(53) Williams, M.L.; Landel, R.F.; Ferry, J.D. *J.Amer.Chem.Soc*. **1955**, 77, 3701.

(54) Ref.(14), p 534.

(55) Ref (20), p 125

(56) Kurata, M.; Osaki, K.; Elinaga, Y.;Surgie, T. *J.Polym.Sci.,Polym,Phys.Ed.* **1974**, 12, 849.

(57) Bohn, L. *Kunststoffe* **1963**, 53, 93.

(58) Jacoby, P.; Bersted, B.H.; Kissel, W.J.; Smith, C.E. *J.Polym. Sci., Polym.Phys.Ed.* **1986**, 24, 461.

(59) Rotter, G.; Ishida, H. *Macromolecules* **1992**, 25, 2170.

(60) Park, T.; Snyder, C.; Marand, H.; Ward, T.C. *Amer. Chem. Soc., Div. Polym. Chem., Prepr.* **1993**, 69, 70.

(61) Doi, Y. *Microbial Polyesters*; VCH Publishers: New York, 1990.

(62) Huang, J.C.; Shetty, A.S.; Wang, M.S. *Advances in Polymer Technology* **1990**, 10, 23.

(63) Lemoigne, M. *Ann. Inst. Pasteur* **1925**, 10, 135.

(64) Hughes, L.;Richardson, K.R. *Br. Patent* 0 046 344 (1981)

(65) *National Geographic* Feb, 1994.

(66) Kepes, A.; Peaud, L.C. *Bull.Soc.Chim.Biol.* **1952**, 34, 563.

(67) Fukada, E.; Ando,Y. *Int.J.Biol.Macromol.* **1986**, 34, 563.

(68) Barham, P.J.; Keller, A.; Otun, E.L.; Holmes, P.A. *J.Mater.Sci.* **1984**, 19, 2781.

(69) Cornibert, J.; Marchessault, R.H. *J.Mol.Biol.* **1972**, 71, 735.

(70) Barham, P.J.; Keller, A. *J.Polym.Sci.,Polym.Phys.Ed.* **1986**, 24, 69.

(71) King, P.P. *J.Chem.Tech.Biotechnol.* **1982**, 32, 2.

(72) Holmes, P.A. *U.S.Patent* 4 477 654 (1984)

(73) Hori, Y. *Macromolecules*, **1992**, 25, 5117.

(74) Kemnitzer,J.; McCarthy, S.P.; Gross, R.A. *Macromolecules* **1993**, 26, 6143 and 1221

(75) Reeve, M.S.; McCarthy, S.P.; Gross, R.A. *Macromolecules*, **1993**, 26, 888.

(77) McCarthy, S.P.; Gross, R.A. *Proc. of Environmentally Degradable Polymers: Technical, Business, and Public Perspectives*, Chelmsford, MA, 1991.

(78) Ziska, J.J.; Barlow, J.W.; Paul, D.R. *Polymer*, **1981**, 22, 918.

(79) Holmes, P.A. *U.S.Patent* 4 393 167 (1983)

(80) Avella, M.; Martucelli, E. *Polymer* **1988**, 29, 1731.

(81) Abbate, M.; Martuscelli, E.; Ragosta, G.; Scarinzi, G. *J.Polym.Sci.* **1991**, 26, 1119.

(82) Pearce, R.; Jesudason, J.;Orts, W.; Marchessault, R.H.; Bloembergen, S. *Polymer* **1992**, 33, 4647.

(83) Ceccorulli, G.; Pizzoli, M.; Scandola,M. *Macromolecules* **1993**, 26,6722.

(84) Abe, H.; Doi, Y. Michael, M.S.; Noda, I. *Macromolecules* **1994,** 27, 50.

(86) Marchessault, R.H.;Coulombe, S.; Morikawa, H.; Okamura, K.; Revol, J.F. *Can.J.Chem.* **1981**, 5, 38.

(87) Barham, P.J. *J.Mater.Sci.* **1984,**19,3826.

(88) Scandola, M.;Pizzoli,M.;Ceccorulli, G.; Cesaro, A.; Paoletti, S.; Navarini, L. *Int.J.Biol.Macrmol.* **1988**,10,373.

(89) Revol, J.F.; Chanzy,H.D.; Deslandes, Y.; Marchessault, R.H. *Polymer* **1989**, 30, 1973.

(90) Doi, Y.; Kanesawa, Y.; Kunioka, M. *Macromolecules* **1990**, 23, 26.

(91) Owen, A.J.; Heinzel, J.; Skrbic, Z.; Divjakovic, V. *Polymer* **1992**, 33, 1563.

(92) Burger, H.M.; Muller, H.M.; Seebach, D.; Bornsen, K.O.; Schar, M.; Widmen, H.M. *Macromolecules* **1993**, 26, 4783.

(93) Brandrup, J.; Immergut, E.H. *Polymer Handbook*, 3rd ed., VII-24; John Wiley & Sons: New York, 1989.

(94) Performed by Chad C. Snyder, Dept. of Chemistry, Virginia Tech.

(95) Mohamed, J.L.; Walsch, J. eds. *Numerical Algorithms*; Clarendon Press: Oxford, 1986.

(96) Bevington, P.R. *Data reduction and error analysis for the physical sciences*; McGraw-Hill: New York, 1969.

(97) Ando, Y.; Fukada, E. *J.Polym.Sci.Polym.Phys.Ed.* **1984**, 22, 1821.

(98) Information from Dr.Herve Marand, Dept. of Chemistry, Virginia Tech.

(99) Schegel, H.G.; Gottschalk, G.; Bartha, R. *Nature* **1961**, no 4787, 463.

(100) Kolarik, J. *Adv.Polym.Sci.* **1982**, 46, 119.

(101) George Dallas, Ph.D. dissertation, Virginia Polytechnic Institute & State University.

(102) Saikat Joardar, Ph.D. dissertation, Virginia Polytechnic Institute & State University.

Appendices

All programs in Appendix A and B were

i) written in Microsoft Basic version 1.00E
ii) compiled and executed on MacIntosh Quadra 800

The program in Appendix C was

i) written in Mathematica version 2.2.1
ii) executed on MacIntosh Quadra 800

Appendix A:

Nonlinear Least Squares Method of Levenberg-Marquardt

(a) Constrained parameter method

This method works very well in practice and has been the standard of nonlinear squares routines.[95, 96]

One thing to remark about in utilizing this algorithm , especially for Appendix B-3, is the parameter constraint problem. If this is not considered, this algorithm does not work at all in many cases. Usually when minimizing some function whose parameters are a_1, a_2, .. and so on, the parameters can take any signs during the iteration process. However, if the function has components such as a power function with odd or fractional index or log function, the parameter should be always positive. In this case all parameters should be replaced with positive ones using the following technique.

For the minimization of given function

$$f(x; a_1, a_2, a_3,..) = 0 , \quad a_i > 0 , \ i = 1,2,...$$

1) Replace a_i with α_i where $a_i = \alpha_i^2$

2) Then the function is rewritten in terms of α_i

$$f(x; \alpha_1, \alpha_2, \alpha_3,..) = 0 , \qquad i = 1,2,...$$

3) For the analytic derivative, which is always favored over the numerical one in the Levenberg-Marquardt algorithm, use the chain rule

$$\frac{\partial f}{\partial \alpha_i} = \frac{\partial f}{\partial a_i} \cdot \frac{\partial a_i}{\partial \alpha_i}$$

to avoid any logic and illegal function error.

(b) Common Subroutines

Within the programs in the appendix, "Subroutine MATINV" corresponds to the following routine.

```
REM    ==============SUBROUTINE MATINV================

                          MATINV:

     DET = 1

     FOR k =1 TO NORDER

    REM -----FIND LARGEST ELEMENT ARRAY(I,J) IN REST OF MATRIX

        AMAX = 0

500     FOR I = k TO NORDER
            FOR J = k TO NORDER
              D = ABS(AMAX) - ABS(ARRAY(I,J))
              IF D > 0 THEN GOTO 510
              AMAX = ARRAY(I,J)
              IK(k) = I
              JK(k) = J
510         NEXT J
        NEXT I


    REM ----INTERCHANGE ROWS AND COLUMNS TO PUT AMAX IN ARRAY(K,K)

      IF AMAX <> 0 THEN GOTO 520
      DET = 0: GOTO 1000

520           I = IK(k)
```

```
                II = I - k
                IF II < 0  THEN GOTO 500
                IF II = 0 THEN GOTO  530
                FOR J = 1 TO NORDER
                     SSAVE = ARRAY(k,J)
                     ARRAY(k,J) = ARRAY(I,J)
                     ARRAY(I,J) = -SSAVE
                NEXT J

530             J = JK(k)
                JJ = J - k
                IF JJ < 0 THEN GOTO 500
                IF JJ = 0 THEN GOTO 540
              FOR I = 1 TO NORDER
                   SSAVE = ARRAY(I,k)
                   ARRAY(I,k) = ARRAY(I,J)
                   ARRAY(I,J) = -SSAVE
                NEXT I

    REM ---- ACCUMULATE ELEMENTS OF INVERSE MATRIX

540         FOR I = 1 TO NORDER
                II = I - k
                IF II = 0 THEN GOTO 550
                ARRAY(I,k) = -ARRAY(I,k) / AMAX
550         NEXT I

            FOR I = 1 TO NORDER
                FOR  J = 1 TO NORDER
                II = I - k
                IF II = 0 THEN GOTO 570
                JJ = J- k
                 IF JJ = 0 THEN GOTO 560
                  ARRAY(I,J) = ARRAY(I,J) + ARRAY(I,k)*ARRAY(k,J)
560             NEXT J
570         NEXT I

              FOR J = 1 TO NORDER
                JJ = J - k
                IF JJ = 0 THEN GOTO 580
              ARRAY(k,J) = ARRAY(k,J) / AMAX

580           NEXT J
            ARRAY(k,k) = 1 / AMAX
            DET = DET*AMAX
    NEXT k

  REM   -----RESTORE ORDERING OF MATRIX

    FOR L = 1 TO NORDER
            k  = NORDER - L  + 1
            J = IK(k)
            JJ = J - k
            IF JJ =< 0 THEN GOTO 800
            FOR I = 1 TO NORDER
```

```
            SSAVE = ARRAY (I,k)
            ARRAY(I,k) = -ARRAY(I,J)
            ARRAY(I,J) = SSAVE
            NEXT I

800          I = JK(k)
             II = I - k
             IF II =< 0 THEN GOTO 900
             FOR J = 1 TO NORDER
              SSAVE = ARRAY(k,J)
              ARRAY(k,J) = -ARRAY(I,J)
              ARRAY(I,J) = SSAVE
             NEXT J
900   NEXT L
1000  RETURN
```

Within the programs in the appendix, "Subroutine Sing" corresponds to the following routine.

```
                                    Sing:
    SOUND 1046,1,100 :SOUND 988,1,100:SOUND 1046,2,100
    SOUND 784,2,100:SOUND 784,2,100: SOUND 784,1,100
    SOUND 698,1,100:SOUND 659,1,100: SOUND 784,1,100
    SOUND 1046,2,100:SOUND 1046,2,100

  RETURN
```

Within the programs in the appendix, "Subroutine FCHISQUARE" corresponds to the following routine.

```
REM   ==============SUBROUTINE FCHISQUARE=============

                        FCHISQUARE:

            CHISQ = 0
                 FOR II = 1 TO NPTS
                   CHISQ = CHISQ + ((Y(II)-YFIT(II))^2)
                 NEXT II
            FREE = NFREE
            FCHISQ = CHISQ / FREE
```

```
RETURN
```

Within the programs in the appendix, "Subroutine CURVFIT" corresponds to the following routine.

```
REM  ===============SUBROUTINE CURVFIT===============

                          CURVFIT:

    NFREE = NPTS-NTERMS

    REM  -----EVALUATE ALPHA AND BETA MATRICES

255     FOR J = 1 TO NTERMS
    BETA(J) = 0
      FOR k = 1 TO J
      ALPHA(J,k) = 0
      NEXT k
    NEXT J

    FOR I = 1 TO NPTS
        GOSUB FDERIV
            FOR J = 1 TO NTERMS
                GOSUB FUNC1
      BETA(J) = BETA(J) +  ( Y(I) - FUNCTN )*DERIV(J)
                FOR k = 1 TO J
      ALPHA(J,k) = ALPHA(J,k) + DERIV(J)*DERIV(k)
                NEXT k
            NEXT J
    NEXT I

      FOR J = 1 TO NTERMS
          FOR k = 1 TO J
            ALPHA(k,J) = ALPHA(J,k)
          NEXT k
      NEXT J


    REM --------EVALUATE CHI SQUARE AT STARTING POINT

          FOR I = 1 TO NPTS
              GOSUB FUNC1
                  YFIT(I) = FUNCTN
          NEXT I
        GOSUB FCHISQUARE
            CHISQ1 = FCHISQ

    REM---------INVERT MODIFIED CURVATURE MATRIX
    REM---------TO FIND NEW PARAMETERS
```

```
300         FOR J = 1 TO NTERMS
                    FOR k = 1 TO NTERMS
            ARRAY(J,k) = ALPHA(J,k) / SQR( ALPHA(J,J) * ALPHA(k,k))
                    NEXT k
            ARRAY(J,J) = 1 + FLAMDA
          NEXT J
        NORDER = NTERMS
                              GOSUB MATINV

        FOR J = 1 TO NTERMS
          B(J) = A(J)
            FOR k = 1 TO NTERMS
              B(J) = B(J) + BETA(k) *ARRAY(J,k)/ SQR(ALPHA(J,J)*ALPHA(k,k))
            NEXT k
        NEXT J

        REM   ----- IF CHI SQUARE IS INCREASED,
        REM   -----INCREASE FLAMDA AND TRY AGAIN

      FOR I = 1 TO NPTS
          GOSUB FUNC2
          YFIT(I) = FUNCTN
      NEXT I

          GOSUB FCHISQUARE
          DCHI = CHISQ1 - FCHISQ
          IF DCHI >= 0 GOTO 350
          FLAMDA = 5*FLAMDA

      GOTO 300


        REM   -----EVALUATE PARAMETERS AND UNCERTAINTITIES

350 FOR J = 1 TO NTERMS
          A(J) = B(J):SIGMAA(J) = SQR(ARRAY(J,J)/ALPHA(J,J))
      NEXT J
      FLAMDA = FLAMDA/5

    RETURN
```

Appendix B:

Appendix B-1:

Multiple Gaussian Curves with Exponential Baseline

```
REM  ****************************
REM       Curve Resolution
REM  ****************************

REM   PURPOSE:  CURVE RESOLUTION OF COMPOSITE CURVE INTO
REM   THREE GAUSSIAN CURVES AND ONE EXPONENTIAL CURVE
REM   USING A NONLINEAR LEAST SQUARES METHOD BASED ON
REM   MARQUARDT'S ALGORITHM

REM  ================================
REM  DESCRIPTION OF PARAMETERS
REM  ================================

REM  X-          ARRAY OF DATA POINTS FOR INDEPENDENT VARIABLE
REM  Y-          ARRAY OF DATA POINTS FOR DEPENDENT VARIABLE
REM  A-          ARRAY OF PARAMETERS
REM  DELTAA-      ARRAY OF PARAMETER INCREMENTS
REM  SIGMAA       ARRAY OF STANDARD DEVIATIONS FOR A PARAMETERS
REM  SIGMAY-      ARRAY OF STANDARD DEVIATION FOR Y DATA POINTS
REM  NPTS-       NUMBER OF PAIRS OF DATA POINTS
REM  NTERMS-      NUMBER OF PARAMETERS
REM  NFREE-      NUMBER OF DEGREE OF FREEDOM
REM  NORDER-      DEGREE OF MATRIX
REM  FLAMDA-      PROPORTION OF GRADIENT SEARCH INCLUDED
REM  YFIT-       ARRAY OF CALCULATED VALUES OF Y
REM  CHISQ-       REDUCED CHI SQUARE FOR FIT

DIM  X(300),Y(300),YFIT(300),A(15),B(15),SIGMAA(15)
DIM  ALPHA(15,15),BETA(15),ARRAY(15,15)
DIM  DERIV(15),IK(15),JK(15)

    CLS:
5    GOSUB Title: GOSUB Sing
     CALL TEXTSIZE(12) :CALL TEXTFACE(33):backcolor 30:forecolor 205
7    LOCATE 11,5: INPUT "  Ready for Analysis (y/n)       "; R$
          IF R$ = "n" GOTO 125
          IF R$ <> "y" GOTO 7

8   CLS: GOSUB Title
    CALL TEXTSIZE(12): CALL TEXTFACE(33):backcolor 30: forecolor 409
    LOCATE 12,5: INPUT " I.       Max. Amplitude of 1st curve --->";A(1)
    LOCATE 13,5: INPUT "          Center of 1st curve --->";A(2)
    LOCATE 14,5: INPUT "          FWHM of 1st curve --->";A(3)

    LOCATE 15,5: INPUT " II.      Max. Amplitude of 2nd curve --->";A(4)
    LOCATE 16,5: INPUT "          Center of 2nd curve --->";A(5)
    LOCATE 17,5: INPUT "          FWHM of 2nd curve --->";A(6)
```

```
    LOCATE 18,5: INPUT " III.      Max. Amplitude of 3rd curve --->";A(7)
    LOCATE 19,5: INPUT "          Center of 3rd curve --->";A(8)
    LOCATE 20,5: INPUT "          FWHM of 3rd curve --->";A(9)

    LOCATE 21,5 : INPUT "IV.       Pure exponential region x1  ==>";XE1
    LOCATE 22,5 : INPUT "          Pure exponential region y1  ==>";YE1
    LOCATE 23,5 : INPUT "          Pure exponential region x2  ==>";XE2
    LOCATE 24,5 : INPUT "          Pure exponential region y2 ==>";YE2

    LOCATE 25,5:forecolor 137
    PRINT" ************************************"
    LOCATE 26,5 : INPUT " Number of data point pair  --->";NPTS
    LOCATE 27,5 : INPUT " Input data file name   ---> ";F$
    LOCATE 28,5
    PRINT" ************************************"
    forecolor 205
9   LOCATE 29,5 : INPUT " Any corrections (y/n)        "; C$
    IF C$ = "n"  GOTO 10
    IF C$ <> "y" GOTO 9
    GOTO 8
10  CLS : forecolor 409
    LOCATE 5,5:INPUT " Output data file name   ---> ";FF$:CLS: forecolor 409
    LOCATE 10,5 :PRINT " Iteration Process Started"
    TEXTSIZE(12):TEXTFACE(0):backcolor 30:forecolor 33
      OPEN F$ FOR INPUT AS 1
      FOR I = 1 TO NPTS : INPUT #1, X(I),Y(I): NEXT I
      CLOSE #1

  OPEN FF$ FOR OUTPUT AS 2


REM -------Begin Nonlinear Regression ----------


        NTERMS = 11
        FLAMDA = .01

        A(10) = LOG(YE2/YE1) / (XE2-XE1)
        A(11) = XE2 - LOG(YE2) / A(10)

 REM  ================================================
 REM  ITERATION OF  CHI-SQUARE CALCULATION
 REM  ================================================
                    IT = 0

  FOR I = 1 TO 5 : PRINT #2," " : NEXT I

      PRINT        "#";"   A1   A2   A3   A4   A5   A6   A7   A8  A9 A10 A11  CHI2"
      PRINT #2,    "#";" A1   A2   A3   A4   A5   A6    A7   A8  A9 A10 A11  CHI2"

      PRINT         IT; A(1); A(2);A(3);A(4);A(5);A(6);A(7);A(8);A(9);A(10);A(11)
      PRINT #2,    IT,A(1), A(2),A(3),A(4),A(5),A(6),A(7),A(8);A(9);A(10);A(11)

        GOSUB CURVFIT
```

```
                              IT = IT +1

          PRINT  " FIRST CHI-SQUARE VALUE",CHISQ1
          PRINT #2," FIRST CHI-SQUARE VALUE",CHISQ1

   PRINT   " ========================================="
   PRINT #2, "========================================="
                              OLDCHI = FCHISQ

50  GOSUB  CURVFIT

          PRINT       IT, FCHISQ
          PRINT #2,   IT,FCHISQ

          FOR I =  1 TO NTERMS
            PRINT A(I); : PRINT #2,A(I);
          NEXT I
            PRINT " "
            PRINT #2," "

         NEWCHI = FCHISQ

         E = ABS((OLDCHI-NEWCHI)/OLDCHI)

         IF E =<.0001    GOTO 100

         OLDCHI = NEWCHI : IT = IT +1

        GOTO 50

100       PRINT "============================="
          PRINT #2,"============================="
          PRINT " FINAL RESULT ": PRINT " "
          PRINT #2," FINAL RESULT ": PRINT #2," "

          PRINT IT,FCHISQ
          PRINT #2,IT,FCHISQ

      FOR I = 1 TO NTERMS
       PRINT A(I) :PRINT #2,A(I)
       NEXT I

      PRINT "FITTING ACCOMPLISHED AFTER";IT;"TIMES ITERATION"
      PRINT #2,"FITTING ACCOMPLISHED AFTER";IT;"TIMES ITERATION"

      CLOSE 2

125       END

   REM   >>>>>>>>>>>>>>>>>>>>>SUBROUTINES<<<<<<<<<<<<<<<<<<<<<<<
```

Subroutine CURVFIT

```
      REM   ============SUBROUTINE FDERIV================
```

```
                    FDERIV:
   xi = X(I)
   DERIV(1) = EXP(-LOG(2)*(2*(xi-A(2))/A(3))^2)
   DERIV(2) = (8*LOG(2)*A(1)*(xi-A(2))*DERIV(1))/((A(3))^2)
   DERIV(3) = (xi-A(2))*DERIV(2)/A(3)

   DERIV(4) = EXP(-LOG(2)*(2*(xi-A(5))/A(6))^2)
   DERIV(5) = (8*LOG(2)*A(4)*(xi-A(5))*DERIV(4))/((A(6))^2)
   DERIV(6) = (xi-A(5))*DERIV(5)/A(6)

   DERIV(7) = EXP(-LOG(2)*(2*(xi-A(8))/A(9))^2)
   DERIV(8) = (8*LOG(2)*A(7)*(xi-A(8))*DERIV(7))/((A(9))^2)
   DERIV(9) = (xi-A(8))*DERIV(8)/A(9)


   DERIV(10) = (xi-A(11))*EXP(A(10)*(xi-A(11)))
   DERIV(11) = -A(10)*EXP(A(10)*(xi-A(11)))


     RETURN

REM  ==========SUBROUTINE FUNCTN==========

                    FUNC1:

   IF A(3) <0 THEN A(3) = -A(3)
   IF A(6) <0 THEN A(6) = -A(6)
   IF A(9) <0 THEN A(9) = -A(9)
 FUNCTN = 0
    xi = X(I)
Z1 = (xi-A(2))/A(3)
Z2 = (xi-A(5))/A(6)
Z3 = (xi-A(8))/A(9)
Z12 = (Z1)^2
Z22 = (Z2)^2
Z32 = (Z3)^2
ZZ1= EXP(-4*LOG(2)*Z12)
ZZ2= EXP(-4*LOG(2)*Z22)
ZZ3= EXP(-4*LOG(2)*Z32)
ZZ4 =EXP(A(10)*(xi-A(11)))
FUNCTN = FUNCTN + A(1)*ZZ1+A(4)*ZZ2 + A(7)*ZZ3 + ZZ4


RETURN

                    FUNC2:

   IF B(3) <0 THEN B(3) = -B(3)
   IF B(6) <0 THEN B(6) = -B(6)
   IF B(9) <0 THEN B(9) = -B(9)
 FUNCTN = 0
 xi = X(I)
Z1 = (xi-B(2))/B(3)
Z2 = (xi-B(5))/B(6)
Z3 = (xi-B(8))/B(9)
```

```
Z12 = (Z1)^2
Z22 = (Z2)^2
Z32 = (Z3)^2
ZZ1= EXP(-4*LOG(2)*Z12)
ZZ2= EXP(-4*LOG(2)*Z22)
ZZ3= EXP(-4*LOG(2)*Z32)
ZZ4 =EXP(B(10)*(xi-B(11)))
FUNCTN = FUNCTN + B(1)*ZZ1+B(4)*ZZ2 + B(7)*ZZ3 + ZZ4

RETURN
```

Subroutine FCHISQUARE

Subroutine MATINV

```
                                    Title:
  backcolor 273 : forecolor 409
  CALL TEXTSIZE(33): CALL TEXTFACE(33)
  LOCATE 2,3 :PRINT " CURVE DECONVOLUTION "
  CALL TEXTSIZE(12): CALL TEXTFACE(33)
  LOCATE 7,20:backcolor 30:PRINT " © Dr. Thomas C Ward's Lab "
   CALL TEXTSIZE(14):forecolor 205
  LOCATE 7,10: PRINT " [  v 1.0    In-House program  Polypkem 6/25/93 ] "
  forecolor 341
  LINE (35,34)-(475,150), ,B
  LINE (34,33)-(476,151), ,B
  LINE (32,31)-(478,153), ,B
  forecolor 137
  FOR xi = 35 TO 475 STEP 5
  FOR yi = 34 TO 150 STEP 5
  PSET (xi,yi)
  NEXT yi
  NEXT xi
RETURN
```

Subroutine Sing

Appendix B-2:

Kohlaursch-Williams-Watts

```
      REM  ****************************
      REM  Kohlaursch-Williams-Watts Analysis
      REM  ****************************

      REM   This program, first, evaluates parameter beta of
      REM   Kohlaursch-Williams-Watts function using the
      REM   linear regression forced to the origin for the
      REM   x,y data pairs of (LOG10( TIME),auto-correlation function value )
      REM   The beta obtained is used as the initial guess of
      REM   nonlinear least square method which use MARQUARDT'S ALGORITHM
      REM   to obtain fine tuned beta

      REM  ============================
      REM  DESCRIPTION OF PARAMETERS
      REM  ============================
      REM   yt = 1/e
      REM  X- ,XR-    ARRAY OF DATA POINTS FOR INDEPENDENT VARIABLE
      REM  Y- ,YR-    ARRAY OF DATA POINTS FOR DEPENDENT VARIABLE
      REM  A-         ARRAY OF PARAMETERS
      REM  B-         ARRAY OF PARAMETERS
      REM  IK-,JK-        TEMPORARY STORAGE IN SUBROUTINE MATINV
      REM  DERIV-         ARRAY OF DERIVATIVES
      REM  ALPHA-,BETA-   ARRAY FOR GRADIENTS IN SUBROUTINE CURVFIT
      REM  YFIT-          ARRAY OF CALCULATED VALUES OF Y
      REM  NPTS           NUMBER OF PAIRS OF DATA POINTS
      REM  NTERMS         NUMBER OF PARAMETERS
      REM  NFREE          NUMBER OF DEGREE OF FREEDOM
      REM  NORDER         DEGREE OF MATRIX
      REM  FLAMDA         PROPORTION OF GRADIENT SEARCH INCLUDED
      REM  TAUCENT        CENTRAL RELAXATION TIME
      REM  CHISQ          REDUCED CHI SQUARE FOR FIT
      REM  ============================================================

        DIM    XR(200),YR(200),X(200),Y(200),YFIT(200)
        DIM    A(5),ALPHA(5,5),BETA(5),ARRAY(5,5)
        DIM   DERIV(5),b(5),IK(5),JK(5)

          CLS:
5      GOSUB Title: GOSUB Sing
       CALL TEXTSIZE(12) :CALL TEXTFACE(33):backcolor 30:forecolor 205
7      LOCATE 11,5: INPUT "  Ready for Analysis (y/n)       "; R$
               IF R$ = "n" GOTO 200
               IF R$ <> "y" GOTO 7
8     CLS: GOSUB Title
      CALL TEXTSIZE(12): CALL TEXTFACE(33):backcolor 30: forecolor 409
      LOCATE 11,5 : INPUT " Sample ID --->";samp$
       LOCATE 12,5
      PRINT"************************************"
      LOCATE 13,5 : INPUT " Number of data point pair  --->";N
      LOCATE 14,5 : INPUT " Input data file name   ---> ";F$
```

```
    LOCATE 15,5
    PRINT"************************************"
    forecolor 205
9   LOCATE 20,5 : INPUT " Any corrections (y/n)        "; C$
    IF C$ = "n"  GOTO 10
    IF C$ <> "y" GOTO 9
    GOTO 8
10  CLS
    LOCATE 5,5:INPUT " Output data file name  ---> ";FF$:CLS: forecolor 409
    LOCATE 10,5 :PRINT " Iteration Process Started"
    CALL TEXTSIZE(12): CALL TEXTFACE(0):backcolor 30:forecolor 33

    OPEN F$ FOR INPUT AS 1
    FOR I = 1 TO N   :   INPUT #1,XR(I),YR(I)   :   NEXT I   :   CLOSE #1
    OPEN FF$ FOR OUTPUT AS 2
          PRINT "*****KWW analysis of ";samp$;" ***** "
          PRINT #2,   "*****KWW analysis of ";samp$;" ***** "
          yt = .367879
             FOR I = 1 TO N
             IF YR(I) =< yt  THEN GOTO 25
             NEXT I
25      k2 = I  :  k1 = k2 - 1
        logtau = (yt-YR(k2))*(XR(k2)-XR(k1))/(YR(k1)-YR(k2)) +XR(k1)
        taucent = 10^(logtau)
    PRINT "   Central relaxtion time =  ";  taucent
    PRINT #2,   "   Central relaxtion time =   ";  taucent

        FOR I = 1 TO  N
     X(I) =  LOG(10)*(XR(I)-logtau) :Y(I) = LOG(-LOG(YR(I)))
        NEXT I

    sumxy = 0 : sumx2=0 :sumy2 =0
    FOR  I = 1 TO N
    sumxy = sumxy + X(I)*Y(I)
    sumx2 = sumx2 + (X(I))^2
    sumy2 = sumy2 + (Y(I))^2
    NEXT I

    delta2 = sumy2-(sumxy)^2 / sumx2
    slope = sumxy / sumx2
    stdslope = (delta2/(N-1))/sumx2
    coeff = sumxy / (SQR(sumx2) * SQR(sumy2))

    PRINT "   beta =   ";slope :   PRINT #2,"   beta =   ";slope

    PRINT "   Standard deviation of beta =  ";stdslope
    PRINT #2,   "   Standard deviation of beta =  ";stdslope
    PRINT "   Coefficient of correlation =   " ; coeff
    PRINT #2,   "   Coefficient of correlation =   " ; coeff

    CHISQ =0
    FOR I = 1 TO N
    J =  (10^(XR(I) ))  / (10^(logtau)) : K = J^(slope)
    CHISQ = CHISQ + ( YR(I) - EXP(-K))^2/(N-1)
    NEXT I
```

```
      PRINT "    Chi-square (linear) =     ";CHISQ
      PRINT #2,    "    Chi-square (linear) =     ";CHISQ
      PRINT "    "
      PRINT #2,    " "

     REM     ========Begin nonlinear regression==========

       NPTS = N : NTERMS = 1: FLAMDA = .001: A(1)=slope

     REM    -------REFRESH X(I),Y(I)
     FOR I = 1 TO NPTS : X(I) = 10^(XR(I)) :Y(I)=YR(I) : NEXT I

     REM    -----ITERATION OF  CHI-SQUARE CALCULATION
                              IT = 0
       PRINT         "-----Nonlinear regression----- "
       PRINT #2,    "-----Nonlinear regression----- "

                        GOSUB CURVFIT
                            IT = IT +1
          PRINT   " ============================="
          PRINT #2, "============================="
          OLDCHI = FCHISQ
          PRINT   "    Iteration / beta / Chi-square   "
          PRINT #2, "    Iteration / beta / Chi-square   "

50                       GOSUB   CURVFIT
          PRINT       IT;" / ";A(1);" / "; FCHISQ
          PRINT #2,  IT;" / ";A(1);" / "; FCHISQ
          PRINT " "
          PRINT #2," "

          NEWCHI = FCHISQ

          E = ABS((OLDCHI-NEWCHI)/OLDCHI)

          IF E =<.001    GOTO 100

          OLDCHI = NEWCHI : IT = IT +1

          GOTO 50

100       PRINT " ============================="
          PRINT #2," ============================="
          PRINT "           <<FINAL RESULT>> ": PRINT " "
          PRINT #2,"           <<FINAL RESULT>> ": PRINT #2," "

           PRINT "        beta =   ";A(1) : PRINT #2,    "    beta =  ";A(1)
     PRINT "    Chi-square =  ";FCHISQ
     PRINT #2,    "    Chi-square =  ";FCHISQ
     PRINT " "
     PRINT #2," "
     PRINT "FITTING ACCOMPLISHED AFTER";IT;"TIMES ITERATION"
     PRINT #2,"FITTING ACCOMPLISHED AFTER";IT;"TIMES ITERATION"
```

```
    CLOSE #2
200     END

    REM   >>>>>>>>>>>>>>>>>SUBROUTINES<<<<<<<<<<<<<<<<<<<<<<<<<
```

Subroutine CURVFIT

```
    REM   ===========SUBROUTINE FDERIV===============

                        FDERIV:
      xi = X(I)
      D1 =   -EXP(  -( xi/taucent)^(A(1))    )
      D2 =   ( xi / taucent ) ^ ( A(1) ) * LOG( xi / taucent )
      DERIV(1) = D1 * D2
    RETURN

   REM   =============SUBROUTINE FUNCTN====================

                          FUNC1:
      FUNCTN = 0 : xi = X(I)
      FUNCTN = FUNCTN + EXP(  -( xi/taucent)^(A(1))    )
    RETURN

                          FUNC2:
      FUNCTN = 0 :  xi = X(I)
      FUNCTN = FUNCTN + EXP(  -( xi/taucent)^(b(1))    )
   RETURN
```

Subroutine FCHISQUARE

Subroutine MATINV

```
                                    Title:
    backcolor 273 : forecolor 409
    CALL TEXTSIZE(33): CALL TEXTFACE(33)
    LOCATE 2,7 :PRINT " KWW-Analysis "
    CALL TEXTSIZE(12): CALL TEXTFACE(33)
    LOCATE 7,20:backcolor 30:PRINT " © Dr. Thomas C Ward's Lab "
     CALL TEXTSIZE(14):forecolor 205
    LOCATE 7,10: PRINT " [  v 1.0    In-House program  Polypkem 6/25/93 ] "
    forecolor 341
    LINE (35,34)-(475,150), ,b
    LINE (34,33)-(476,151), ,b
    LINE (32,31)-(478,153), ,b
    forecolor 137
    FOR xi = 35 TO 475 STEP 5
    FOR yi = 34 TO 150 STEP 5
    PSET (xi,yi)
    NEXT yi
    NEXT xi

RETURN
```

Subroutine Sing

Appendix B-3:

Havriliak-Negami and its special cases

The partial derivatives of Havriliak-Negami equation were derived by the author and their validities were tested with theoretical data. For Eq.(2.2.3-2),

With

$$\frac{\partial r}{\partial \tau} = 2\,\omega(\omega\tau)^{-\alpha}(1-\alpha)\left[\sin\left(\frac{\alpha\pi}{2}\right) + (\omega\tau)^{1-\alpha}\right]$$

$$\frac{\partial \theta}{\partial \tau} = \omega(\omega\tau)^{-\alpha}(1-\alpha)\cos\left(\frac{\alpha\pi}{2}\right)$$

$$\frac{\partial r}{\partial \alpha} = 2(\omega\tau)^{1-\alpha}\left[\frac{\pi}{2}\cos\left(\frac{\alpha\pi}{2}\right) - \sin\left(\frac{\alpha\pi}{2}\right)\ln(\omega\tau) - (\omega\tau)^{1-\alpha}\ln(\omega\tau)\right]$$

$$\frac{\partial \theta}{\partial \alpha} = \frac{-(\omega\tau)^{1-\alpha}\left[\cos\left(\frac{\alpha\pi}{2}\right)\cdot\ln(\omega\tau) + \frac{\pi}{2}\sin\left(\frac{\alpha\pi}{2}\right) + \frac{\pi}{2}(\omega\tau)^{1-\alpha}\right]}{\left[(\omega\tau)^{1-\alpha} + \sin\left(\frac{\alpha\pi}{2}\right)\right]^2 + \left[\cos\left(\frac{\alpha\pi}{2}\right)\right]^2}$$

Partial derivatives are

$$\frac{\partial \varepsilon''(\omega)}{\partial(\varepsilon_s - \varepsilon_\infty)} = r^{-\frac{\gamma}{2}}\sin(\theta\gamma)$$

$$\frac{\partial \varepsilon''(\omega)}{\partial \alpha} = \gamma(\varepsilon_s - \varepsilon_\infty)\, r^{-\frac{\gamma}{2}}\left[\cos(\theta\gamma)\frac{\partial \theta}{\partial \alpha} - \frac{1}{2r}\cdot\frac{\partial r}{\partial \alpha}\cdot\sin(\theta\gamma)\right]$$

$$\frac{\partial \varepsilon''(\omega)}{\partial \gamma} = (\varepsilon_s - \varepsilon_\infty)\, r^{-\frac{\gamma}{2}}\left[\theta\cdot\cos(\theta\gamma) - \frac{1}{2}\ln r\cdot\sin(\theta\gamma)\right]$$

$$\frac{\partial \varepsilon''(\omega)}{\partial \tau} = \gamma(\varepsilon_s - \varepsilon_\infty)\, r^{-\frac{\gamma}{2}}\left[\frac{\partial \theta}{\partial \tau}\cos(\theta\gamma) - \frac{1}{2r}\cdot\frac{\partial r}{\partial \tau}\cdot\sin(\theta\gamma)\right]$$

For the Cole-Cole and the Davidson-Cole model, one can use partial derivatives derived in a similar manner as in the Havriliak-Negami model. However as the degree of freedom in the minimization routine is important, all the subroutines in the Havriliak-Negami program were simply constrained according to each model and this approach was found to guarantee more rugged convergence to minimum chi-square.

(a) Havriliak-Negami Analysis

```
REM  ****************************
REM       Havriliak-Negami Analysis
REM  ****************************

REM   This program evaluates the Havriliak-Negami parameters
REM  from the data point pairs X,Y ( frequency , loss permittivity)
REM  through nonlinear regression which use MARQUARDT'S ALGORITHM

REM  ==============================
REM  DESCRIPTION OF PARAMETERS
REM  ==============================

REM  FQ-          FREQUENCY in Hertz
REM  LOSS-        LOSS PERMITTIVITY
REM  X-           ARRAY OF DATA POINTS FOR INDEPENDENT VARIABLE
REM  Y-           ARRAY OF DATA POINTS FOR DEPENDENT VARIABLE
REM  A-,B-        ARRAY OF PARAMETERS. the orders are
REM               oscillator strength / alpha / beta / tau
REM  IK-,JK-      TEMPORARY STORAGE IN SUBROUTINE MATINV
REM  DERIV-       ARRAY OF DERIVATIVES
REM  ALPHA-,BETA-  ARRAY FOR GRADIENTS IN SUBROUTINE CURFIT
REM  DELTAA-      ARRAY OF PARAMETER INCREMENTS
REM  NPTS-        NUMBER OF PAIRS OF DATA POINTS
REM  NTERMS-      NUMBER OF PARAMETERS
REM  NFREE-       NUMBER OF DEGREE OF FREEDOM
REM  NORDER-      DEGREE OF MATRIX
REM  FLAMDA-      PROPORTION OF GRADIENT SEARCH INCLUDED
REM  YFIT-        ARRAY OF CALCULATED VALUES OF Y
REM  CHISQ-       REDUCED CHI SQUARE FOR FIT

DIM  X(20),Y(20),YFIT(20),A(5),b(5),AA(5),BB(5)
DIM  ALPHA(20,20),BETA(20),ARRAY(20,20),SIGMAA(20)
DIM  DERIV(20),IK(20),JK(20),FQ(20),LOSS(20)
     CLS:
5    GOSUB Title: GOSUB Sing
     CALL TEXTSIZE(12) :CALL TEXTFACE(33):backcolor 30:forecolor 205
7    LOCATE 11,5: INPUT "  Ready for Analysis (y/n)       "; R$
          IF R$ = "n" GOTO 200
          IF R$ <> "y" GOTO 7

8    CLS: GOSUB Title
     CALL TEXTSIZE(12): CALL TEXTFACE(33):backcolor 30: forecolor 409
     LOCATE 12,5: INPUT " I.        Number of data point --->";NPTS
     IF NPTS < 4  THEN GOTO 200

     FOR I =1 TO NPTS
     LOCATE 12+I,5: PRINT "          Frequecncy";I;"  = ";:INPUT FQ(I):NEXT I

     FOR I = 1 TO NPTS
     LOCATE 13+NPTS+I,5:PRINT "          Loss dielectric constant";I;"  = ";
     INPUT LOSS(I):NEXT I
     forecolor 205
9    LOCATE 14+2*NPTS,5 : INPUT " Any corrections (y/n)       "; C$
```

```
      IF C$ = "n"  GOTO 10
      IF C$ <> "y" GOTO 9
      GOTO 8
10      CLS
     forecolor 409
     LOCATE 24,5 : INPUT " Output data file name  ---> ";F$
          LOCATE 25,5 :PRINT " Iteration Process Started"
         CALL TEXTSIZE(12):CALL TEXTFACE(0):backcolor 30:forecolor 33


  REM   =======INPUT RAW DATA AND INITIAL  VALUES=====

       PI = 3.141593 :  NTERMS =4 : FLAMDA = .0001
      HP = PI / 2


  FOR I = 1 TO NPTS   : X(I) = 2*PI*FQ(I): Y(I) = LOSS(I)  : NEXT I



   REM   <<<<<%%%%%RAW DATA END%%%%%>>>>>
   PRINT " Computation going on,Please don't disturb"

      OPEN F$ FOR OUTPUT AS 1

INPUT " Initial value ,Oscillator Strength";DEM
INPUT " Initial value ,alpha";ALM
INPUT " Initial value ,beta";BEM
INPUT " Initial value ,tau";TAM

                PRINT #1,ALM;BEM;DEM;TAM


          A(1) = DEM :   A(2)=ALM :   A(3)=BEM   :  A(4) =TAM
          AA(1) = SQR(DEM):   AA(2)= SQR(ALM)
           AA(3)= SQR(BEM):   AA(4)= SQR(TAM)

  REM   ---Begin nonlinear search------
  PRINT "---Begin nonlinear search------"

  REM   ==========================================
  REM   ITERATION OF  CHI-SQUARE CALCULATION
  REM   ==========================================
                        IT = 0

30      FOR I = 1 TO 5 : PRINT #1," " : NEXT I

       PRINT          " OS      alpha      beta      tau        "
       PRINT #1,       " OS  /  alpha   / beta  / tau  "

       PRINT           A(1), A(2),A(3),A(4)
       PRINT #1,      A(1), A(2),A(3),A(4)

         GOSUB CURVFIT
```

```
                        IT = IT +1

        OLDCHI = FCHISQ

50  GOSUB   CURVFIT


        PRINT #1,    "Iteration# = "; IT,"Chi-square = ";FCHISQ
        FOR I = 1 TO NTERMS: A(I) = (AA(I)^2) : NEXT I
        FOR I =  1 TO NTERMS
        PRINT #1,A(I);
        NEXT I

        PRINT #1," "

       NEWCHI = FCHISQ

      E = ABS((OLDCHI-NEWCHI)/OLDCHI)

       IF E =<.00001    GOTO 100

       OLDCHI = NEWCHI : IT = IT +1

      GOTO 50

100     PRINT "************************"
        PRINT #1,"************************"
        PRINT " FINAL RESULT ": PRINT " "
        PRINT #1," FINAL RESULT ": PRINT #1," "

        PRINT    "Iteration # = ";IT;"Chi-square"; FCHISQ
        PRINT #1,"Iteration # = ";IT;"Chi-square"; FCHISQ

    PRINT #1, "Oscillator strength = ";A(1)
    PRINT #1,  "Alpha = ";A(2)
    PRINT #1,  "Beta = ";A(3)
    PRINT #1, "Tau = ";A(4)


    PRINT "FITTING ACCOMPLISHED AFTER";IT;"TIMES ITERATION"
    PRINT #1,"FITTING ACCOMPLISHED AFTER";IT;"TIMES ITERATION"

    CLOSE 1
    PRINT "Thanks! Computation finished"
    PRINT " The data is stored in file ";F$

200     END


  REM   >>>>>>>>>>>>>>>>>>>>>>SUBROUTINES<<<<<<<<<<<<<<<<<<<<<<<<
```

Subroutine CURVFIT

```
REM  ==========SUBROUTINE FDERIV==========

                    FDERIV:

        xi = X(I)
R1 = (xi*A(4))^(1-A(2))
R2 = (xi*A(4))^(-A(2))
RS = SIN(A(2)*HP)
RC = COS(A(2)*HP)
OM = LOG(xi*A(4))
RT = (1+R1*RS)^2 + (R1*RC)^2
TH = ATN((R1*RC)/(1+R1*RS))
RB = (RT)^(-A(3)/2)
STB = SIN(TH*A(3))
CTB = COS(TH*A(3))
DRDA = 2*R1*(HP*RC-OM*RS-OM*R1)
DTDAU = -R1*(OM*RC+HP*RS+HP*R1)
DTDAB = (R1+RS)^2 + (RC)^2
DTDA = DTDAU / DTDAB
DRDT = 2*xi*R2*(1-A(2))*(RS + R1)
DTDTU = xi*(1-A(2))*R2*RC
DTDTB = (R1+RS)^2 + (RC)^2
DTDT = DTDTU / DTDTB
DEDC = A(1)*RB*A(3)
    DERIV(1) = RB*STB*2*AA(1)
    DERIV(2) = DEDC*(-DRDA*STB/(2*RT) + CTB*DTDA)*2*AA(2)
    DERIV(3) = A(1)*RB*(TH*CTB-STB*LOG(RT)/2)*2*AA(3)
    DERIV(4) = DEDC*(-DRDT*STB/(2*RT) + CTB*DTDT)*2*AA(4)

    RETURN

REM  ==========SUBROUTINE FUNCTN==========

                    FUNC1:
          FUNCTN = 0
              xi = X(I)
      F1 = (xi*(AA(4))^2)^(1-(AA(2))^2)
      F2 = SIN((AA(2))^2*HP)
      F3 = COS((AA(2))^2*HP)
      F4 = (1+F1*F2)^2  + (F1*F3)^2
      F5 = ATN((F1*F3)/(1+F1*F2))
      FUNCTN = FUNCTN + ((AA(1))^2)*(  (F4)^(-((AA(3))^2)/2)  )*SIN(F5*(AA(3))^2)

RETURN

                    FUNC2:
          FUNCTN = 0
              xi = X(I)
      F1 = (xi*(BB(4))^2)^(1-(BB(2))^2)
      F2 = SIN((BB(2))^2*HP)
      F3 = COS((BB(2))^2*HP)
      F4 = (1+F1*F2)^2  + (F1*F3)^2
      F5 = ATN((F1*F3)/(1+F1*F2))
      FUNCTN = FUNCTN + ((BB(1))^2)*(  (F4)^(-((BB(3))^2)/2)  )*SIN(F5*(BB(3))^2)
```

```
RETURN
```

Subroutine FCHISQUARE

Subroutine MATINV

```
                                INITIAL:

                              xi = X(P)
          INIT = 0
             F1 = (xi*TA)^(1-AL)
             F2 = SIN(AL*HP)
             F3 = COS(AL*HP)
             F4 = (1+F1*F2)^2  + (F1*F3)^2
             F5 = ATN((F1*F3)/(1+F1*F2))
            INIT = INIT + DE*(  (F4)^(-BE/2)  )*SIN(F5*BE)

  RETURN

END

                                        Title:
    backcolor 273 : forecolor 409
    CALL TEXTSIZE(33): CALL TEXTFACE(33)
    LOCATE 2,3 :PRINT "Havriliak-Negami Analysis"
    CALL TEXTSIZE(12): CALL TEXTFACE(33)
    LOCATE 7,20:backcolor 30:PRINT " © Dr. Thomas C Ward's Lab "
     CALL TEXTSIZE(14):forecolor 205
    LOCATE 7,10: PRINT " [  v 1.0    In-House program  Polypkem 6/25/93 ] "
    forecolor 341
    LINE (25,34)-(475,150), ,b
    LINE (24,33)-(476,151), ,b
    LINE (22,31)-(478,153), ,b
    forecolor 137
    FOR xi = 25 TO 475 STEP 5
    FOR yi = 34 TO 150 STEP 5
    PSET (xi,yi)
    NEXT yi
    NEXT xi
```

Subroutine Sing

(b) Cole-Cole Analysis

```
REM  ****************************
REM            Cole-Cole Analysis
REM  ****************************

REM   This program evaluates the Cole-Cole parameters
REM   from the data point pairs X,Y ( frequency , loss permittivity)
```

```
REM   through nonlinear regression which use MARQUARDT'S ALGORITHM

REM   ============================
REM   DESCRIPTION OF PARAMETERS
REM   ============================

REM   FQ-          FREQUENCY in Hertz
REM   LOSS-        LOSS PERMITTIVITY
REM   X-           ARRAY OF DATA POINTS FOR INDEPENDENT VARIABLE
REM   Y-           ARRAY OF DATA POINTS FOR DEPENDENT VARIABLE
REM   A-,B-        ARRAY OF PARAMETERS. the orders are
REM                oscillator strength / alpha / beta / tau
REM   IK-,JK-      TEMPORARY STORAGE IN SUBROUTINE MATINV
REM   DERIV-       ARRAY OF DERIVATIVES
REM   ALPHA-,BETA-   ARRAY FOR GRADIENTS IN SUBROUTINE CURFIT
REM   DELTAA-      ARRAY OF PARAMETER INCREMENTS
REM   NPTS-        NUMBER OF PAIRS OF DATA POINTS
REM   NTERMS-      NUMBER OF PARAMETERS
REM   NFREE-       NUMBER OF DEGREE OF FREEDOM
REM   NORDER-      DEGREE OF MATRIX
REM   FLAMDA-      PROPORTION OF GRADIENT SEARCH INCLUDED
REM   YFIT-        ARRAY OF CALCULATED VALUES OF Y
REM   CHISQ-       REDUCED CHI SQUARE FOR FIT

DIM   X(20),Y(20),YFIT(20),A(5),B(5),AA(5),BB(5)
DIM   ALPHA(20,20),BETA(20),ARRAY(20,20),SIGMAA(20)
DIM   DERIV(20),IK(20),JK(20),FQ(20),LOSS(20)
      CLS:
5     GOSUB Title: GOSUB Sing
      CALL TEXTSIZE(12) :CALL TEXTFACE(33):backcolor 30:forecolor 205
7     LOCATE 11,5: INPUT "  Ready for Analysis (y/n)       "; R$
            IF R$ = "n" GOTO 200
            IF R$ <> "y" GOTO 7

8     CLS: GOSUB Title
      CALL TEXTSIZE(12): CALL TEXTFACE(33):backcolor 30: forecolor 409
      LOCATE 12,5: INPUT " I.        Number of data point --->";NPTS
      IF NPTS < 4   THEN GOTO 200

      FOR I =1 TO NPTS
      LOCATE 12+I,5: PRINT "            Frequecncy";I;"  = ";:INPUT FQ(I):NEXT I

      FOR I = 1 TO NPTS
      LOCATE 13+NPTS+I,5:PRINT "            Loss dielectric constant";I;"  = ";
      INPUT LOSS(I):NEXT I
      forecolor 205
9     LOCATE 14+2*NPTS,5 : INPUT " Any corrections (y/n)         "; C$
      IF C$ = "n"  GOTO 10
      IF C$ <> "y" GOTO 9
      GOTO 8
10      CLS
      forecolor 409
      LOCATE 24,5 : INPUT " Output data file name   ---> ";F$
            LOCATE 25,5 :PRINT " Iteration Process Started"
           CALL TEXTSIZE(12):CALL TEXTFACE(0):backcolor 30:forecolor 33
```

```
REM   =======INPUT RAW DATA AND INITIAL  VALUES=====

      PI = 3.141593 :  NTERMS =4 : FLAMDA = .0001
     HP = PI / 2


FOR I = 1 TO NPTS   :  X(I) = 2*PI*FQ(I): Y(I) = LOSS(I)  : NEXT I



 REM   <<<<<%%%%%RAW DATA END%%%%%>>>>>
 PRINT " Computation going on,Please don't disturb"

    OPEN F$ FOR OUTPUT AS 1

INPUT " Initial value ,Oscillator Strength";DEM
INPUT " Initial value ,alpha";ALM
INPUT " Initial value ,beta";BEM
INPUT " Initial value ,tau";TAM

              PRINT #1,ALM;BEM;DEM;TAM


        A(1) = DEM :   A(2)=ALM :   A(3)=BEM   :  A(4) =TAM
        AA(1) = SQR(DEM):   AA(2)= SQR(ALM)
         AA(3)= SQR(BEM):   AA(4)= SQR(TAM)

 REM   ---Begin nonlinear search------
 PRINT "---Begin nonlinear search------"

 REM   ================================================
 REM   ITERATION OF  CHI-SQUARE CALCULATION
 REM   ================================================
                    IT = 0

30     FOR I = 1 TO 5 : PRINT #1," " : NEXT I

      PRINT        " OS     alpha     beta      tau       "
      PRINT #1,     " OS  /  alpha   / beta  / tau  "

      PRINT          A(1), A(2),A(3),A(4)
      PRINT #1,     A(1), A(2),A(3),A(4)

        GOSUB CURVFIT

                    IT = IT +1

        OLDCHI = FCHISQ

50  GOSUB   CURVFIT
```

```
        PRINT #1,    "Iteration# = "; IT,"Chi-square = ";FCHISQ
        FOR I = 1 TO NTERMS: A(I) = (AA(I)^2) : NEXT I
        FOR I =  1 TO NTERMS
        PRINT #1,A(I);
        NEXT I

        PRINT #1," "

       NEWCHI = FCHISQ

      E = ABS((OLDCHI-NEWCHI)/OLDCHI)

       IF E =<.00001    GOTO 100

       OLDCHI = NEWCHI : IT = IT +1

      GOTO 50

100     PRINT "************************"
        PRINT #1,"************************"
        PRINT " FINAL RESULT ": PRINT " "
        PRINT #1," FINAL RESULT ": PRINT #1," "

        PRINT    "Iteration # = ";IT;"Chi-square"; FCHISQ
        PRINT #1,"Iteration # = ";IT;"Chi-square"; FCHISQ

    PRINT #1, "Oscillator strength = ";A(1)
    PRINT #1,  "Alpha = ";A(2)
    PRINT #1,  "Beta = ";A(3)
    PRINT #1, "Tau = ";A(4)


    PRINT "FITTING ACCOMPLISHED AFTER";IT;"TIMES ITERATION"
    PRINT #1,"FITTING ACCOMPLISHED AFTER";IT;"TIMES ITERATION"

    CLOSE 1
    PRINT "Thanks! Computation finished"
    PRINT " The data is stored in file ";F$

200     END


  REM   >>>>>>>>>>>>>>>>>>>>>>SUBROUTINES<<<<<<<<<<<<<<<<<<<<<<<<
```

Subroutine CURVFIT

```
    REM   ===========SUBROUTINE FDERIV==========

                        FDERIV:
A(3) = 1:AA(3) = 1
            xi = X(I)
  R1 = (xi*A(4))^(1-A(2))
  R2 = (xi*A(4))^(-A(2))
  RS = SIN(A(2)*HP)
```

```
    RC = COS(A(2)*HP)
    OM = LOG(xi*A(4))
    RT = (1+R1*RS)^2 + (R1*RC)^2
    TH = ATN((R1*RC)/(1+R1*RS))
    RB = (RT)^(-A(3)/2)
    STB = SIN(TH*A(3))
    CTB = COS(TH*A(3))
    DRDA = 2*R1*(HP*RC-OM*RS-OM*R1)
    DTDAU = -R1*(OM*RC+HP*RS+HP*R1)
    DTDAB = (R1+RS)^2 + (RC)^2
    DTDA = DTDAU / DTDAB
    DRDT = 2*xi*R2*(1-A(2))*(RS + R1)
    DTDTU = xi*(1-A(2))*R2*RC
    DTDTB = (R1+RS)^2 + (RC)^2
    DTDT = DTDTU / DTDTB
    DEDC = A(1)*RB*A(3)
        DERIV(1) = RB*STB*2*AA(1)
        DERIV(2) = DEDC*(-DRDA*STB/(2*RT) + CTB*DTDA)*2*AA(2)
        DERIV(3) = A(1)*RB*(TH*CTB-STB*LOG(RT)/2)*2*AA(3)
        DERIV(4) = DEDC*(-DRDT*STB/(2*RT) + CTB*DTDT)*2*AA(4)

        RETURN

    REM   ==============SUBROUTINE FUNCTN==============

                                FUNC1:
A(3) = 1:AA(3) = 1
                    FUNCTN = 0
                            xi = X(I)
            F1 = (xi*(AA(4))^2)^(1-(AA(2))^2)
            F2 = SIN((AA(2))^2*HP)
            F3 = COS((AA(2))^2*HP)
            F4 = (1+F1*F2)^2  + (F1*F3)^2
            F5 = ATN((F1*F3)/(1+F1*F2))
            FUNCTN = FUNCTN + ((AA(1))^2)*(  (F4)^(-((AA(3))^2)/2)  )*SIN(F5*(AA(3))^2)

    RETURN

                                FUNC2:
B(3) = 1:BB(3) = 1
                        FUNCTN = 0
                                xi = X(I)
            F1 = (xi*(BB(4))^2)^(1-(BB(2))^2)
            F2 = SIN((BB(2))^2*HP)
            F3 = COS((BB(2))^2*HP)
            F4 = (1+F1*F2)^2  + (F1*F3)^2
            F5 = ATN((F1*F3)/(1+F1*F2))
            FUNCTN = FUNCTN + ((BB(1))^2)*(  (F4)^(-((BB(3))^2)/2)  )*SIN(F5*(BB(3))^2)

  RETURN
```

Subroutine FCHISQUARE

Subroutine MATINV

```
                                INITIAL:
A(3) = 1: AA(3) = 1
                                xi = X(P)
        INIT = 0
          F1 = (xi*TA)^(1-AL)
          F2 = SIN(AL*HP)
          F3 = COS(AL*HP)
          F4 = (1+F1*F2)^2  + (F1*F3)^2
          F5 = ATN((F1*F3)/(1+F1*F2))
         INIT = INIT + DE*(  (F4)^(-BE/2)  )*SIN(F5*BE)

  RETURN


END

                                Title:
    backcolor 273 : forecolor 409
    CALL TEXTSIZE(33): CALL TEXTFACE(33)
    LOCATE 2,6 :PRINT "Cole-Cole Analysis"
    CALL TEXTSIZE(12): CALL TEXTFACE(33)
    LOCATE 7,20:backcolor 30:PRINT " © Dr. Thomas C Ward's Lab "
     CALL TEXTSIZE(14):forecolor 205
    LOCATE 7,10: PRINT " [  v 1.0   In-House program  Polypkem 8/10/93 ] "
    forecolor 341
    LINE (25,34)-(475,150), ,B
    LINE (24,33)-(476,151), ,B
    LINE (22,31)-(478,153), ,B
    forecolor 137
    FOR xi = 25 TO 475 STEP 5
    FOR yi = 34 TO 150 STEP 5
    PSET (xi,yi)
    NEXT yi
    NEXT xi


RETURN
```

Subroutine Sing

(c) Davidson-Cole Analysis

```
REM  ******************************
REM       Davidson-Cole Analysis
REM  ******************************

REM   This program evaluates the Davidson-Cole parameters
REM  from the data point pairs X,Y ( frequency , loss permittivity)
REM  through nonlinear regression which use MARQUARDT'S ALGORITHM
```

```
   REM  ==============================
   REM  DESCRIPTION OF PARAMETERS
   REM  ==============================

   REM  FQ-          FREQUENCY in Hertz
   REM  LOSS-        LOSS PERMITTIVITY
   REM  X-           ARRAY OF DATA POINTS FOR INDEPENDENT VARIABLE
   REM  Y-           ARRAY OF DATA POINTS FOR DEPENDENT VARIABLE
   REM  A-,B-        ARRAY OF PARAMETERS. the orders are
   REM               oscillator strength / alpha / beta / tau
   REM  IK-,JK-      TEMPORARY STORAGE IN SUBROUTINE MATINV
   REM  DERIV-       ARRAY OF DERIVATIVES
   REM  ALPHA-,BETA- ARRAY FOR GRADIENTS IN SUBROUTINE CURFIT
   REM  DELTAA-      ARRAY OF PARAMETER INCREMENTS
   REM  NPTS-        NUMBER OF PAIRS OF DATA POINTS
   REM  NTERMS-      NUMBER OF PARAMETERS
   REM  NFREE-       NUMBER OF DEGREE OF FREEDOM
   REM  NORDER-      DEGREE OF MATRIX
   REM  FLAMDA-      PROPORTION OF GRADIENT SEARCH INCLUDED
   REM  YFIT-        ARRAY OF CALCULATED VALUES OF Y
   REM  CHISQ-       REDUCED CHI SQUARE FOR FIT

   DIM  X(20),Y(20),YFIT(20),A(5),B(5),AA(5),BB(5)
   DIM  ALPHA(20,20),BETA(20),ARRAY(20,20),SIGMAA(20)
   DIM  DERIV(20),IK(20),JK(20),FQ(20),LOSS(20)
      CLS:
5    GOSUB Title: GOSUB Sing
     CALL TEXTSIZE(12) :CALL TEXTFACE(33):backcolor 30:forecolor 205
7    LOCATE 11,5: INPUT "  Ready for Analysis (y/n)       "; R$
           IF R$ = "n" GOTO 200
           IF R$ <> "y" GOTO 7

8    CLS: GOSUB Title
     CALL TEXTSIZE(12): CALL TEXTFACE(33):backcolor 30: forecolor 409
     LOCATE 12,5: INPUT " I.        Number of data point --->";NPTS
     IF NPTS < 4  THEN GOTO 200

     FOR I =1 TO NPTS
     LOCATE 12+I,5: PRINT "          Frequecncy";I;"  = ";:INPUT FQ(I):NEXT I

     FOR I = 1 TO NPTS
     LOCATE 13+NPTS+I,5:PRINT "          Loss dielectric constant";I;"  = ";
     INPUT LOSS(I):NEXT I
     forecolor 205
9    LOCATE 14+2*NPTS,5 : INPUT " Any corrections (y/n)        "; C$
     IF C$ = "n"  GOTO 10
     IF C$ <> "y" GOTO 9
     GOTO 8
10     CLS
     forecolor 409
     LOCATE 24,5 : INPUT " Output data file name  ---> ";F$
          LOCATE 25,5 :PRINT " Iteration Process Started"
          CALL TEXTSIZE(12):CALL TEXTFACE(0):backcolor 30:forecolor 33
```

```
REM   =======INPUT RAW DATA AND INITIAL  VALUES=====

      PI = 3.141593 :  NTERMS =4 : FLAMDA = .0001
     HP = PI / 2


FOR I = 1 TO NPTS    : X(I) = 2*PI*FQ(I): Y(I) = LOSS(I)  : NEXT I


 REM    <<<<<%%%%%RAW DATA END%%%%%>>>>>
 PRINT " Computation going on,Please don't disturb"

    OPEN F$ FOR OUTPUT AS 1

INPUT " Initial value ,Oscillator Strength";DEM
INPUT " Initial value ,alpha";ALM
INPUT " Initial value ,beta";BEM
INPUT " Initial value ,tau";TAM

              PRINT #1,ALM;BEM;DEM;TAM


         A(1) = DEM :   A(2)=ALM :   A(3)=BEM   :  A(4) =TAM
         AA(1) = SQR(DEM):   AA(2)= SQR(ALM)
          AA(3)= SQR(BEM):   AA(4)= SQR(TAM)

 REM   ---Begin nonlinear search------
 PRINT "---Begin nonlinear search------"

 REM   ==============================================
 REM   ITERATION OF  CHI-SQUARE CALCULATION
 REM   ==============================================
                    IT = 0

30      FOR I = 1 TO 5 : PRINT #1," " : NEXT I

      PRINT        " OS      alpha      beta      tau        "
      PRINT #1,     " OS  /  alpha   / beta  / tau  "

      PRINT          A(1), A(2),A(3),A(4)
      PRINT #1,     A(1), A(2),A(3),A(4)

        GOSUB CURVFIT

                    IT = IT +1

        OLDCHI = FCHISQ

50  GOSUB   CURVFIT


        PRINT #1,   "Iteration# = "; IT,"Chi-square = ";FCHISQ
        FOR I = 1 TO NTERMS: A(I) = (AA(I)^2) : NEXT I
```

```
        FOR I =  1 TO NTERMS
        PRINT #1,A(I);
        NEXT I

        PRINT #1," "

       NEWCHI = FCHISQ

      E = ABS((OLDCHI-NEWCHI)/OLDCHI)

       IF E =<.00001   GOTO 100

       OLDCHI = NEWCHI : IT = IT +1

      GOTO 50

100     PRINT "************************"
        PRINT #1,"************************"
        PRINT " FINAL RESULT ": PRINT " "
        PRINT #1," FINAL RESULT ": PRINT #1," "

        PRINT    "Iteration # = ";IT;"Chi-square"; FCHISQ
        PRINT #1,"Iteration # = ";IT;"Chi-square"; FCHISQ

    PRINT #1, "Oscillator strength = ";A(1)
    PRINT #1,  "Alpha = ";A(2)
    PRINT #1,  "Beta = ";A(3)
    PRINT #1, "Tau = ";A(4)


    PRINT "FITTING ACCOMPLISHED AFTER";IT;"TIMES ITERATION"
    PRINT #1,"FITTING ACCOMPLISHED AFTER";IT;"TIMES ITERATION"

    CLOSE 1
    PRINT "Thanks! Computation finished"
    PRINT " The data is stored in file ";F$

200     END


  REM   >>>>>>>>>>>>>>>>>>>>>SUBROUTINES<<<<<<<<<<<<<<<<<<<<<<<<
```

Subroutine CURVFIT

```
    REM   ==========SUBROUTINE FDERIV==========

                          FDERIV:
A(2) = .000001:AA(2) = .001
            xi = X(I)
  R1 = (xi*A(4))^(1-A(2))
  R2 = (xi*A(4))^(-A(2))
  RS = SIN(A(2)*HP)
  RC = COS(A(2)*HP)
```

```
    OM = LOG(xi*A(4))
    RT = (1+R1*RS)^2 + (R1*RC)^2
    TH = ATN((R1*RC)/(1+R1*RS))
    RB = (RT)^(-A(3)/2)
    STB = SIN(TH*A(3))
    CTB = COS(TH*A(3))
    DRDA = 2*R1*(HP*RC-OM*RS-OM*R1)
    DTDAU = -R1*(OM*RC+HP*RS+HP*R1)
    DTDAB = (R1+RS)^2 + (RC)^2
    DTDA = DTDAU / DTDAB
    DRDT = 2*xi*R2*(1-A(2))*(RS + R1)
    DTDTU = xi*(1-A(2))*R2*RC
    DTDTB = (R1+RS)^2 + (RC)^2
    DTDT = DTDTU / DTDTB
    DEDC = A(1)*RB*A(3)
        DERIV(1) = RB*STB*2*AA(1)
        DERIV(2) = DEDC*(-DRDA*STB/(2*RT) + CTB*DTDA)*2*AA(2)
        DERIV(3) = A(1)*RB*(TH*CTB-STB*LOG(RT)/2)*2*AA(3)
        DERIV(4) = DEDC*(-DRDT*STB/(2*RT) + CTB*DTDT)*2*AA(4)

        RETURN

    REM   ==============SUBROUTINE FUNCTN==============

                              FUNC1:
A(2) =.000001:AA(2) =.001
                    FUNCTN = 0
                          xi = X(I)
            F1 = (xi*(AA(4))^2)^(1-(AA(2))^2)
            F2 = SIN((AA(2))^2*HP)
            F3 = COS((AA(2))^2*HP)
            F4 = (1+F1*F2)^2  + (F1*F3)^2
            F5 = ATN((F1*F3)/(1+F1*F2))
            FUNCTN = FUNCTN + ((AA(1))^2)*(  (F4)^(-((AA(3))^2)/2)  )*SIN(F5*(AA(3))^2)

    RETURN

                              FUNC2:
B(2) = .000001:BB(2) = .001
                    FUNCTN = 0
                          xi = X(I)
            F1 = (xi*(BB(4))^2)^(1-(BB(2))^2)
            F2 = SIN((BB(2))^2*HP)
            F3 = COS((BB(2))^2*HP)
            F4 = (1+F1*F2)^2  + (F1*F3)^2
            F5 = ATN((F1*F3)/(1+F1*F2))
            FUNCTN = FUNCTN + ((BB(1))^2)*(  (F4)^(-((BB(3))^2)/2)  )*SIN(F5*(BB(3))^2)

  RETURN
```

Subroutine FCHISQUARE

Subroutine MATINV

```
                              INITIAL:
```

```
AL = .000001
                        xi = X(P)
      INIT = 0
        F1 = (xi*TA)^(1-AL)
        F2 = SIN(AL*HP)
        F3 = COS(AL*HP)
        F4 = (1+F1*F2)^2  + (F1*F3)^2
        F5 = ATN((F1*F3)/(1+F1*F2))
       INIT = INIT + DE*(  (F4)^(-BE/2)  )*SIN(F5*BE)

  RETURN


END

                                Title:
    backcolor 273 : forecolor 409
    CALL TEXTSIZE(33): CALL TEXTFACE(33)
    LOCATE 2,4 :PRINT "Cole-Davidson Analysis"
    CALL TEXTSIZE(12): CALL TEXTFACE(33)
    LOCATE 7,20:backcolor 30:PRINT " © Dr. Thomas C Ward's Lab "
     CALL TEXTSIZE(14):forecolor 205
    LOCATE 7,10: PRINT " [  v 1.0   In-House program  Polypkem 8/10/93 ] "
    forecolor 341
    LINE (25,34)-(475,150), ,B
    LINE (24,33)-(476,151), ,B
    LINE (22,31)-(478,153), ,B
    forecolor 137
    FOR xi = 25 TO 475 STEP 5
    FOR yi = 34 TO 150 STEP 5
    PSET (xi,yi)
    NEXT yi
    NEXT xi


RETURN
```

Subroutine Sing

Appendix C:

Half sided cosine transformation

```
**************************************
  Autocorrelation Function for ten DECADES
**************************************
```

1. This program calculates auto correlation values of dielectric relaxation from given parameters of Havriliak-Negami Analysis and returns results in data file COMP and DOCU where COMP contains numerical data in column format and DOCU contains integration variable information.
2. It is extremely important that the alpha in this program corresponds to (1 - alpha[HN]) where alpha is defined according to original literature.
3. Time scale used is " constant log-time ".

```
"Clearing up the parameters";

w =.;   "angular frequency";
d =.;   "oscillator strength";
a =.;   "1-alpha in H-N equation";
g =.;   "gamma in H-N equation";
tau =.; "time constant of H-N equation";
k =.;   "user defined variable";
r =.;   "user defined variable";
theta =.; "user defined variable";

lt =. ; " log-time";
t =.;   "time";
hp =. ; " half period ";

amp =.; "amplitude of omega space";
obj =.; "total integrand";
sm =.;  "sum of all half period integration";
m =.  ; "instantaneous half period integration (hpi)";

l1 =. ; " initial integration limit for hpi ";
l2 =. ; " final integration limit for hpi ";


" Assigning values to parameters";

  "Havriliak-Negami constants";

        d = 0.117;
        a = 0.7;
        g = 0.5;
        tau = 0.022;
```

```
"calculation part";

        k=( (1-a) Pi / 2 );

        amp[w_] := (
        theta=ArcTan[((w tau)^a Cos[k]) / (1+((w tau)^a) Sin[k])] ;
  r=( 1 + (( w tau )^a) Sin[k])^2+((w tau)^a Cos[k])^2;
  am = ( 2/ Pi) r^(-g / 2) Sin[ theta g]          )


OpenWrite["COMP"];
OpenWrite["DOCU"];

        Print[" beginning do loop "] ;


Do[
         t= 10 ^ ( lt ) ;

  hp= N[ Pi / t ];
  Print["========================================="];
  Print["hp ",hp];
  sm= 0 ;
  l1 = 0 ;l2= l1 + hp ;

  obj =  amp[w]  ( Cos[ w t ] /  w );

  Print[ " " ];


( Label[again];

   m = NIntegrate[obj,{w,l1,l2},MaxRecursion->40];

                sm = sm + m ;
           l1 += hp ; l2 += hp ;

     If[ Abs[m] > 10 ^ -6, Goto[again] ] );



 Print[" acf at t= ",t," is ", sm," up to w= ",l2];
 Write["DOCU"," acf at t= ",t," is ", sm," up to w= ",l2];
 Write["COMP",lt,"tab",sm,"tab"]
                                                  ,{lt,-10,-0.1,0.1}];
 Close["DOCU"];
 Close["COMP"];

  Print[" "];
  Print[" All 10 dedcades' ACF have been calculated "]
```

VITAE

Taigyoo Park was born to Bongryeol Park and Seonhee Kim Park in Pusan, Korea on June 18, 1960. After graduating from Baejeong high school in Pusan with honors, he entered Seoul National University, Korea, majoring in Chemical Engineering. He obtained a Bachelor of Science degree in Chemical Engineering in February 1984 and began R & D in the Lucky Central Research Institute as a process /polymer engineer for five years, in replacement of military service. In 1989 when the military option was finished, he enrolled in a doctoral program in the Chemistry department of Virginia Polytechnic Institute & State University and subsequently joined Professor Thomas C. Ward's group. He mainly worked in the area of dielectric relaxation in order to find a viable way of toughening biodegradable polymer poly(3-hydroxybutyrate). He defended and received his doctorate in April, 1994.

Taigyoo Park